

Mohammad H. Vadjed Samiei

Interaction of a radio-handset and a human head at 1900 MHz using the FDTD method

Thèse  
présentée  
à la Faculté des études supérieures  
pour l'obtention  
du grade de Philosophiae Doctor (Ph. D.)

Département de Génie Electrique  
FACULTÉ DES SCIENCES ET DE GÉNIE

UNIVERSITÉ LAVAL

QUÉBEC

DÉCEMBRE 1999

© Mohammad H. Vadjed Samiei, 1999



**National Library  
of Canada**

**Acquisitions and  
Bibliographic Services**

**395 Wellington Street  
Ottawa ON K1A 0N4  
Canada**

**Bibliothèque nationale  
du Canada**

**Acquisitions et  
services bibliographiques**

**395, rue Wellington  
Ottawa ON K1A 0N4  
Canada**

*Your file Votre référence*

*Our file Notre référence*

**The author has granted a non-exclusive licence allowing the National Library of Canada to reproduce, loan, distribute or sell copies of this thesis in microform, paper or electronic formats.**

**The author retains ownership of the copyright in this thesis. Neither the thesis nor substantial extracts from it may be printed or otherwise reproduced without the author's permission.**

**L'auteur a accordé une licence non exclusive permettant à la Bibliothèque nationale du Canada de reproduire, prêter, distribuer ou vendre des copies de cette thèse sous la forme de microfiche/film, de reproduction sur papier ou sur format électronique.**

**L'auteur conserve la propriété du droit d'auteur qui protège cette thèse. Ni la thèse ni des extraits substantiels de celle-ci ne doivent être imprimés ou autrement reproduits sans son autorisation.**

**0-612-52264-4**

**Canada**



Ce 7<sup>e</sup> jour du mois de AVRIL 19<sup>2000</sup>, les personnes soussignées, en leur qualité de membres du jury de la thèse de M. M. - HASHEM VADJED-SAMEI ont assisté à la soutenance de cette thèse. M. M. - HASHEM VADJED-SAMEI

NOMS	UNIVERSITÉ	SIGNATURE
<u>GILLES DELISLE</u>	<u>U. Laval</u>	
<u>MICHEL TÉTU</u>	<u>U. Laval</u>	
<u>MICHEL LECOURS</u>	<u>U. Laval</u>	
<u>MARIA STUCHLY</u>	<u>U. of VICTORIA</u>	

## Résumé

Ce travail porte sur l'analyseur théorique et expérimentale de l'interaction entre un modèle de crâne humain et un téléphone cellulaire opérant à 1900 MHz. Cette analyse utilise la méthode des différences finies aux variations temporelles (FDTD). En utilisant un modèle homogène, l'impédance d'entrée et le diagramme de rayonnement associés au téléphone cellulaire sont calculés en utilisant et en l'absence du modèle de la tête. L'effet de combiné téléphonique sur le débit d'un système spécifique (SAR) est calculé sur quatre modèles de têtes différents, homogène et non-homogène. Des mesures de l'impédance d'entrée d'entrée et du diagramme de rayonnement du combiné ont été effectués pour vérifier les prédictions analytiques.

Notre étude montre que les effets de la présence de la tête modélisée sur le modèle de l'antenne utilisée sont une légère déviation de la fréquence centrale du combiné lorsque celui-ci est à une distance de 1.5 à 2 cm et un effet de masque significatif sur le diagramme de rayonnement de l'antenne dans la direction de la tête.

De plus, même si la valeur du SAR n'est pas sensible l'hétérogénéité, on observe une réduction de celui-ci de l'ordre de 5% lorsque l'on ajoute un cou au modèle et cette décroissance est la même si la dimension du modèle de la tête est réduite de 10%.

---

M. Hashem Vadjed Samiei  
Étudiant Ph.D.

Gilles-Y. Delisle  
Directeur de thèse



## Abstract

The problem of the interaction between a human head model and a radio-handset at the frequency of 1900 MHz is studied, both theoretically and experimentally. Our analysis is performed using the method of FDTD. The input impedance and the radiation pattern of the radio-handset in two cases of with and without the head model are calculated, using a simple homogeneous model. The effect of the radio-handset on the head is studied by calculation of the SAR (Specific Absorption Rate) in four different head models, both homogeneous and heterogeneous. A series of measurements on the input impedance and on the radiation pattern of the radio-handset are performed to confirm the theoretical results. Our studies indicate that the effects of the presence of the head model on the antenna model used in our study are a small shift in the centre frequency of the radio-handset, when the head handset distance is around 1.5-2 cm, and a significant shadowing effect on the radiation pattern of the antenna in the direction toward the head. In addition, while the SAR value is not sensitive to the heterogeneity, it reduces by 5% when the neck is added to the model and increases by the same 5% when the size of the head model decreases by 10%.

M. Hashem Vadjed Samiei  
Ph.D. Student


Gilles-Y. Delisle  
Thesis Advisor

## Sommaire

Ce travail a pour objectif d'analyser, à la fois analytiquement et expérimentalement, l'interaction entre un combiné-radio et la tête d'un usager à la fréquence de 1900 MHz pour laquelle on ne retrouve pas suffisamment de résultats dans la littérature malgré l'importance du problème. La plupart des recherches courantes ont été effectuées pour une fréquence de 900 MHz. Les effets de la tête sur les performances du combiné-radio sont estimés à partir de calcul de l'impédance d'entrée et du diagramme de rayonnement entre 0 et 6 GHz, alors que les effets du combiné-radio sur la tête sont étudiés en calculant la moyenne temporelle du SAR spatial maximal sur des modèles de la tête. Notre analyse s'appuie sur la méthode FDTD, un modèle du combiné-radio constitué d'un monopole  $\lambda/4$  monté sur un boîtier métallique et des modèles de la tête homogène et hétérogène. Dans les calculs de l'impédance et du diagramme de rayonnement, un modèle homogène simple, à une distance de 1 cm du combiné-radio est utilisé alors que, pour le calcul du SAR, quatre modèles différents de la tête, à la fois homogène et hétérogène à une distance de 15-50 cm de la source fonctionnelle est utilisé.

Les modèles hétérogènes s'appuient sur trois types de tissus du cerveau, des muscles et de l'humeur dont les formes, positions relatives et dimensions sont compatibles avec les données anatomiques disponibles. Les modèles de la tête consiste en une partie sphérique de rayon 10 cm, montée sur une portion cylindrique de rayon de 6 cm, remplie avec les tissus appropriés. Pour les calculs du SAR, les effets de la grosseur de la tête, du cou et de l'hétérogénéité des modèles sont étudiés. Une série de mesures de l'impédance d'entrée entre 0 et 3 GHz et des diagrammes de rayonnement dans les trois plans ont été effectuées pour valider les résultats théoriques. Nos résultats montrent que la présence de la tête introduit une légère déviation de la fréquence centrale du combiné lorsque la distance entre la tête et le combiné est autour de 1.5-2 cm, et un effet de masque important sur le diagramme de rayonnement si l'antenne est pointée vers la tête.

Dans les calculs de SAR, où aucune sensibilité à l'hétérogénéité n'a été décelée, l'addition du cou amène une réduction de 5% du SAR maximal et une augmentation du même ordre si la dimension de la tête du modèle est réduite de 10%. Les résultats de notre étude sont comparés avec ceux obtenus par d'autres chercheurs et il apparaît clairement que les modèles simples pour la tête sont fiables pour estimer les effets mutuels entre le combiné-radio et la tête d'un usager.

 Hashem Vadjed Samiei  
Étudiant Ph.D.

Gilles-Y. Delisle  
Directeur de thèse

## Summary

The aim of this study is to investigate, both theoretically and experimentally, the interaction of a radio-handset and the head of its user at the frequency of 1900 MHz for which there are not enough results in the literature in spite of the importance of the problem. Most of the current investigations were done for the effects at 900 MHz. Effects of the head on the radio-handset performance are estimated by calculation of the input impedance and the radiation patterns of the radio-handset in the 0-6 GHz range, while the effects of the radio-handset on the head are studied by calculations of the time average of the spatial peak of the SAR in the head models. Our analysis in impedance and pattern calculations is based on the FDTD method, a radio-handset model consisting a  $\lambda/4$  monopole antenna mounted on a metallic box and a simple homogeneous model of the head, at a distance of 1 cm from the handset, while for the SAR calculations four different head models, both homogeneous and heterogeneous ones, at a distance of 15-50 mm from the source point, are used.

Heterogeneous models are based on three tissue types of a brain, the muscle, and the humour, whose shapes, relative positions and sizes are compatible with the existing anatomical data. Head models consisted of a spherical part, with a radius of 10 cm, mounted on a cylindrical part, with a radius of 6 cm, filled with the relevant tissue type(s). In the SAR calculations the effects of the head size, neck, and heterogeneity of the models on the SAR are studied. A series of measurements on the input impedance, in the 0-3 GHz range, and on the radiation patterns, in three cuts, are performed to confirm the theoretical results. Our studies indicate that the presence of the head introduces a small shift in the centre frequency of the handset, and a significant shadowing effect on the radiation pattern of the antenna in the direction toward the head.

In the SAR calculations, while no sensitivity is detectable due to heterogeneity, adding the neck results in a reduction of 5% in SAR's peak, and an increase by the same amount of 5%, is seen due to a decrease of 10% in the size of the head model. Results obtained in our studies are compared with those of others researchers, and it seems that simple head models are reliable to estimate the mutual effects of the radio-handset and the head of its user.

M. Hashem Vadjed Samiei  
Ph.D. Student

Gilles-Y. Delisle  
Thesis Advisor

## **Acknowledgements**

I would like to express my thanks and appreciation to Professor Gilles-Y. Delisle for his supervision, guidance, encouragement and financial support.

I also want to present my appreciation to all my professors, members of departmental committees, specifically Professor Michel Lecours. I extend also these thanks to the thesis examiners, Dr Michel Têtu and Dr Maria Stuchly.

I would like to thank Laval University to have given me all the opportunities required to pursue my Ph.D. program in good conditions.

Special acknowledgement is extended to the Ministry of Culture and Higher Education of the Islamic Republic of Iran, the Higher Advisory of the Ministry in Canada, Dr Mortazavi and Iran University of Science and Technology for awarding me Graduate Studies Fund and Scholarship.

I would like to thank my parents, my sisters and my brothers for their support and encouragement.

I would like to express my thanks to my wife for her encouragement and patience, and to my son Taha for the happiness and joy he brought to our life.

# Table of Contents

abstract.....	ii
Summary.....	iii
Résumé.....	v
Sommaire.....	vi
Acknowledgements.....	viii
Table des matières.....	ix
<b>Chapter One: Introduction.....</b>	<b>1</b>
1.1-Importance of this research topics.....	1
1.2-Objects of the study.....	1
1.3-Methodology used in the research.....	2
1.4-Thesis Outline.....	2
1.5-Contributions and results.....	4
<b>Chapter Two: General considerations on the interaction of EM radiating systems and biological objects.....</b>	<b>6</b>
2.1-Intrduction.....	6
2.1.1-Generalized interaction problem.....	6
2.1.2-Generated problems.....	7
2.2-EM radiating systems biological objects interaction: A classification .....	7
2.3-EM radiation bioeffects: Disciplines and contributions.....	7
2.3.1-Biophysics.....	8
2.3.2-Electromagnetics.....	9
2.3.2.1-General aspects.....	9
2.3.2.2-Electromagnetic analysis of human body radiating systems interaction.....	10
2.4-Radiofrequency field exposure standards .....	11
2.4.1-Standards related to the mobile communication technology.....	12

<b>Chapter Three: Dielectric properties of biological materials.....</b>	<b>14</b>
3.1-Introduction.....	14
3.2-Dielectric dispersion in tissues.....	15
3.2.1-Conductivity.....	15
3.2.1.1-Losses due to Maxwell-Wagner processes.....	15
3.2.1.2-Losses due to polar structures.....	16
3.2.1.3-Losses due to water content.....	16
3.2.2-Permittivity.....	16
3.2.2.1-Alpha dispersion.....	17
3.2.2.2-Beta dispersion.....	18
3.2.2.3-Gamma dispersion.....	18
3.2.2.4-Delta dispersion.....	18
3.3-Concluding remarks.....	19
<b>Chapter Four: Fundamentals of Electromagnetic analysis of the interaction between human head and cellular phone.....</b>	<b>21</b>
4.1-Introduction.....	21
4.2-Literature review.....	21
4.2.1-Experimental investigation.....	22
4.2.2-Theoretical investigation.....	22
4.2.2.1-Analytic methods.....	22
4.2.2.2-Numerical computation methods.....	23
4.2.2.3-FDTD based studies of the problem.....	24
4.3-Considerations about the current conditions of the research in the subject.....	28
4.3.1-General aspects.....	29
4.3.2-Frequency dependent aspects.....	29
4.3.3-Theory-experiment relationship.....	29
4.3.4-Numerical (FDTD) Models of the head.....	29
4.3.5-Data on the values of tissues's dielectric constant.....	30
4.3.6-Results and discussion.....	30
4.4-Human head radio-handset interaction problem at the 1.9 GHz.....	30
4.4.1-Goals, methodology and plan of study.....	30



4.4.2-Programming aspects.....	31
4.4.3-Analysis of the isolated radio-handset.....	33
4.4.3.1-FDTD preliminary calculations.....	34
4.4.3.2-Antenna modeling.....	36
4.4.3.3-Thin wire modeling.....	36
4.4.3.4-Field components modification in the proximity of the wire .....	36
4.4.3.5-Source modeling.....	38
4.4.3.6-Limitations associated with thin wire modeling.....	39
4.4.3.7-Impedance calculation.....	40
4.4.3.8-Calculation of radiation pattern and efficiency.....	40
4.4.4-Typical results for analysis of isolated antenna-box system.....	41
4.4.5-Problems in the analysis of the head handset system.....	42
4.4.5.1-Effects of the radiating system on the Head.....	43
4.4.5.2-Effects of the head on the antenna performace.....	43
4.4.5.3-Limitation of the FDTD modeling of the round objects.....	44
4.5-Conclusions.....	45
<b>Chapter Five: Experimental aspects, measurement methods and considerations.....</b>	<b>46</b>
5.1-Substituting materials.....	46
5.2-Tissue substituting materials.....	46
5.2.1-Solid Mixtures.....	47
5.2.2-Liquid Mixtures.....	47
5.3-The real human head and its models.....	48
5.3.1-Real head.....	48
5.3.2-FDTD model.....	49
5.3.3-Phantom model.....	49
5.3.4-Summary of heads characteristics.....	50
5.4-Measurements.....	52
5.4.1-Impedanc measurement.....	52
5.4.2-Radiation pattern measeurement.....	52
5.4.2.1-Radiation pattern measuring system.....	53
5.4.2.2-Distance requirement.....	54

5.4.2.3-Radiation pattern measuring setup.....	55
<b>Chapter Six: Numerical and Experimental results.....</b>	<b>56</b>
6.1-Introduction.....	56
6.2-Problem definition.....	56
6.3-Preliminary considerations.....	57
6.3.1-Head model.....	57
6.3.1.1-Dielectric constants of the tissues.....	57
6.3.1.2-Anatomic head.....	58
6.3.1.3-Developing a relevant head model.....	58
6.3.2-Calculation of the average dielectric properties of homogeneous models.....	60
6.4-Component concentrations in a liquid filled phantom model.....	61
6.4.1-Error estimation for dielectric constant of the liquid mixture.....	62
6.5-Impedance and radiation patter results.....	63
6.5.1-Isolated radio-handset.....	63
6.5.2-Radio-handset in the presence of the human head model.....	71
6.5.3-Effects of the head on the radiation pattern and input impedance.....	74
6.5.3.1-Effects on the radiation patterns.....	74
6.5.3.2-Effects of the head on the input impedance.....	76
6.5.4-Experimental verification of the results.....	78
6.6-Results of SAR calculations.....	81
6.6.1-Peak of SAR in different tissues.....	81
6.6.2-Effect of the neck on the peak of SAR.....	84
6.6.3-Homogeneity versus heterogeneity.....	84
6.6.4-Effect of head size on the Peak of the SAR.....	87
6.6.5-Power absorbed and radiation efficiency.....	87
<b>Chapter Seven: Discussion and Conclusion.....</b>	<b>89</b>
7.1-Introduction.....	89
7.2-Input impedance.....	89
7.3-Radiation patterns.....	90
7.4-Specific Absorption Rate (SAR).....	90

7.5-Radiation efficiency.....	91
7.6-Difficulties and factors influencing these studies.....	92
7.7-Values of the simple head models.....	92
7.8-Issues for future research.....	93
<b>Bibliography.....</b>	<b>94</b>

# **Chapter 1**

## **Introduction**

This is a short introduction to a large subject. The brevity is justified by the fact that this will serve to open a thesis, and hence only the framework issues are dealt with.

### **1.1 Importance of this research topic**

The problem of the interaction between a radio-handset and its user is of interest and importance from different points of view and at different levels, namely that of a single user, of the public, governmental bodies responsible for radiation protection, industries producing equipment, and of research laboratories. A careful study of the interaction problem would be achievable through a multidisciplinary or even an interdisciplinary project, coordinating researches of related disciplines, compiling, interpreting, and circulating the results among them to be used in further research. Among the disciplines involved in the study are epidemiology, physiology, biophysics, and bioelectromagnetics. Contribution of each discipline is explained briefly in the second chapter.

### **1.2 Objects of the study**

The general objects of an electromagnetic analysis of the interaction between the radio-handset and its operator are explained in the second and fourth chapters. Briefly, by this analysis, one may find the effects of the head on the performance of the radio-handset on one hand and the level of deposited EM power in the head on the other hand. The first effect is quantifiable by determination of the changes in the radiation pattern of the radio-handset and of its input impedance in the presence of the user with respect to the case of the isolated radio-handset. The second effect is expressed quantitatively by using the SAR (Specific

Absorption Rate) which considers both the E field distribution and the biological matter's ability to transform it to heat, in a simple relation:  $SAR = \sigma |E|^2 / \rho$

In addition to the above mentioned general objects, this study is based on some other considerations too, which encompass the working frequency, the models of the head, and the method of analysis. The working frequency is 1900 MHz, for which there are not enough studies in spite of its importance. Simple models of the head with an adjustable degree of heterogeneity have been targeted from the beginning.

### **1.3 Methodology used in the research**

Chapter four reviews what has been done by other researchers until now using different methods. As it is explained in that chapter, the method of FDTD (Finite Difference Time Domain) is the most relevant method of analyzing the head handset interaction problem. This is mainly due to the fact that the human head is a geometrically complex object with a heterogeneous dielectric constant. Our modeling is based on the FDTD method. A simple metallic box model of handset has been considered which a  $\lambda/4$  monopole antenna is mounted on its top, and regarding the human head, four models have been used, named NHN (Nonhomogeneous Head with Neck), NH (Nonhomogeneous Head), HN (Homogeneous Head with Neck), and HS (Homogeneous Spheric head) models. In SAR calculations all four models have been studied while for impedance and radiation pattern calculations just the HS model has been used. These models are mathematically expressible and hence the related code is adaptable to different cell sizes. In addition they are readily upgradeable to include the most important geometrical features of the head. The real value(s) of these models are discussed in chapter seven (conclusions).

### **1.4 Thesis Outline**

Chapter two explains the following subjects: various aspects of the interaction of EM radiation with biological matter, various ways of classification; far field exposure versus near field exposure, or equivalently, interaction with negligible or without coupling versus interaction with (high) coupling; methods of study of the interaction problem considering related disciplines (such as EM analysis method), their methodology and contribution. This chapter contains some information about radiation protection standards.

Chapter three studies the dielectric behavior of biological matter using physical principles to give an insight useful in choosing among the data sources of dielectric constant values which are conflicting in some cases. Variation of conductivity and permittivity for selected tissues, both of high and low water content have been provided as relevant curves on a wide band of frequencies.

Chapter four considers the fundamentals of the EM analysis of the interaction between the human head and the radio-handset. The chapter contains a study of what has been done by other researchers, first experimental studies and then theoretical ones such as analytical methods and various numerical methods including FDTD, considerations about the current conditions of the research in the subject. The chapter then considers “human head radio-handset interaction problem at 1.9 GHz” by discussing the goals, methodology and plan of this study. This section presents the formulation used in our analysis and related details of modeling.

Chapter five reviews briefly experimental aspects, measurement methods and considerations, and includes tissue substituting materials systems, solid mixtures and liquid mixtures, some aspects of the real head versus the FDTD model of the head and the phantom model which is used in measurements, and continues with the method of measuring the input impedance of the antenna and its radiation patterns of it with required equipments and setups.

Chapter six presents numerical and experimental results and includes a definition of the problem to be analyzed; preliminary calculations, both FDTD related and head model ones; validation of the code; results of input impedance calculations in the (0-6 GHz) frequency band in two cases of radio-handset and head-handset; results of radiation pattern calculations in the above two cases at 1.9 GHz; experimental verification of the input impedance and radiation patterns; SAR calculations in four different models of NHN, NH, HN, and HS, information concerning the parameters of related calculations, head model calculations, the results obtained, input impedance, radiation pattern in two cases of isolated radio-handset and head-handset, SAR and efficiency calculations.

Chapter seven considers concluding remarks, and contains some points about what should be done in continuing the study.

### **1.5 Contributions and results**

This work presents a rigorous study of the interaction of human head with a radio-handset at 1900 MHz using simple heterogeneous and homogeneous models of the head and the FDTD method of analysis.

In order to study the effects of the head on the radio-handset, antenna performance characteristics (input impedance and radiation patterns) have been calculated theoretically and then measured experimentally in two cases of isolated radio-handset and head-handset system. Regarding the effects of the radio-handset on the head, spatial peak values of the SAR in four different head models have been calculated. The head model used in impedance and radiation pattern calculations was a simple homogeneous spherical model of 10 cm radius. A distance of 2 cm between the head and the source point of the antenna was considered, which seems to be reasonable. At this distance, the effect of the head on the impedance was just a small decrease in the centre frequency. But the radiation pattern indicates losses at various angles up to 27 dB. SAR calculations are based on four different homogeneous and heterogeneous models and give the values of spatial peaks of the SAR as a function of the distance between the head and the source point of the radio-handset from 15 mm up to 50 mm. In this series of calculations the effects of heterogeneity, the head size, and of adding the neck to the model were studied. Calculations indicate that adding the neck reduces the peak of the SAR by 5%, and by reducing the radius of the spherical section of the head and the radius of the neck model by 10% an increase amounting to the same 5% will result in the peak of the SAR. That means two compensating effects in the above two changes.

In our calculations, the effect of the ears was not considered, a problem that may have a noticeable effect on the peak SAR value. This aspect should be considered in future work on these models.

Regarding the reliability of the results on the peaks of the SAR, one may add that, comparing with the results by other researchers our values are acceptable. For example, in our cal-

calculations on the NHN model, the peak value of the SAR at a distance of 17 mm is 1.54 W/kg, while in the case of Gandhi, [15], the same value of the peak SAR has been obtained at a distance of 13.8 mm between the head and source point of the handset. Our results have been compared with those of Gandhi, because the values of dielectric constants used in both calculations are the same. In our case the value of the SAR for the distance of 13.8 mm has not been calculated, and for this reason the above comparison is based on the distance for which the same value of SAR has been obtained.



## **Chapter 2**

# **General considerations on the interaction of EM radiating systems and biological objects**

### **2.1 Introduction**

At the beginning of a research on a subject such as human head radio handset interaction, there is no easy and straightforward point of departure. This is due to the fact that the subject is situated at the heart of a network of problems, approaches, methods and disciplines. Some of these problems are more general than our subject and involve methods and approaches which are used as a basis of our research. Some others are at the same level of complexity and generality and have mutual relations with our problem so that they influence it and are being influenced by its related results. Finally, the third group are those problems that together constitute the topic of this work and they may be considered as the starting point. They are more specific problems and their complexity is within acceptable limits. From the viewpoint of the subject under study the first group of problems can be called generalized problems, the second ones co-problems and the third ones generated problems. This categorization will be used as part of the definition of the subject by pointing generalized problem(s) and generated problem(s).

#### **2.1.1 *Generalized interaction problem***

In this category, the subject of "biological object EM radiating systems interaction" fits very well. It is a rich domain of studies including, epidemiological, physiological, biophysical, EM engineering studies. In addition, it involves subjects such as exposure standards and safety guides, dosimetry and so on.

### **2.1.2 Generated problems**

As a category, the problem of "human head radio handset interaction" has two basic sub-problems, first, "the effects of human head on the performance of the radio handset", and second, "the effects of EM field of the radio handset on the head". In the following, it will be noted that both of these subproblems require the same method of analysis. Hence, methodologically it is an electromagnetic analysis of the interacting system composed of the human body's model and the EM radiator. Our study begins with the subject of the interaction of EM radiating systems and biological objects.

### **2.2 EM radiating systems biological objects interaction**

Electromagnetic energy, today, is one of the most important forms of energy whose presence and role is very complex in the modern life. This complexity is due to the fact that on the one hand, its presence is inevitable at all levels of private and public life and, on the other hand it is always accompanied with biological hazards. Use of EM energy is accompanied with an environmental pollution, for the majority of cases, or leads to a direct near field exposure on the user in some other cases. Designing and application of the EM energy related equipments, in addition to technical aspects, should be based on a sufficient information about the their interaction with living organisms.

### **2.3 EM radiation bioeffects: Disciplines and contributions**

When a biological object is under exposure of an EM wave, it absorbs EM energy from the field. This absorption may result in biological effects. The nature and level of these effects depend on several factors. A complete study of the matter is an interdisciplinary subject which should consider various aspects of the bioeffects of EM fields. This implies a close cooperation between workers in related fields. The most important aspects mentioned regularly in the literature are Epidemiological, Physiological, Biophysical and Electromagnetic aspects. Evidently each discipline brings with itself its own interests, viewpoints and methodology to the field. Objects of such a study includes obtaining a clear picture of EM biohazard under various circumstances, establishing necessary safety standards, evaluation

of EM field penetration into the body in different situations and so on. Various references contain information about Epidemiological, Physiological, Biophysical, and Electromagnetic approaches [1-13]. Naturally among the disciplines considered, the biophysical approach is closer to electromagnetic approach and in the following these two approaches will be considered briefly.

### **2.3.1 Biophysics**

The object of the biophysical approach to the problem is to provide us with a clear picture of the relation between the physical interaction mechanisms underlying and controlling the interaction of electromagnetic fields with biological systems, on the one hand, and specific experimentally supported biological effects, on the other hand. This approach requires a careful consideration of the involving factors each of which has its own peculiarities. The most important of these factors are the EM field, the human body, the biological effects and the physical interaction mechanisms. A brief consideration of them will be given in the following. Here emphasis is on methodological aspects, not on the details of findings.

**EM field-**The electromagnetic field is composed of E (electric) and B (magnetic) fields, each being specified using two parameters for amplitude and frequency. To the extent that the EM field biological matter interaction, in the context of our work, is concerned, the magnetic field has no important effect. Concerning the electric field bioeffects, amplitude and frequency should be considered separately. As far as the amplitude is concerned, the intensity of the external electric field and the permittivity distribution of the matter determine the local electric field as the final measure of the E field bioeffect. This local field is controllable choosing the relevant intensity of excitation and considering the established exposure standards. But as far as the frequency is concerned, the picture is not so simple. In fact with changing frequency we may find a vast extent of behavior of the EM fields in their interaction with matter, including biological ones. This is mainly because of two important points. First, the mechanism of energy transfer of an EM field in the transmitting medium is frequency dependent. Second, in the higher frequencies the quantum nature of EM radiation will be more important. Regarding the first point, it should be noted that, in the static case (electrostatic or magnetostatic fields), and in the extremely low frequency (ELF) fields the energy transfer mechanism is essentially nonradiative. In the higher frequency bands, energy transfers via the radiative mechanism. Concerning

the second point, with raising frequency the energy of photons will rise to an extent that may be sufficient to do some chemical changes, including ionization, in the structure of macromolecules in biomatters. Here, it may be helpful to review rapidly the ionization effect of EM radiation.

### **2.3.2 Electromagnetics**

#### **2.3.2.1 General aspects**

Electromagnetic theory is a macroscopic theory which can provide us with the distribution of E and H fields in a specified region of space under various conditions, knowing the necessary information concerning the EM field source, the distribution of dielectric constant, the magnetic permeability and electric conductivity of matter in the region and the existing boundary conditions. These parameters should be described macroscopically, otherwise the problem will become practically intractable. Then, having E and H distributions in the matter, we can easily find power deposited per volume.

This picture is evidently not complete and there are other aspects, which should be considered. Really, to the extent that macroscopic electromagnetic theory is concerned this problem is essentially a scattering problem. But if we consider that here the scatterer is basically a living organism interacting with the EM field and therefore a site of coexistence for some EM field induced physical interaction mechanisms and a vast amount of biological and physiological processes which should not be influenced seriously, then we will be able to realize that an EM engineer should go very far away from the traditionally frontiers of macroscopic EM theory.

Using EM methods to analyse human body and EM radiating system interaction means solving Maxwell's equations under the conditions described above. The method of solution may be analytical or numerical. Normally analytical methods are suitable when we need some general results in which the inclusion of the details of the model is not so important. In these cases simple models may be sufficient. Regarding geometrical complexity of biological objects, diversity of their dielectric properties and complexity of the EM radiating systems utilized in the bioelectromagnetics applications, using numerical techniques to characterize and quantify EM field interactions with biological objects, is not only desirable, but essential. Numerical methods, too, have their own specific features, for example,

they heavily rely upon computer resources.

This aspect along with precision requirements impose some limitations. Normally one has to make a trade-off to arrive at an acceptable result. The study of physical parameters of body organs in different frequency bands, the lack of information and the discrepancies in the reported data constitute another dimension of the difficulties encountered in bioelectromagnetics. Any research in this area should be started with a careful consideration of these aspects.

### *2.3.2.2 Electromagnetic analysis of Human body radiating systems interaction*

Having studied briefly the contribution of some disciplines involving the interaction between the human body and radiating systems and having reviewed some general aspects of electromagnetic theory related to this area, the time has come to consider the contribution of this theory to a solution of the problem. This contribution has two sides, theoretical studies and experimental studies as follows.

#### *Theoretical studies*

*Effects of radiating systems on the body-* The object of this type of study is to calculate the EM field distribution and power deposition in the human body under various conditions. Depending on the problem and considering the source, the body and the distance between them, the problem can be treated as a far field exposure problem or a near field exposure one. In the far field exposure calculations one uses a planar model for the EM wave while in the near field calculations the shape of EM field may be very complicated. From the beginning of these types of studies the researchers have used various calculation methods and different models of the human body. Today with the developments of numerical methods in electromagnetics they are able to obtain more precise results even for more complicated models having a relatively high degree of heterogeneity. The FDTD method is being used regularly for this type of investigations because of a series of advantages to be discussed later.

*Body effects on radiating systems-*This aspect too represents an important application, because design and performance prediction for systems which should work in the vicinity of human body are based on the results of such studies. Among these systems, personal radio

handsets and medical applicators for hyperthermia should be mentioned.

### *Experimental studies*

Experimental studies have a complementary role to the theoretical ones. Sometimes they are used as a verifying method for the results obtained in theoretical calculations and modeling and in some cases these studies are the sole method of gaining information and estimation at least in the first phases of investigations. Among them are designing and performing experimental and measuring setups to evaluate field quantities in situations under study. Some examples are: measuring EM leakages from various equipments, measuring EM field in phantom models, and measuring environmental EM pollution. In order to perform these studies some preparatory investigations and experiments are needed regularly such as measuring dielectric constants of biological materials, providing relevant phantom models using suitable artificial dielectrics, and designing more effective probes and other related field sensors.

## **2.4 Radiofrequency field exposure standards**

In an attempt to assess the many and varied biological effects reported in the literature and to identify effects pertinent to a health risk assessment, a number of national and international agencies have provided detailed literature reviews that could form a data base for the development of human RF exposure standards. Reviews of RF bioeffects literature have been produced for example by the World Health Organization (WHO, 1981) by the American National Standards Institute (ANSI, 1982) and by the International Radiational Protection Association (IRPA, 1984). The WHO (1981), and ANSI (1982), and other reviews and literature were used to develop the IRPA (1984) guidelines, and more recent literature and other national standards were used to draft the updated IRPA (1988) guidelines. The International Non-Ionizing Radiation Committee of IRPA has published a revision of its 1984 guideline (IRPA 1988). In this document, as in its preceding document (IRPA 1984), the threshold limit exposures on which the basic limits was derived is: 0.4 W/kg for whole-body exposure to RF field

**Table (2.1) "IRPA occupational exposure limits to radiofrequency fields"**

Frequency (MHz)	unperturbed RMS Field strength		equivalent plane-wave power density (peq)	
	Electric E (V/m)	Magnetic H (A/m)	W/m <sup>2</sup>	mW/cm <sup>2</sup>
>0.1-1	614	1.6f	-	-
>1-10	614/f	1.6/f	-	-
>10-400	61	0.16	10	1
>400-2000	3 f <sup>1/2</sup>	0.008f <sup>1/2</sup>	f/40	f/400
>2000-300,000	137	0.36	50	5

"IRPA occupational exposure limits to radiofrequency fields" is reproduced here in Table (2.1) above. Table (2.2) indicates the "IRPA general public exposure limits to radiofrequency fields".

**Table (2.2) "IRPA general public exposure limits to radiofrequency fields"**

Frequency (MHz)	unperturbed RMS Field strength		equivalent plane-wave power density (peq)	
	Electric E (V/m)	Magnetic H (A/m)	W/m <sup>2</sup>	mW/cm <sup>2</sup>
>0.1-1	87	0.23/f <sup>2</sup>	-	-
>1-10	87/f <sup>2</sup>	0.23/f <sup>2</sup>	-	-
>10-400	27.5	0.073	2	0.2
>400-2000	1.375 f <sup>1/2</sup>	0.0037f <sup>1/2</sup>	f/200	f/2000
>2000-300,000	61	0.16	10	1

#### **2.4.1 Standards related to the mobile communication technology**

To the extent that mobile communication technology is concerned The IEEE has approved various exposure guidelines, among which one should mention the 1982 guideline, and its more recent replacements of 1991 and 1992 [59]. For low-powered devices such as cellular telephones, that are used in 'uncontrolled' environments, ANSI/IEEE C95.1-1992 recommends a specific absorption rate (SAR) as averaged over one gram of tissue of 1.6 W/kg.

Table (2.3) shows the limits recommended for low power devices by ANSI/IEEE C95.1-1992.

**Table 2.3 ANSI/IEEE C95.1-1992 Limits for low power devices.**

	<i>Controlled environment</i>	<i>Uncontrolled environment</i>
Average SAR (100 KHz - 6 GHz)	<0.4 W/kg (whole - body) =<0.8 W/kg (partial - body)	<0.08 W/kg (whole - body) =<1.6 W/kg (partial - body)
Radiated Power (100 KHz - 450 MHz)	7.0	1.4
Radiated Power (100 KHz - 1500 MHz)	7. (450/f)	(1.4).(450/f)



## Chapter 3

### Dielectric properties of biological materials

#### 3.1 Introduction

The bulk electrical properties of biological materials have been of interest for many reasons for over a century. The dielectric properties of tissues are needed for the calculation of the internal electric fields resulting from exposure to nonionizing EM fields, and are thus important in the development of communication equipments, diagnostic and therapeutic medical applications of this energy and studies of potential EM biohazards. Dielectric properties of biological materials other than tissues are important in developing applications of EM fields in a variety of areas, e.g., food processing, other agricultural purposes, and drying of various products. On a more fundamental level, study of these properties gives important information about possible mechanisms by which external fields can produce effects in an organism. A vast amount of research has been conducted in recent decades to develop the computer-controlled instrumentation for precise and rapid measurements of dielectric properties, and a greater understanding of dielectric phenomena in tissues and other complex materials.

Studying the radio-handset human head interaction, too, demands a good understanding of the dielectric properties of biological materials under various conditions. To the extent that EM field biological objects interactions are concerned there are some important points to be considered. These considerations are reflected in the data on the dielectric constant in the literature, [2,16-20], as follows:

- *Dependence of the dielectric constant of the biological materials on living conditions (in vivo, in vitro)*

- *The change with frequency, temperature, and physiological conditions of the living tissues*
- *Lacking of sufficient informations on some organs in some of the frequency bands*
- *Differences among the related data reported in the literature*

The above points sometimes makes the task of choosing among the data and deciding on a reasonable plan of study a demanding and critical task. In this chapter these properties are briefly reviewed, basic responsible mechanisms of the observed properties are considered and relevant data needed in the next chapters are supplied. These data, and an understanding of the mechanisms, are the starting point for widening the scope necessary for precise modeling of the biological object under EM exposure or analyzing the claims of related biological effects

### **3.2 Dielectric dispersion in tissues**

In this section we consider the variations of complex permittivity of tissues. Our considerations here are based on two points. First, we concentrate our study on the UHF and the Microwave bands of frequencies. This is due to limitation of space in this chapter on the one hand and to our interests in these frequency bands in later chapters. Second, while the changes in conductivity with frequency are coupled to changes in permittivity by the Kramers-Kronig relations, it is instructive to consider the conductivity separately, with reference to dielectric mixture theory.

#### **3.2.1 Conductivity**

Conductivity at frequencies above  $100\text{MHz}$ , the conductivity reflects increasingly large contributions from relaxation effects. Three possible mechanisms can be identified.

##### *3.2.1.1 Losses due to Maxwell-Wagner processes*

A Maxwell-Wagner process means interfacial polarization of the electrolyte and relatively nonconducting protein molecules. Assuming appropriate values for the electrical properties of the electrolyte and protein in a typical tissue, relevant equations [21], predict increases

in conductivity of a few hundredths of a millisiemens per meter with a mean relaxation frequency of about 300 MHz. This was suggested as a minor contribution to the dielectric relaxation in barnacle muscle at frequencies between 0.1 to 1 GHz.

### *3.2.1.2 Losses due to polar structures*

A class of losses originate in the dielectric loss of small polar molecules and polar sidechains on proteins. The principal relaxation range of protein molecules is in the low megahertz range; but by virtue of their small size, single amino acids and polar sidechains of protein molecules can undergo a dielectric relaxation at much higher frequencies. In view of the proportionality of the total increase in conductivity to the mean relaxation frequency, such a relaxation process can contribute observably to the loss above 100 MHz even though the corresponding changes in permittivity might be small.

### *3.2.1.3 Losses due to water content*

Dielectric relaxation of water. Pure water exhibits a dielectric relaxation that is nearly characterized by a single time process with relaxation time of 8 psec, corresponding to a relaxation frequency at 20 GHz at 25 C. Consequently, its conductivity will rise approximately quadratically with frequency below the relaxation frequency. For typical high water content tissues, this increase in conductivity becomes comparable to the ionic conductivity at 3 to 5 GHz. Moreover, the conductivity of tissues and protein solutions will include a contribution from dipolar relaxation of the water of hydration, which exhibits a relaxation frequency an order-of-magnitude or more below that of bulk water. It appears that in barnacle muscle tissue, the contribution to the total conductivity, and dipolar relaxation of motionally restricted water, ionic conductivity, and dipolar loss of bulk tissue water are all of roughly comparable magnitude at about 3 to 5 GHz, although the uncertainties in separating the contributions from "bulk like" and motionally altered water are quite large.

## **3.2.2 Permittivity**

Typically, soft tissues exhibit a continuous monotonic decrease in permittivity with frequency, together with an associated increase in conductivity. Permittivity values can exceed  $10^5$  to  $10^6$  at subaudio frequencies and can be expected to reach limiting values of 4

to 5 at frequencies approaching 100 GHz. Three major dispersion regions can be identified (fig 3.3), that would correspond to separate relaxation processes with total dielectric increments,  $\Delta\epsilon_\alpha$ ,  $\Delta\epsilon_\beta$ , and  $\Delta\epsilon_\gamma$ , respectively.

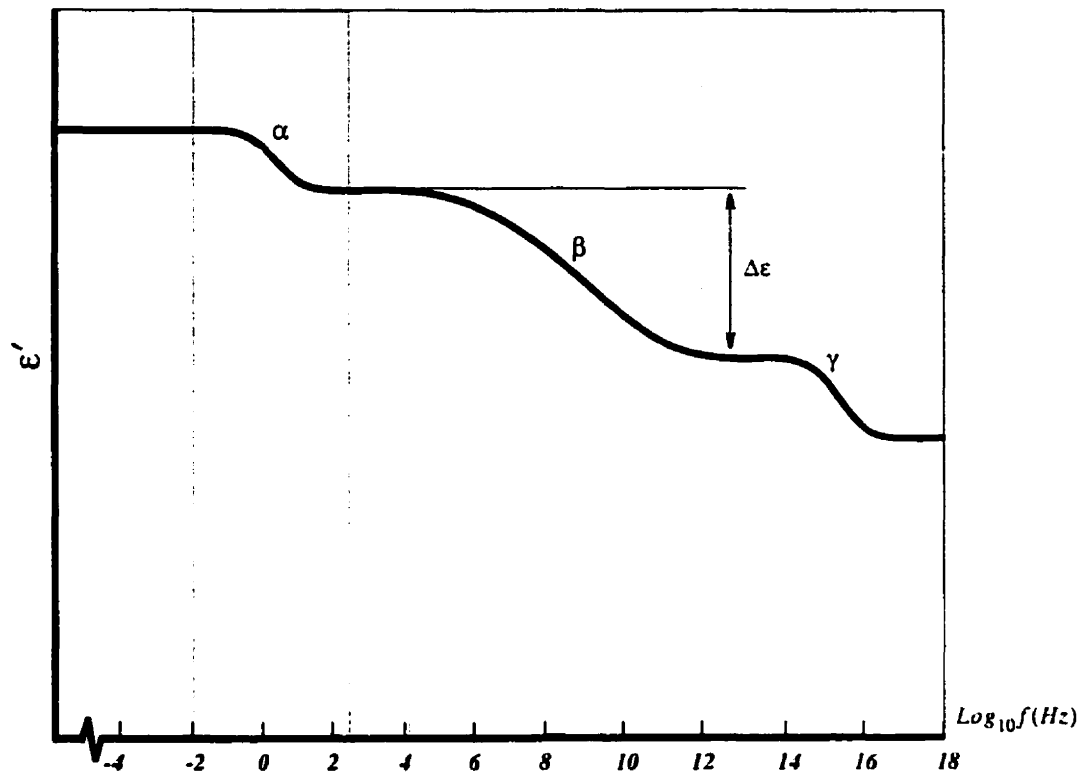


Figure 3.3- The variations of  $\epsilon'$  with frequency for various dielectric dispersion processes

### 3.2.2.1 Alpha dispersion

The alpha dispersion is manifested by the very large increase in permittivity at audio frequencies. In this frequency range, large permittivity values are produced by ionic diffusion processes in micron and larger sized objects; such effects must be presumed to occur in tissues as well as these low frequencies. Other possible low frequency polarization mechanisms that are specific to individual tissues would included active membrane conductance phenomena, the charging of intracellular membrane-bound organelles that connect with the outer cell membrane, and perhaps a frequency dependence in the membrane impedance itself. For a total dielectric increment  $\Delta\epsilon$  of  $10^6$  and relaxation frequency of 100 Hz, the in-

crease in conductivity is expected from the Kramers-Kronig relations to be roughly 0.005 S/m, which is negligible compared to the ionic conductivity of most biological preparations.

At these low frequencies the tissue impedance is overwhelmingly resistive in spite of the tremendous permittivity values that are measured. Consequently, for the engineering applications, the alpha dispersion is of little significance.

#### *3.2.2.2 Beta dispersion*

The beta dispersion occurs at RF due principally to the capacitive charging of cellular membranes in tissues, although smaller contributions are also expected from dipolar relaxation of proteins in the tissue. Blood exhibits a total dielectric increment  $\Delta\epsilon_\beta$  of 2000 and a  $\beta$  relaxation frequency of 3 MHz, and consequently a total conductivity increase of roughly 0.4 S/m of which by far the largest part is due the increase in the volume fraction of the suspension that is available to conduction, i.e., the intracellular as well as extracellular spaces. For tissues, the total change in permittivity through the beta dispersion approaches  $10^4$  relative to free space, and the relaxation frequency is about 500 KHz.

#### *3.2.2.3 Gamma dispersion*

The gamma dispersion occurs with a center frequency near 25 GHz at body temperature, due to the dipolar relaxation of the water that constitutes 80% of the volume of most soft tissues. For a total dielectric increment  $\Delta\epsilon_\gamma$  of 50 (typical of soft tissues containing 80% water) and relaxation frequency of 25 GHz, the total increase in conductivity is about 70 S/m.

#### *3.2.2.4 Delta dispersion*

In addition to the above three major dispersion regions, there is a smaller, rather poorly defined delta dispersion in the range of 0.1 to 3 GHz, for which no single, dominant relaxation process has been identified. In tissues, the total observed changes in relative permittivity between 0.1 and 1 GHz are typically in the 10 to 20 range relative to free space, with associated increase in conductivity of 0.4 to 0.5 S/m. This is presumed to arise in part from the dipolar relaxation of water of hydration, and in part from rotational relaxation of polar

sidechains, and possibly also from ionic effects of the Maxwell-Wagner type or counterion diffusion along small regions of charged surfaces. The lack of a single, dominant mechanism makes the analysis of this dispersion region in tissues rather difficult.

### 3.3 Concluding remarks

The calculations needed to analyse the interaction of an EM system with biological matter finally involve a series of values to be regarded as dielectric constants of related tissues at the working frequency, In reality one should consider some theoretical facts based on physical principles and some global insight concerning the behaviour of dielectric constants of tissues in a sufficiently wide band of frequencies around the working frequency. Considering these aspects the researcher would be able to do the following steps.

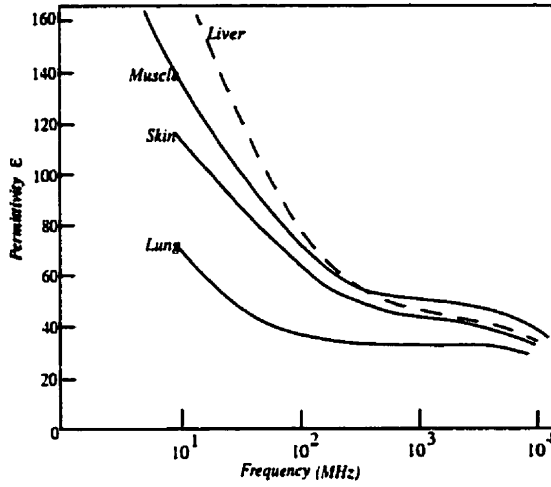
- Choose the relevant values for dielectric constant among the existing sources
- Interpolate and extrapolate the dielectric constants at other frequencies to obtain the required values at the working frequency

Regarding the first point one should consider for example that the real part of the dielectric constant is a monotonically decreasing function of frequency. This implies a rule for any given tissue as:

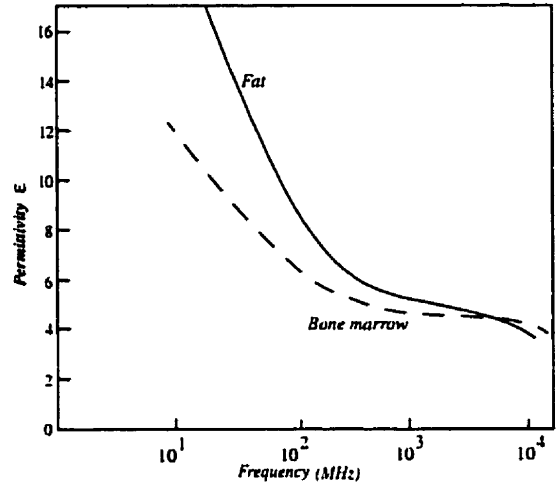
$$\epsilon_{tissue}(f_1) \geq \epsilon_{tissue}(f_2) \quad (2-1)$$

where  $f_2 \geq f_1$ . Figure (3.4) show the global behaviour of some selected tissues, both with low and high water content.

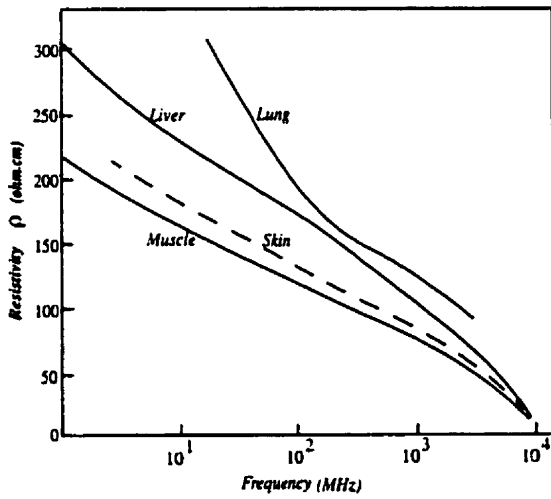
Regarding the second point researchers have conducted studies about parametrization of media dispersive properties, such as dielectric properties of biological matter, Mrozowski, M. and Stuchly, M.A. [23].



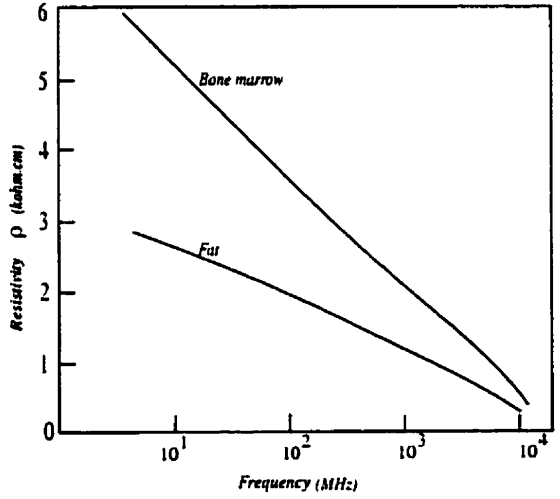
(a): Permittivity  $\epsilon$  of some typical tissues of high water content



(c): Permittivity  $\epsilon$  for fat and bone marrow



(b): Resistivity  $\rho$  of some typical tissues of high water content



(d): Resistivity  $\rho$  for fat and bone marrow

**Figure (3.4)** Dielectric properties of some selected tissues of high and low water content, [22]

## **Chapter 4**

# **Fundamentals of electromagnetic analysis of the interaction between human head and cellular phone**

### **4.1 Introduction**

This chapter analyses a system composed of a cellular phone and head, from an electromagnetic theory point of view. To situate it in the context, a review of the works which have been reported in the literature, together with a comparison of related methods, will be given. Then the important points which motivated this study will be mentioned and our method of choice will be justified. An analysis of the problem along with the relevant formulation regarding the different parts of calculations will follow.

### **4.2 Literature review**

Research on the subject of interaction of radiotelephone operator with EM fields interaction goes back to at least three decades ago. At that time, numerous investigations have been conducted with mainly experimental studies. Theoretical studies based on analytical methods and simple models of the head started later. With the advances in the computer technology, which promoted research and advancements in numerical methods, another approach based on computer simulation and using more sophisticated models arose. Today, one sees a coexistence of various approaches and methods used by researchers around the world. Among these approaches, the numerical computation using the FDTD method has shown a high degree of accountability, so that it may be considered as the canonical approach to the problem where a high degree of accuracy in the results is required. Before



considering what the researchers have done using the FDTD method, a rapid review of other approaches is presented below giving samples of ideas and results reported in the literature.

#### **4.2.1 Experimental investigations**

In these studies the temperature rise or the electric field in the head phantoms are measured. For example Balzano et al., [24,25], measured the temperature increase in human head phantoms in the vicinity of a 6 W portable radio antenna at 150 MHz and 800 MHz. Chatterjee et al., [26], measured the electric field in a phantom human body using an implantable probe, the head model being exposed to the EM field from a portable radio transceiver operating at 50, 150, 450, and 800 MHz. Another experimental study reported by Cleveland and Athey [27] dealt with the measurement of the electric field in the head models under exposure from a hand-held radio transmitting at frequencies in the 800 MHz band. In another report Balzano et al., [28], explained a method to quantify the RF exposure of the users of portable cellular phones in terms of SAR, using a robotic system to accurately position an isotropic  $E$ -field probe. They exposed the phantom through a dipole antenna situated very close to its surface. Using the following relation

$$SAR \cdot \Delta t = c \Delta T \quad (4-1)$$

in which  $\Delta t$  is the exposure time (30 sec),  $c$  (2.7 joules/C/g) is the thermal capacity of the simulated tissue and  $\Delta T$  is the temperature increase due to the RF exposure, they found the SAR and, putting it into relation (4-2)

$$SAR = \frac{|E|^2 \cdot \sigma}{\rho} \quad (4-2)$$

where  $\sigma$  is the simulated tissue dielectric loss and  $\rho$  its density, they obtained  $|E|^2$ .

#### **4.2.2 Theoretical investigation**

##### **4.2.2.1 Analytic methods**

Amemiya and Uebayashi, [29], have derived closed-form formula for a homogeneous sphere irradiated by a half-wavelength dipole antenna. They modelled the human head as

a dielectric lossy sphere and then calculated the power deposition inside the sphere by using the theoretical equations. Kamimura et al., [30], based their studies on the theoretical works of Amemiya and Uebayashi, compared actual radiation sources with a  $\lambda/2$  dipole model investigated the impedance variation in the presence of the phantom model, and concluded that the  $\lambda/2$  dipole model is quite useful for describing the exposure of a human head to the incident fields from portable radios. They also added that a correction factor depending on the antenna type might be necessary for more rigor.

#### *4.2.2.2 Numerical computation methods*

Various methods have been described in the literature for numerical calculation of human head radio-handset interaction. The approaches to this problem consist of numerically solving Maxwell's equations in either differential or integral form. These approaches fall into the two categories of time domain or frequency domain methods. The most successful frequency domain method is the method of moments (MOM). However, the MOM requires computer storage and computation time on the order of  $3(N)^2$  and  $3(N)^3$ , respectively, where  $N$  is the number of cells. Numerically efficient algorithms have been developed, but at best, time requirements are reduced to  $N \cdot \log N_2$ , [31], which is still very large for the needed high-resolution methods where  $N$  may be on the order of several thousands to ten thousands. Among the time domain methods are the finite-element and the finite-difference method. In contrast to the MOM method, the finite-difference time-domain (FDTD) method has time requirements proportional to a constant times  $N$  and storage requirements proportional to  $N^{4/3}$  [32]. Even though  $N$  is considerably greater for the FDTD method because of an overhead of free space cells around the body, when bodies of 20 000 cells (cell number in a  $27 \times 27 \times 27$  FDTD space) are contemplated, any method whose resource requirements increases linearly rather than geometrically presents an attractive alternative. The relative advantages of the FDTD method with respect to other numerical methods, specifically for analyzing of a problem such as human head radio-handset interaction, are not limited to time and computer storage aspects. M.F. Iskander has studied, [33], the broader context of applications in bioelectromagnetics and has shown that how these two methods along with the spherical-wave expansion method should be considered as complementary to one another in this highly diverse field. In our case, the complexity of both the geometry and material distribution of the head on the one hand, and the details

needed in the information about the SAR distribution in the head on the other hand, make the FDTD method practically the method of promise.

#### 4.2.2.3 FDTD based studies of the problem

Using the FDTD method in analyzing the human head radiating systems interactions goes back to the first years of this decade. In 1991, Dimbylow, [34], used the method to calculate the SAR distribution in a realistic heterogeneous model of the head for plane-wave exposure from 600 MHz to 3 GHz. His concerns in this study were an enhanced absorption due to resonance in the head, hot spots in the brain, and in higher frequencies the increasingly superficial deposition of energy particularly in the eyes. However their exposure was a uniform plane wave which is not the subject of our study. In fact a more intense local pattern of absorption will be produced by the anisotropic fields from sources close to the head. The same author then considered the calculations of the SAR for a dipole closely coupled the head at 600 MHz and 1.9 GHz in another study, [35]. In this study he calculated the power absorption in the eye using a detailed model of the eye including 4 tissue types and arrived at the SAR as a function of distance between the EM source and the eye surface. Their result for the frequency of 1900 MHz is shown in Figure (4.1)

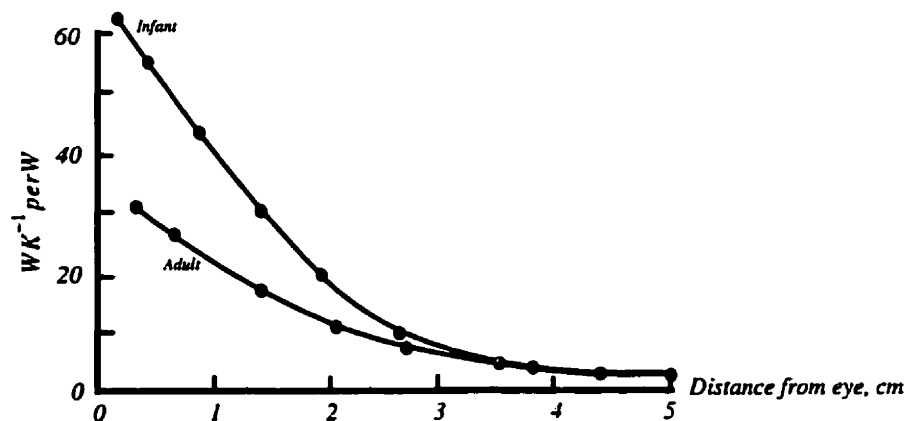


**Figure (4.1)** The SAR averaged over the eye as a function of the separation between the dipole and the surface of the eye at 1.9 GHz, [35].

Toftgard et al., [36], analysed the problem using an homogenous and spherical model of head, a block model of the hand and a box model of the radio-handset at the frequencies of 914 MHz and 1890 MHz. Based on their findings half of the power is absorbed in the hand and head. Most of the absorbed power (96%) is deposited in the head and just (4%) is deposited in the hand. Martens, [37,38], conducted similar studies at 900 MHz, using a MRI (Magnetic Resonance Imagery) based model of the head and for a monopole mounted on a box. Absorbed power ratio reported by Martens is 50%, in [37], and 15%, in [38]. Figure (4.2) shows the effect of the head model on the H plane pattern [37].

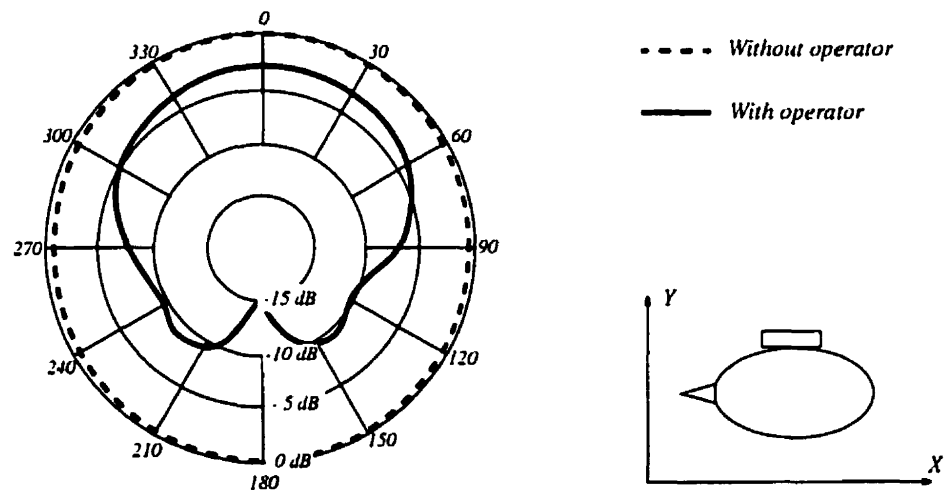


**Figure (4.2)** Far-field radiation pattern with and without the presence of operator, [37].

Jensen and Rahmat-Samii, [14], studied the problem at 900 MHz, using a MRI based model of the head including 5 tissue types and considering four models of antennas and reported an absorption of 48 to 68% of the total power in the head and hand. Hombach and colleagues conducted another study, [39], at 900 MHz using realistic models of the head with different sizes and shapes and models of the internal anatomy. They observed an independence of the SAR properties from the size and shape of models. Regarding the details of the model they observed that although local SAR values depend significantly on local inhomogeneities and electric properties, the volume-averaged spatial peak SAR obtained with the homogeneous phantoms only slightly overestimates that of the worst-case exposure in the inhomogeneous phantoms. Meier, Hombach et al. in a more recent study [40], based on the same methodology at 1800 MHz, used a dipole antenna and a

realistic model of the head. In this study they used the Mafia software package to analyse complex head phantoms. This code based on the finite-integration technique (FIT) is conceptually slightly different from the FDTD technique, but nevertheless results in the same numerical scheme. They concluded that a homogeneous representation of the head is suitable for assessing the maximum specific absorption rate SAR in the head if appropriate parameters are chosen. Figure (4.3) shows SAR profiles obtained at 900 MHz and 1800 MHz, in homogeneous head models.

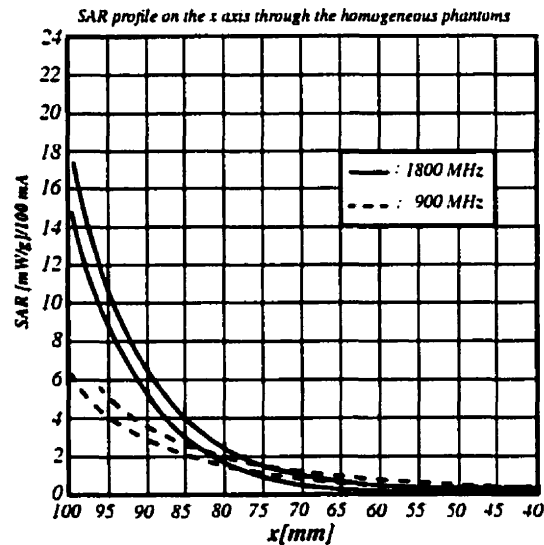


**Figure (4.3)** SAR profiles in homogeneous head models, at 900 MHz, [39], and at 1800 MHz, [40].

Watanabe and co-workers, [41], used a realistic model including the auricle at 900 MHz and 1.5 GHz, although they did not explain how they modeled the auricle considering a cell size of 2.5 mm. As they intended to study the influence of auricles to maximum values of local SAR this aspect seems to be important. They studied also the effects of the antenna size on the maximum local SAR. In the head model they have used the dielectric constant for fat has been considered equal to 4.67 at 900 MHz and 9.70 at 1500 MHz. This does not seem to be correct from the physical point of view, as the dielectric constant of materials should decrease when increasing the frequency. The point is that they used different sources for dielectric constant of tissue types they needed without verifying the compatibility among them at least to the extent that the general theory of dielectrics is concerned. Gandhi et al., [15], worked on the same problem, at 835 MHz and 1.5 GHz, for a  $\lambda/4$  and a  $3\lambda/8$  monopole antennas, with realistic MRI based models of the heads of an adult person, of ten years child and of 5 years child, with resolutions down to 1 mm. They too calculated the

SAR distribution in the head. They observed that using homogeneous models of the head leads to gross overestimations in the results of SAR calculations. Table (4.1) indicates the results they reported regarding head models of an adult male and of a 10 years old child at 1900 MHz.

*Table (4.1) Comparisons for models of an adult and 10-year-old child at frequency of 1900MHz. [15]*

<i>Quantity</i> \ <i>Model</i>	<i>Adult male</i>	<i>10-years-old-child</i>
<i>Peak 1-voxel SAR (W/kg)</i>	3.90	4.90
<i>Peak 1-gr SAR* (W/kg)</i>	1.11 (1.03 g)	0.90 (1.02g)
<i>Peak 1-voxel SAR for brain (W/kg)</i>	0.20 (1.00 g)	0.25 (1.07g)
<i>Power absorbed by head and neck</i>	35.6 %	34.4 %
<i>Power absorbed by head and hand</i>	13.8 %	9.4 %
<i>Peak 1-voxel SAR for brain (W/kg)</i>	0.29	0.42
<i>Time averaged radiated power = 125 mw</i> <i>a <math>\lambda/4</math> antenna above a handset is taken for the calculations</i> <i>* <math>5 \times 5 \times 5</math> cells; <math>0.987 \times 0.987 \times 1.200</math> cm; <math>1.170</math> cm<sup>3</sup> for the adult male</i> <i><math>7 \times 7 \times 4</math> cells; <math>1.057 \times 1.057 \times 0.939</math> cm; <math>1.049</math> cm<sup>3</sup> for the 10-year-old child</i>		

Okoniewski and Stuchly reported another study, [42], at 915 MHz using various boxes, spherical and realistic head models to consider the effects of the head, hand and ear. They reported that the hand holding the handset absorbs a significant proportion of the antenna power output, a proportion which can be considerably decreased by modifying the geometry of the handset metal box. Table (4.2) indicates dependence of power deposition in various models they studied on the separation between the antenna and the head model.

**Table (4.2) Effects of the distance between the antenna and the Head Model; 915 MHz, 1W, [42]**

<b>Model</b>	<b>Separation (cm)</b>	$\eta$ (%)	$P_{abs}(W)$	<b>SAR in the head (W/kg)</b>		
				<b>Peak</b>	<b>1 g</b>	<b>10 g</b>
<b>Homogeneous Box</b>	1.5	16	0.84	18.1	14.1	9.25
	2.0	25	0.75	11.1	8.5	5.6
	2.5	40	0.60	5.7	4.3	3.1
	3.0	51	0.49	3.2	2.6	1.9
<b>Homogeneous Sphere</b>	1.5	46	0.54	13.4	10.9	7.0
	2.0	57	0.43	8.5	6.8	4.6
	2.5	66	0.34	5.5	4.4	3.0
	3.0	73	0.27	3.7	3.0	2.1
<b>Gent Head</b>	1.5	51	0.49	11.2	8.6	4.8
	2.0	57	0.43	7.1	5.6	3.3
	3.0	72	0.28	3.2	2.4	1.4
<b>Yale Head</b>	1.5	60	0.40	3.5	2.65	1.8
	2.0	67	0.33	2.4	1.7	1.4
	2.5	73	0.27	1.9	1.2	0.9
	3.0	77	0.23	1.7	1.1	0.8

### 4.3 Considerations about the current conditions of research in the subject

The above review indicates the most important aspects of the research in the subject and to some extent indicates the complexity of this interaction problem which in its turn has been reflected in the complexities and ranks of the specific research laboratories working on the matter. For this reason, in addition to various research labs. in U.S., Canada, Japan, Switzerland, an European project too is involved in the matter, [37]. In this European project, a multi-disciplinary group of engineers, physicians, and biologists are investigating the link between the fields absorbed in the head of the operator of a wireless and possible health effects. To this one should add the controversy regarding the value different research groups appreciate the models used by other groups, such as disagreement about the value of homogeneous models of human head as indicated above, [39,40,15]. Here the general and specific aspects of the subject as explained above are mentioned to provide at the same time a basis for definition of our research subject and its planing.

### **4.3.1 General aspects**

The most important studies have been done using FDTD method. These studies have been done from the first years of this decade and have essentially concentrated on the 900 MHz band, although some other studies around 1.8 GHz, have also been reported. Present studies are concentrating on finding the SAR values in different conditions and with different head models.

### **4.3.2 Frequency dependent aspects**

Results at higher frequencies can to some extent be different from results at lower frequencies. This is due to the complexity of the interaction problem. For example knowing the value of homogeneous models in assessing the spatial-peak power absorption at 900 MHz, as Meier et al., [40], observed, will not be sufficient to make the same judgement about its applicability at higher frequencies, for example in the frequency band from 1.5 to 2.5 GHz. In this frequency band some tissue layers have a thickness in the range of  $\lambda/2$ - $\lambda/4$ . At higher frequencies the relation between absorption and anatomical details becomes even more complex. To this, one should add the necessity of using more memory space to model the objects under analysis, which leads to the necessity of using supercomputers for studies concerned with frequencies of several GHz.

### **4.3.3 Theory-experiment relationship**

The experimental studies in this field are not solely to confirm the simulation results. They are the best sources of information to guide the workers even in their initial modeling because the head model is neither fixed nor unique. Precise results in these experiments require various elements such as carefully prepared head phantoms, suitable probes and precision positioning. Precise implementing systems to place probes using robots have been reported

### **4.3.4 Numerical (FDTD) Models of the head**

Both MRI based models and geometrically simple models have been used. Both heterogeneous and homogeneous models have been used.



### ***4.3.5 Data on the values of tissues' dielectric constant***

One of the problems that complicates the comparison between the reported results is the vast discrepancy among the values used for the dielectric constants of tissues. To this, one should add the lack of data for some tissues at a specific frequency which may oblige a researcher to use another data source. Sometimes these data are not compatible as indicated above in the case of Watanabe, [41].

### ***4.3.6 Results and discussion***

There are differences on the reported SAR and absorption rates by various researchers and even discrepancy between the results reported by the same researcher on the same quantity, [37,38]. Another problem is the value of a homogeneous model of the head, [39,40,15].

## **4.4 Human head radio-handset interaction problem at the 1.9 GHz**

### ***4.4.1 Goals, methodology and plan of study***

Regarding the potential biohazards of cellular radio handsets and the rapid development of their use, the problem of estimation and evaluation of the related bioeffects has always been a concern to the public, to governmental bodies, companies, and researchers. Commercial producers should satisfy the health regulations and criteria in order to be permitted on the market. These criteria are formulated as worst case maximum SAR in the head of the user. Most studies until now were conducted for a working frequency around 900 MHz and those ones performed at 1900 are limited. Our aim in this study is to investigate the interaction problem using simple homogeneous and heterogeneous head models. In the literature normally the head models are MRI based or in the case of simple ones the models used are a sphere. In this study in addition to use a simple homogeneous spherical head model, simple heterogeneous models containing three tissue types and nasal and mouth cavities are studied. Hence it is possible to develop simple models to assimilate more anatomical aspects of real head and at the same time keep the model mathematically expressible so that it will be applicable with various cell sizes, for example in higher frequencies applications, with little effort. The effects of the head size, adding the neck to the model, effects of heterogeneity on the peak value of SAR in a reasonable head-handset distance are studied.

The head effect of the performance of the radio-handset is studied by calculation of the radiation patterns and input impedance and the radiation efficiency of the handset in absence and in the presence of the simple spherical head model. The effect of the handset on the head is studied using 4 different models, both homogeneous and heterogeneous, to find the average value of the spatial peak of SAR and the total power absorbed in the head.

#### ***4.4.2 Programming aspects***

The code is based on the FDTD program provided in the reference [32] and after its correction and verification by the example available at the end of that reference, relevant subroutines have been developed for near field to far field transformation and SAR calculations. Our near field to far field transformation is a time marching one to calculate the E field components in a far observation point using the surface equivalent theorem. The following section considers the verification of the core and near field to far field transformation of the program.

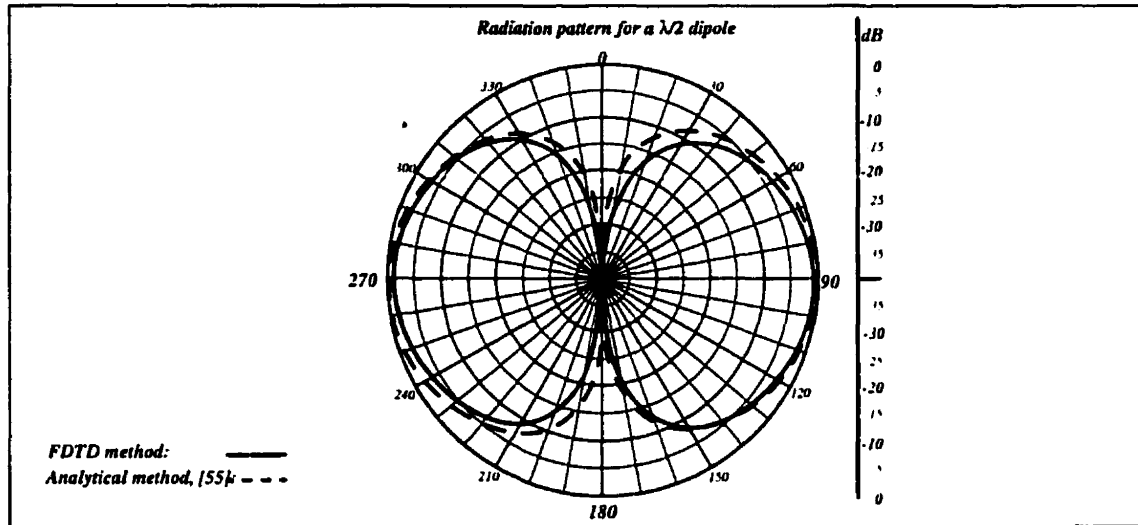
##### ***A-Core of the program***

*a-Verification of the core of the program* Core of the program has been verified using the example of a lossy sphere illuminated with a Gaussian pulse plane wave, provided in the text. In the FDTD space four observation points have been selected and E (or H) field components are saved at each step. These values are used to verify the core comparing the results obtained with those ones tabulated in the text.

##### ***B-Near field to far field transformation***

*b1-Verification using an abstract radiator*-In this method, in the absence of any radiator in the FDTD space, the closed surface which should contain the radiator is supposed to carry constant electric and magnetic current densities on each of its six plates. The E field distribution at a far observation point has been calculated using our FDTD program and compared with the result of analytical calculations. This method may be considered as a reliable verification of the near field to far field transformation part of the program.

*b2-verification using a canonical problem*-In this method the radiation pattern of a  $\lambda/2$  antenna was used to verify the result its related FDTD calculation. Figure (4.4) shows the comparison.



**Figure(4.4)**-Radiation pattern of a dipole antenna

In our simulations, performed at 1.5 GHz, the cell size is  $5\text{ mm} \times 5\text{ mm} \times 5\text{ mm}$ , the number of steps are 820, distances from the antenna to the ABC surfaces are 20 cells and time step is calculated using the relation  $\Delta t = \Delta / (2 \cdot c)$ . Its value is around 8.33 ps.

*b3-verification using the results for noncanonical problems in the literature*- In this method the radiation pattern and input impedance of a monopole antenna mounted on a metallic box have been calculated at 1.5 GHz and compared with those one reported in the literature. Relevant data for these calculations for 1.5 GHz will follow. The next section contains the results on input impedance and radiation pattern calculations of monopole mounted on a metallic box at 1.5 GHz in comparison with the corresponding results reported in the literature. These results may be considered as verification of the code used.

**Experimental verification of the results**-Experimental verification of the results is based on steps such as, finding a relevant system of phantom fabrication, measuring the antenna input impedance in a specified band of frequencies, measuring the antenna radiation pattern in some cuts. Evidently measurements are performed in two cases of with and without head

phantom. Antenna input impedance measurement is possible in the presence of a volunteer, as operator, to replace the phantom.

#### 4.4.3 Analysis of the isolated radio-handset, [53]

The object in this section is to analyze the basic radio-handset model, shown in Figure (4.5). The system is composed of a  $\lambda/4$  monopole antenna mounted on a metallic box.

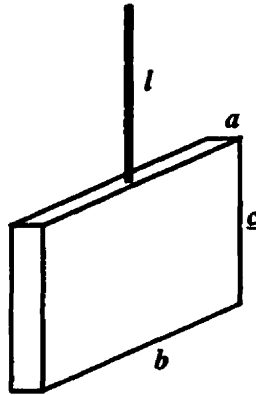


Figure (4.5)- Antenna-box system

The rationale for the choice of this model is that the model is essentially a simple one, at the same time it is sufficiently near to reality, it is in use by manufacturers, and there are some results in the literature to be used in the comparisons. The center frequency  $f_0$ , corresponding to  $\lambda$ , for this structure is determined by the antenna length ( $l=\lambda/4$ ) although the dimensions of the box has relatively little shifting effects on the centre frequency, as has been observed by Luebbers et al. [53]. Evidently there are some errors in centre frequency and radiation resistance calculations such as field approximations around the antenna wire to be considered later and rounding off the antenna length which should be compensated. However our object is to find the real and imaginary parts of the impedance at the working frequency  $f_0$ , and finding radiation pattern diagrams of the radio-handset. At this frequency the real part of impedance should be equal to a specified value ( $50\Omega$  in our case) while the imaginary part should be zero. These are adjusted using relevant values for the radius of the antenna wire and the dimensions of the box. In the following we consider the details of the antenna-box calculations for a working frequency of  $1.5GHz$ . At the centre frequency of  $1.5GHz$ , the wavelength,  $\lambda$ , is  $200mm$ .

#### 4.4.3.1 FDTD preliminary calculations

In analysing an object using FDTD calculations, first one should find some parameters related to FDTD space, its cell sizes, time step, the distance between the object and boundary surfaces, and the total number of time steps. These are based on some criteria and may be calculated as follows:

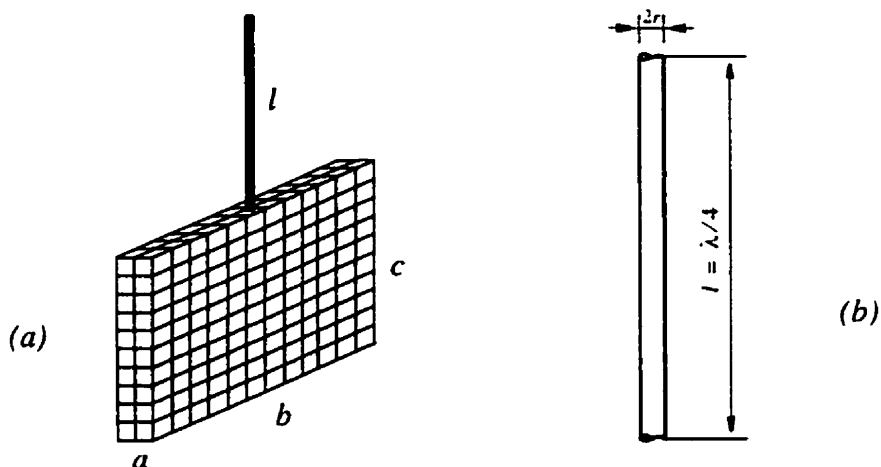
*a-Cell size calculation*-The criteria used in determining the cell size is the precision one need in the results on the one hand, and the memory available on the other hand. Using more cells per wavelength means more precision in the sampling of the field to update it at each step. But at the same time this necessitates using more memory space to keep the results at each step. In some calculations coarse cells down to 4 cells per wavelength is sufficient, while in some calculations one may need to use a fine mesh up to 40 cells per wavelength. As in the general case the medium is a heterogeneous one, different wavelengths in different media are unavoidable. In determining the cell size one should consider the minimum wavelength in the FDTD space which is corresponding to the highest value of the permittivity of the heterogeneous object at the working frequency. This may be expressed in the following relation:

$$\Delta = \lambda_{min}/n \quad (4-3)$$

In our calculations  $n=40$  for radiation pattern measurements which leads to cell sizes of  $5mm \times 5mm \times 5mm$ . For Impedance calculations a cell size of  $2.5mm \times 2.5mm \times 2.5mm$  is used. The dimensions of the box in mm and their ratio to wavelength are indicated in Table (4.3). Using this cell size the resulting discrete system in FDTD coordinates  $I, J, K$  is shown in Figure (4.6 a). In order to model the box, it is just needed to equal the relevant  $E$  field components to zero for example  $E_x$  and  $E_y$  components of the  $E$  field at the top of the box are tangent to the perfect conductor surface of the box. These components, specified by their  $I, J, K$  coordinates, are equated to zero for all time steps.

**Table (4.3)-Dimension of the radio-handset**

Dimension	in [mm]	in $\lambda$	in cells
<i>a</i>	10	0.05	2
<i>b</i>	60	0.30	12
<i>c</i>	50	0.25	10
<i>l</i>	50	0.25	8
<i>r</i>	0.5	0.0025	0.1

**Figure (4.6)-(a): Discrete antenna-box system (b): antenna wire size**

**b-Time step**-Finding this parameter is based on stability considerations which sets a limit on its maximum value as expressed by the following relation

$$c \cdot Dt \leq 1 / (\sqrt{\Delta x^{-2} + \Delta y^{-2} + \Delta z^{-2}}) \quad (4-4)$$

which reduces to the below relation in the case of cubic cells with  $\Delta x = \Delta y = \Delta z = \Delta$ :

$$Dt \leq \frac{\Delta}{\sqrt{3} \cdot c} \quad (4-5)$$

In our calculations  $Dt = \Delta / (2 \cdot c)$  is used.

**c-FDTD space size**-This parameter depends on the size of the objects under analysis in cells and the distance between them and the boundary surfaces (white space). Normally a distance in the range  $\lambda/2$  to  $\lambda/4$  is chosen depending on the conditions. In this calculations a distance of 20 cells is used.

**d-Total number of steps**-This parameter is typically on the order of ten times the number of

cells on each side of the FDTD space. The following relation gives an estimate to the number of steps:  $T = 10 \cdot \sqrt{3} \cdot N^{1/3}$ . In this relation  $N$  is the number of cells in one side of the FDTD space.

#### 4.4.3.2 Antenna modeling

The antenna used in this system is simply a  $\lambda/4$  monopole antenna made of a thin wire excited through a coaxial cable. Its modeling is done in three steps of thin wire modeling,  $E$  and  $H$  field components correction, and source (gap) modeling. These steps are considered below.

#### 4.4.3.3 Thin wire modeling

In our case the antenna wire radius is  $0.5\text{mm}$  which is well below the cell size,  $r/DX = 0.1$ . Hence to the extent that the  $E$  field components on the wire are concerned it is sufficient to let them equal to zero.

#### 4.4.3.4 Field components modification in the proximity of the wire

Figure (4.7) shows a section of antenna wire. In the vicinity of the thin wire the normal FDTD equations for free space should not be used to find the  $E$  and  $H$  field components. The field components in that region and in the direction normal to the wire, should be replaced by other relevant relations.

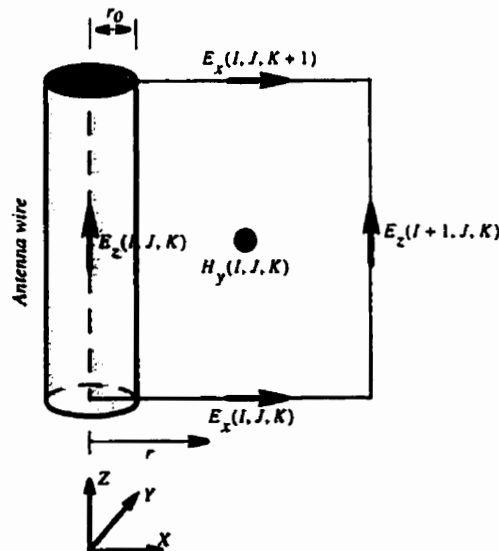


**Figure (4.7)-Field components around a thin wire**

The relevant relations for  $E$  and  $H$  field components may be a  $1/\rho$  variation where  $\rho$  is the radial distance from the center of the wire. Considering the dimension of the wire radius with respect to the wavelength  $r/\lambda = 0.5\text{mm}/200\text{mm} = 0.0025$ , this is a good approximation which follows that described by Umashankar and Taflove [43]. A conducting wire of radius  $r_0$  is positioned to be aligned with and centered on the  $EZ(I, J, K)$  field component. With the above assumptions, the spatial dependence of the fields in the vicinity of the wire is approximated as

$$H_y(r, J, K) \approx H_y(I, J, K) \cdot \frac{\Delta x}{2r} \quad (4-6)$$

within the contour as

$$E_x(r, J, K) \approx E_x(I, J, K) \cdot \frac{\Delta x}{2r} \quad (4-7)$$

along the upper and lower integration contours, with  $E_z(I, J, K) = 0$  all along the wire axis, and  $E_x(I+1, J, K)$  assumed to be uniform along the right contour. Applying Faraday's equation to the contour passing through the four electric field locations the following relation will be obtained.

$$\begin{aligned} & 0 + \int_{r_0}^{\Delta x} E_x(I, J, K+1) \frac{\Delta x dr}{2} \\ & - E_z(I+1, J, K+1) \Delta z - \int_{r_0}^{\Delta x} E_x(I, J, K) \frac{\Delta x dr}{2} \\ & = -\mu \Delta z \frac{\partial}{\partial r} \int_{r_0}^{\Delta x} H_y(I, J, K) \frac{\Delta x dr}{2} \end{aligned} \quad (4-8)$$

This relation reduces to the following finite difference equivalent expression, by evaluating the integrals and derivatives.



$$H_y^{n+1/2}(I, J, K) = H_y^{n-1/2}(I, J, K) + \frac{\Delta t}{\mu \Delta z} [E_x^n(I, J, K) - E_x^n(I, J, K+1)] - \frac{2\Delta t}{\mu \Delta x \ln\left(\frac{\Delta x}{r_0}\right)} E_z^n(I+1, J, K) \quad (4-9)$$

#### 4.4.3.5 Source modeling

There are various possibilities to represent the antenna excitation, which although differing in their details are not so differing in the precision of the related results. Two basic excitation variants are shown in the figure (4.8), (a) and (b), [32].

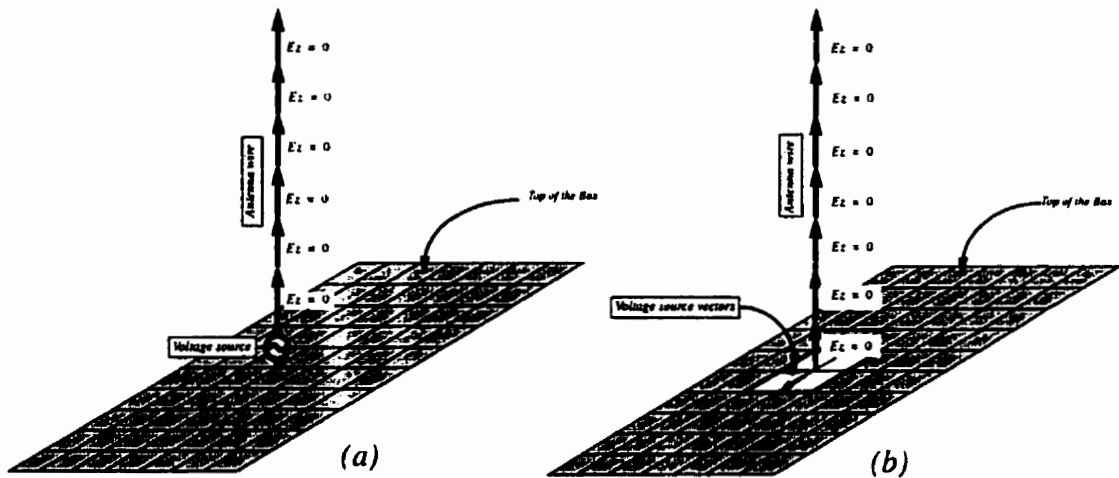


**Figure (4.8)-Two basic source models (a): Vertical gap model (b): Horizontal aperture model**

These cases are essentially FDTD equivalents of a wire monopole antenna delivered through a coaxial cable. Case (a) models the voltage source,  $V_s$ , as a vertical gap at the base of the antenna. Through this gap, the source excites the  $E_z$  component. The magnitude of this component is found through the equation  $E_z = V_s/\Delta z$ . Case (b) models the voltage source through a horizontal aperture situated at the antenna base. This source simulates the coaxial cable cross sectional aperture by exciting the  $E_x$  and  $E_y$  components.

Here it will be assumed that a good approximation to the source of case (b) is a  $1/r$  dependence. Thus the  $E_x$  and  $E_y$  source components on the top of the box at the base of the monopole as shown in figure (4.8 b) are given as

$$E_x^n(I, J, K) = -E_x^n(I-1, J, K) = \frac{-V_1(n\Delta t)}{\ln\left(\frac{\Delta x}{r}\right)} \quad (4-10)$$

$$E_y^n(I, J, K) = -E_y^n(I, J-1, K) = \frac{-V_1(n\Delta t)}{\ln\left(\frac{\Delta y}{r}\right)} \quad (4-11)$$

This approach corresponds to the magnetic frill method for exciting wires in the MOM, since one can consider these impressed electric fields to be equivalent to a magnetic current source circulating around the wire.

#### 4.4.3.6 Limitations associated with thin wire modeling [60-63]

The quasistatic approximation used in our calculations to modify the field components in the vicinity of the antenna wire leads to acceptable results for radiation pattern even with cell sizes up to  $\lambda/10$ . But the accuracy of this method in calculating the input impedance and resonance frequency is not satisfactory. One way to improve the accuracy is to use smaller cell sizes. This is the method applied in our calculations and naturally needs more memory space. But in addition to memory requirements there are limiting aspects which has been studied by workers as follows. The quasistatic approximation limits the wire radius to a half cell size ( $0.5 \Delta$ ), because the magnetic field calculation is unstable when the wire radius approaches the location of the tangential magnetic field components. It has been observed by Hocksman [61], that the above approximation leads to satisfactory agreement with the corresponding results via MOM method when the wire radius is twenty percent of the FDTD cell size ( $0.2 \Delta$ ). Under this condition a 3% difference in half-wave resonance frequency and a 8.5% in the resistance at the half-wave resonance for an antenna with a thin wire radius  $a=0.005 \lambda$  is reported, where  $l=40 \Delta$ . In addition to above limitations the model selected does not consider the finite gap (one cell) effect nor the effect of the singularity of the field at the wire end. These problems have been studied and reported by Soichi and M. Taki [60], and M. Douglas et al. [62,63] respectively.

#### 4.4.3.7 Impedance calculation

Using a sufficiently narrow pulse width one is able to calculate real and imaginary parts of the impedance for the antenna box system in a frequency band of interest. Impedance as a function of frequency is related to source voltage and antenna input current through the following relation

$$Z = \frac{\bar{V}}{\bar{I}} \quad (4-12)$$

in which  $\bar{V}$  and  $\bar{I}$  are the complex Fourier transforms for the source voltage  $V(nDt)$  and the antenna input current  $I((n + 1/2)Dt)$ . At each time step  $(n+1/2)$ , the antenna input current is calculated using Ampere's relation using the  $H$  field component values around the antenna wire and at the antenna base using the following relation

$$I = \oint H_x \cdot dx + H_y \cdot dy \quad (4-13)$$

After establishment of the stability, the complex Fourier transforms for the resulting transient current and the Gaussian excitation voltage will be obtained. Dividing them at each frequency gives the input impedance of the antenna.

#### 4.4.3.8 Calculation of radiation pattern and efficiency

In order to obtain radiation pattern there is no need to do more than a routine FDTD calculation in the problem space and then a near field to far field transformation. This transformation may be done using a steady state (single frequency) or a transient (wideband) excitation. Our radiation pattern calculations are based on a time domain transformation at the working frequency. A closed surface of integration including the objects under analysis, radio-handset and head model, is considered. In our calculations the distance between the surface and the boundary surfaces (ABC surfaces) are considered as adjustable parameters, but normally a distance of 4 cells gives satisfactory results.

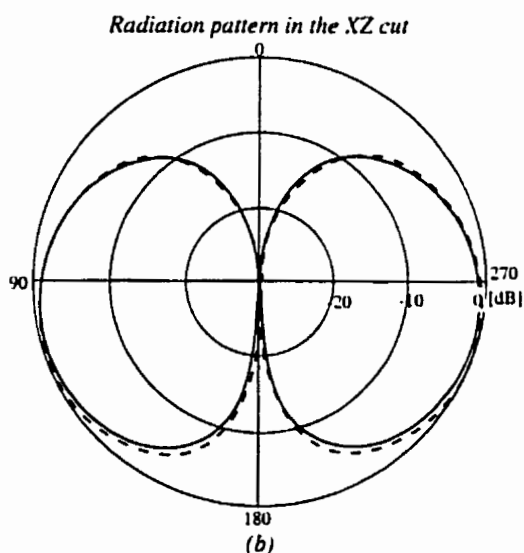
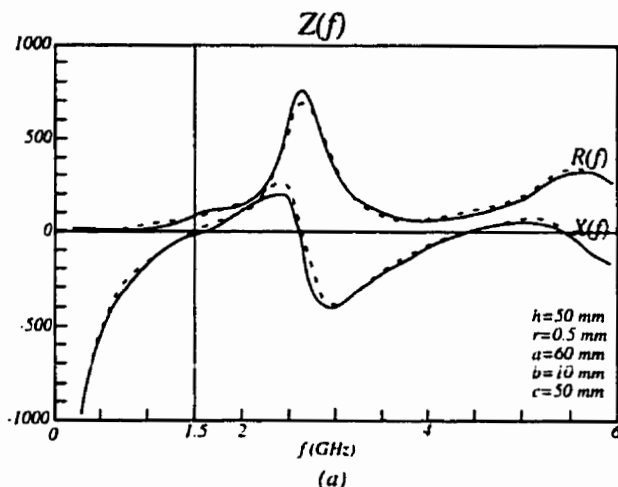
The result of the transformations are the far field distribution of the  $E(\phi, \theta)$  and  $H(\phi, \theta)$  fields. Formulas for calculating the radiation pattern and efficiency are as follows:

$$G(\phi, \theta) = \frac{|E(\phi, \theta)|^2 / \eta_0}{P_{in} / 4\pi} \quad (4-14)$$

$$Efficiency = \frac{P_{in} - P_{abs}}{P_{in}} \quad (4-15)$$

#### **4.4.4 Typical results for analysis of the isolated antenna-box system**

Figure (4.9) shows isolated antenna-box input impedance in the 0-6 GHz frequency band and radiation pattern in the XZ cut. The dimensions of the box and of the antenna mounted on it are shown in the table (4.4). Cell sizes are  $5mm \times 5mm \times 5mm$  for radiation pattern calculations and  $2.5mm \times 2.5mm \times 2.5mm$  for impedance calculations. In both cases the time step is calculated using the relation  $\Delta t = \Delta / (2 \cdot c)$ , and the distance between the object and the ABC is 20 cells. In impedance calculations total number of steps are 1100. A nonmodulated 130 ps pulse is used to give a 0-6 GHz frequency band.



————— : Results reported by Luebbers et al.      - - - - - : Results of our simulations

**Figure (4.9)** Comparison of the results of the analysis of an isolated radio-handset working at 1.5 GHz reported by Luebbers et al. [53], and our corresponding simulation results

#### 4.4.5 Problems in the analysis of the head handset system

That part of the body which is in close proximity to the cellular phone and hence, more than any other part, is under radiation exposure is the head. The hand, is also under exposure, but its sensitivity to the resulted effects is evidently much less than the head's sensitivity. It has already been shown, [44], that the human body cellular phone interaction can be reduced, with a good degree of precision, to the interaction of the head with the cellular

phone. In some calculations we may need to add the hand in our model to obtain more precise results. However, in the following, in explaining the theoretical aspects, just the head as the interacting part of the body is considered. This will not influence the generality of the discussion. Studying the problem of interaction between the body and the radiating system will be done in the following three steps. Firstly, decomposing the interaction into two effects each one originating from one of the interacting parts and affecting the other part. Secondly, characterizing the quantitative measure(s) of the related effects. And thirdly, calculating the related quantities and confirming the results. Regarding the first step the two following effects are readily distinguished: first, *Effects of the radiating system on the head* and second, *Effects of the head on the radiating system*. In the following these effects will be explained separately considering quantitative measure(s) of the related effects as mentioned above.

#### 4.4.5.1 *Effects of the radiating system on the Head*

The most practical way to characterize the effects of radiation on the human body is to use the SAR (Specific Absorption Rate) of the electromagnetic energy in the body. The SAR is a local function that indicates the spacial distribution of the absorbed EM energy. The cumulative effect of this absorption in a volume (of the head, for example) will be specified using another function  $P_b$  which is the summation over the related volume. The SAR and  $P_b$  functions are calculated using the following relations:

$$SAR = \frac{|E|^2 \cdot \sigma}{\rho} \quad (4-16)$$

$$P_b = \Sigma SAR(\Delta v_n \cdot \rho_n) \quad (4-17)$$

SAR and  $P_b$  values depend on the arrangement of the head antenna system, head model used in the calculation and the power level of the radiated field.

#### 4.4.5.2 *Effects of the head on the antenna performance*

Antenna input impedance and radiation pattern may be influenced by the presence of the head in its proximity. The effect of the head on the antenna impedance appears first, as a shift in the resonance frequency, and second, as a change in the values of  $R(f)$  and  $X(f)$ ,

especially around the resonance frequency. Both of these changes are detectable very well on the curve representing  $|S_{11}(f)|$  at the antenna input. As the head is a lossy dielectric under the exposure of the radiating system in its vicinity, it will naturally absorb some percent of the radiated energy. In fact in addition to this energy absorption, which is evidently a directive one, the radiating behavior of the antenna will change due to the presence of the scattering head and this is best analyzed using Maxwell equations, which are the base of our FDTD calculations. However, the effects of the head on the radiation characteristics of the antenna are reflected in its radiation patterns as directive losses in the different cuts.

#### 4.4.5.3 Limitation of the FDTD modeling of the round objects

In the FDTD modeling of the human head normally some parts of the model are eliminated due to rounding effect inherent in the method. This is common to every round object to be modeled via FDTD method and leads to some error. In our calculations these errors are not considered. But in order to reduce them a method is proposed as follows.

Figure (4.10) shows a round object (a 3-dimensional arbitrary round one) inside a FDTD uniform mesh. As is seen two types of cells are present, those that are completely filled by the material-1 described as  $(\epsilon_1, \sigma_1)$  and those that are filled by material-1 and material-2 described as  $(\epsilon_2, \sigma_2)$ , which may be the air with  $(\epsilon_0, 0)$ . This may be generalized to any number of materials filling a cell.

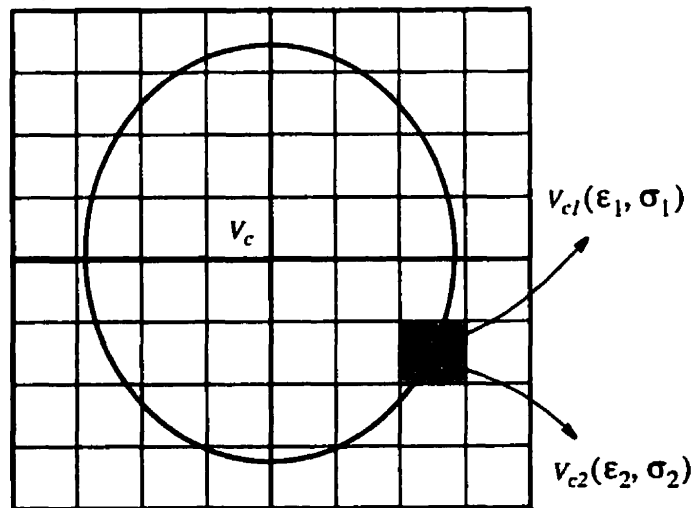


**Figure (4.10)** Averaging the parameters of the cells at the borders of a round object in a FDTD mesh

Then using the following relation one may find an average value for the related parameters

to be used in the cell.

$$P_{ave} = \frac{1}{V_T} \times \sum P_i \cdot V_i \quad (4-18)$$

This is the method of calculations of the average values of dielectric constants for the homogeneous models of the head which is based on the simple mixture theory and explained in the chapter 6. In the case of the bodied of revolution finding the partial volumes in each cell filled by specific material is a simple matter.

#### **4.5 Conclusions**

In this chapter a survey of some important works done by researchers in the field are presented. The goals, methodology and plan of our study, its relation to the works previously done in the field explained. Steps of FDTD analysis of the antenna handset interaction problem in two cases of isolated handset and head-handset, related parameters and preliminary calculations, basic formulation of the problem to be used in post processing phase, along with typical results are described. In addition the limitations associated with the antenna model used in the study giving some references is investigated. Regarding the limitations of our method of FDTD head modeling a suggestion is provided to ameliorate the results although it has not been implemented in our calculations.



## **Chapter 5**

### **Experimental aspects, measurement methods and considerations**

#### **5.1 Substituting materials**

In some problems one needs to study experimentally the interaction of EM waves with various structures to confirm the results obtained in theoretical studies. Evidently the object under study has, in addition to structural specifications, some material dependent specifications and properties. In the case of EM waves scattering structures these properties are the permittivity and permeability of the related materials. Two important cases are the study of the performance of the antenna in the earth, [45], and effects of the EM waves on the human tissues. In these cases one needs to prepare a substitute which is normally a kind of mixture. In studying the EM waves biological matters the mixture should have a specific permittivity characteristics in a frequency band. In addition they should be: nontoxic, nonflammable, noncorrosive, relatively inexpensive, stable (with time and with temperature), reusable (solids) and they should have the desired electrical and mechanical (solids) properties. Evidently there are other requirements, too, which are application dependent.

#### **5.2 Tissue substituting materials**

Various mixtures have been investigated and reported as being suitable substitutes for biological materials. They may be in the solid or in liquid phases. Depending on the application and on the frequency band of interest one may choose among them. Here we explain briefly these systems.

### **5.2.1 Solid mixtures**

Solid mixtures have been used and reported in a vast range of applications. Normally in an experimental study on a subject related to EM radiation dosimetry in a human body, using solid materials is indispensable. This is to some extent due to the mechanical properties of the solid models. They are prepared using a mixture of up to five materials, each one in a definite percentage. Water is normally one of the constituting materials in these mixtures and gelatin is a commonly used material. In the literature, one may find the recipes for different mixtures and in different frequency bands. Duck, [16], provided a review of the literature, up to 1990, in this regard. However, solid mixtures can be constructed in one of two ways: the first one consists of a jelly agent, polyethylene powder, sodium chloride and water; and the second one consists of agar, sodium chloride and water. The disadvantages of constructing phantom models using these materials is that the models cannot be used repeatedly since they dry out and decompose over time. To avoid this, nonhydrated phantom models made of ceramic were developed to simulate muscle tissue, but these materials could not be cut or reshaped easily. Based on these facts flexible nonhydrated phantom models have been developed in order to overcome the shortcomings of their preceding generation. These new models are made of materials composed of silicon rubber and carbon fiber compounds, [46]. Using suitable composition ratios one can control the complex permittivity of the phantom models corresponding to the permittivities of low water and high water content human tissues.

### **5.2.2 Liquid mixtures**

Liquid mixtures, too, have been used extensively. Their use up to 35 GHz is reported in the literature as reviewed by Duck, [16]. In these mixtures sodium chloride is normally used to adjust the conductivity and there are a series of alternative materials to adjust the permittivity of the mixture, such as sugar, ethanol, or other organic materials. There is another liquid mixture system, named emulsion, in which oil is used. The relative permittivity of oil is around 2 and that of water is around eighty. Thus a wide range of permittivities are realizable using emulsions. Here the water is matrix phase and the oil is disperse phase. The conductivity of the mixture is adjusted by controlling the concentration of sodium chloride in the aqueous (matrix) phase. As oil and water do not form a stable mixture, adding a sta-

bilizing agent, called emulsifier and acting as a surface active agent, is necessary. Smith, [45], reported using these mixtures and provided relevant information to find the necessary concentrations. Liquid mixtures may be easily used to fabricate homogeneous models. Nonhomogeneous models demand specific arrangements to juxtapose various mixtures without being mixed together, for example by using relevant containers. One practical point with the liquid based phantoms is their penetrability to electric field measurement probes which is an advantage in some applications.

### **5.3 The real human head and its models**

In the studies about the interaction of EM waves and the human head we are concerned with the object interacting with the radiating system in three different forms depending on the context. The interacting object may be the real head of the user or operator, the FDTD model, or the phantom model. From now on we use the generic name of IHR (for Interacting Head with the Radiating system) for any of the above cases depending on the context. The real head is the interacting object in the real application of the equipment. In addition we may use it (head of a volunteer) in some measurements (impedance) as has been used by Jensen et al., [14]. The FDTD model is the model used in the FDTD calculations, and the phantom model is the model used in the experimental study. Each of the above variants has a different role in the study but there is a specific relation between them that should be considered in detail by a research worker in the field. A detailed grasp of this relation emerges at the expense of doing a good amount of FDTD calculations and experimental works. We now discuss the specifications of each of these IHRs.

#### **5.3.1 Real head**

As anatomy and our daily experience tell us, there are a vast amount of variations in the real head's shape and size specifications. Some of these variations are depending on sex (men, women), age (child, adults), and ethnic group while others are distinguishable even in the samples in each group. It can easily be claimed that there is no unique head. The situation becomes even more complex if we consider other facts, as observed too by Hombach et al, [39], such as the variations of the electrical properties of the human body with the level of physical and metabolic activity, health, and age.

### **5.3.2 FDTD model**

The FDTD model should reflect the biological and anatomical aspects of the head and may take different forms. There are always differences between the specifications of the real head and those which are represented by its FDTD counterpart. There are reasons for their differences, some of which are inherent to the FDTD method such as staircase approximation errors or finiteness of the cell size, while some depend on the anatomic information source of the model. These informations may come from various sources such as MRI data on the head, anatomic data books, a first order global approximation, or a combination of these sources. Accordingly they will lead to one of the following FDTD head models: Anatomic, Nonanatomic, and Semianatomic. Choosing among the above systems depends on factors such as computer resources, parameters to be calculated, frequency, and scope and object of the study. Exact calculation of the peak SAR in the model demands a MRI based FDTD model, while for a calculation of impedance, radiation pattern of the radio-handset, and average SAR, a semianatomic and even a nonanatomic model is sufficient. However all of the above systems are used by researchers. Models consisting of up to 13 tissues, Hombach et al [39], have been considered. There is no agreement about the value of the homogeneous models.

### **5.3.3 Phantom model**

Phantom models cannot be a precise reflection either of the peculiarities of the real head, or even of an anatomic FDTD model. In the experimental realm there is no place for such a flexibility as that given by FDTD modeling in adaptation to details and sophistication. In addition, lack of agreement about the exact values of the dielectric constant of the tissues adds to the difficulties. The process of realization of a phantom model may be complex due to mechanical aspects. However in this process one should consider the following aspects: General material requirements, Electrical properties, Mechanical aspects, Model's sophistication, Measuring system. Each of the above aspects can cause some errors. The first two have been discussed earlier. Mechanical aspects on the one hand depends on the applications of the model (e.g., a standing entire model of the body for dosimetric experiments or a head model for impedance and pattern measurements), and on the other hand depends on the available mechanical facilities. The next factor, which will be considered below, is the

degree of sophistication or details in the phantom model. In addition to these, some considerations come from the measuring dimension.

*Details of the phantom model*-In the FDTD calculations one may choose among a series of alternatives based on the objects of study. Sometimes the object of study is precise SAR calculations, peak and average SAR: a MRI based head model is then preferable. Sometimes the object of study, as in our case, is to obtain, along with the antenna impedance and radiation pattern changes in the vicinity of the user's head, an estimation of the SAR inside the phantom. In this second case a homogeneous model of the head is sufficient, even to verify the results of FDTD calculations based on the models which include a degree of non-homogeneity. This is because the input impedance and the radiation pattern of the radio-handset is not highly sensitive to the details of the head model. But evidently the size and to some extent the shape of the head model may influence the results. In our measurements two head models similar in shape to a real head of an adult and a child and filled with a liquid mixture have been used. As will be seen in chapter 6, the dielectric constant of the liquid mixture was calculated to be equal to the volume average of dielectric constants of tissues in our heterogeneous head model which is near 46 for its permittivity and 1.60 for its conductivity. The outer layer of the phantom was made from fiber glass whose dielectric constant is near 4. Figure (5.1) shows these head models

#### ***5.3.4 Summary of heads characteristics***

In table (5.1) a summary of the characteristics and descriptions of different head models have been indicated, relative to size, shape, number of tissue types, material distribution details, and tissue substituting materials for real heads, FDTD models, and phantom models.

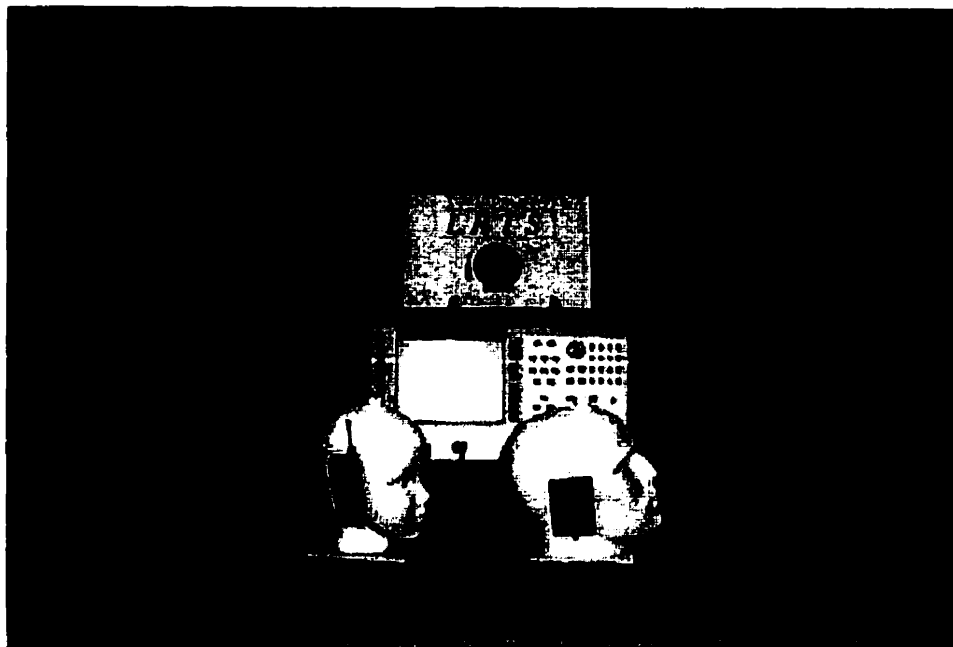


Figure (5.1) Two head models used in measurements

Table (5.1) Head model characteristics versus real head

Head Models characteristics versus real head

<b>Model</b>	<b>Characteristics</b>	<b>Description</b>
<b>Real head</b>	<i>size</i>	<i>child size, adult size</i>
	<i>shape</i>	<i>gender dependent aspects other (e.g.: race) aspects</i>
	<i>tissue type number</i>	<i>up to 130 tissue types reported, [39]</i>
<b>FDTD model</b>	<i>size</i>	<i>child size, adult size</i>
	<i>shape</i>	<i>anatomic, semianatomic, simple</i>
	<i>cell size</i>	<i>down to 1 mm reported, [15]</i>
	<i>material distribution detail</i>	<i>homogeneous, heterogeneous (up to 13 tissue type reported, [39])</i>
<b>Phantom model</b>	<i>size</i>	<i>child size, adult size</i>
	<i>shape</i>	<i>semianatomic, simple</i>
	<i>material distribution detail</i>	<i>homogeneous, heterogeneous</i>
	<i>tissue substituting materials system</i>	<i>Solid, liquid</i>

## 5.4 Measurements

The measurements needed in experimental verification of the calculations are impedance measurement and radiation pattern measurement. Each of these measurements should be performed in two cases of isolated radio-handset and of head-handset. SAR calculations were not supposed to be checked experimentally, from the beginning.

### 5.4.1 Impedance measurement

As the input impedance of the radio-handset is an important electrical characteristic of the handset, and may show the effect of the head on the handset, it should be measured in two cases with and without the head in its proximity. The magnitude of the input impedance,  $|S_{11}(f)|$  is sufficient to give the necessary information. The related measuring setup is indicated in Figure (5.2).

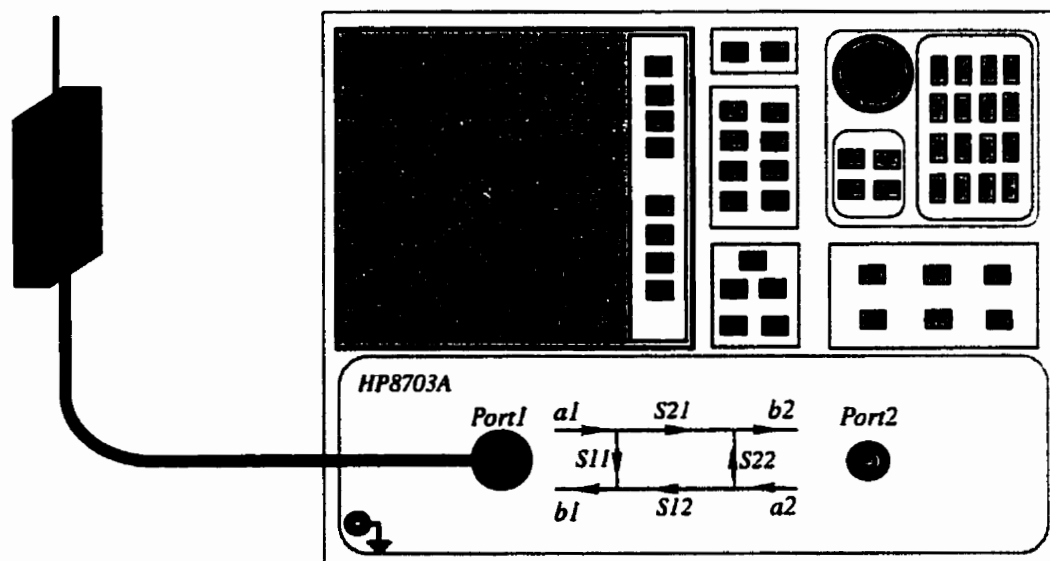


Figure (5.2) Impedance measuring setup

### 5.4.2 Radiation pattern measurement [47-48]

The radiation pattern of an antenna is one of its most important characteristics. It is essentially a three dimensional pattern, and its complete description requires field measurements in all directions in space. In this section a brief description of the radiation pattern measurement method will be given. Our description will cover mainly those aspects which are

needed in our measurements.

Figure (5.3) indicates an antenna situated at the origin of the coordinate system. On an imaginary sphere of large radius centered at the origin, patterns of the  $\theta$  and  $\phi$  components of the electric field are measured along latitude circles ( $\theta$ =constant). These patterns are measured as a function of the longitude or azimuth (longitude) angle  $\phi$ .

Although comprehensive patterns are sometimes necessary, it is frequently possible to obtain sufficient information with only a few patterns. For an horizontally polarized antenna with its major lobe of radiation in the x direction two patterns may be sufficient. In one of these patterns, one measures  $E_{\phi}(\phi)$  on the xy plane ( $\theta=90$ ), while in the other pattern,  $E_{\theta}(\theta)$  on the xz plane ( $\phi=0$ ) should be measured.

In our experiments  $E_{\theta}$  and  $E_{\phi}$  in the three different planes of XZ, XY, and YZ are measured. This is due to the effects that head may have, in different directions, on the radiation pattern of the handset.

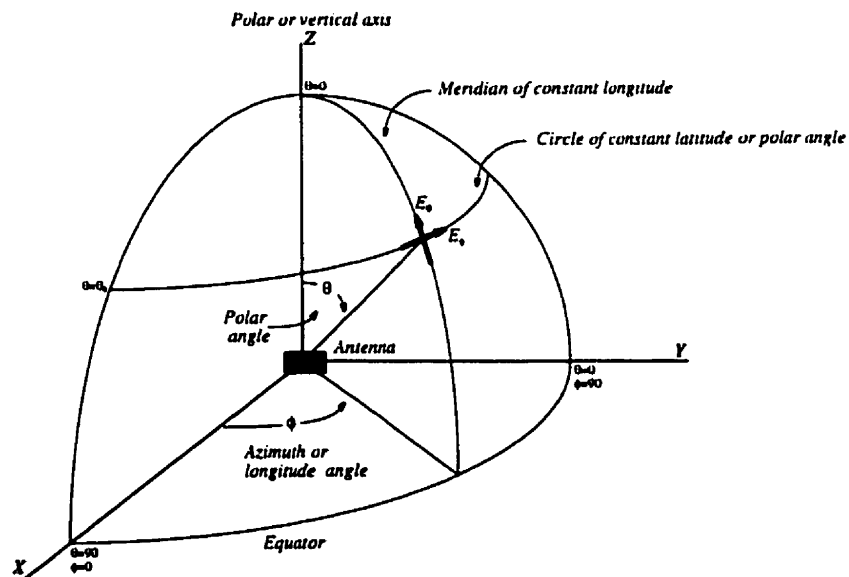


**Figure (5.3) Antenna and coordinate system for pattern measurements**

#### 5.4.2.1 Radiation pattern measuring system

Figure (5.4) shows the basic configuration of a radiation pattern measuring system including a transmitting antenna and its related oscillator, the antenna under test, the turning table,



and the receiver. In pattern measurements it is usually convenient to operate the antenna under test as a receiver, illuminated by a transmitting antenna as illustrated in the Figure (5.4).

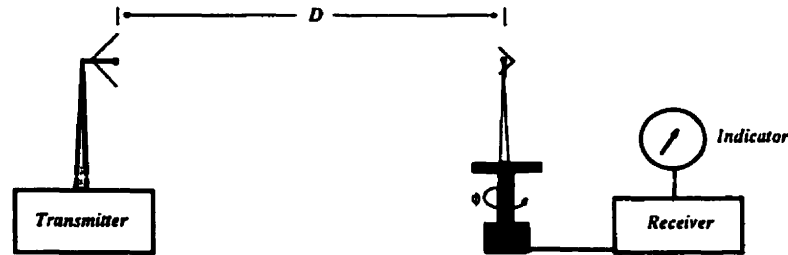


**Figure (5.4) Basic antenna pattern measuring system**

The transmitting antenna is fixed in position, and the antenna under test is rotated around the vertical axis using a controller. Controlling the turning table, taking informations about transmitted and received signals, analyzing and plotting the radiation patterns is done under computer control. Using anechoic chambers one may minimize the unwanted reflections perturbing the results.

#### 5.4.2.2 Distance requirement [49]

For an accurate far-field or Fraunhofer pattern of an antenna a first requirement is that the measurements be made at a sufficiently large distance. These far-field conditions are summarized as follows.

$$r > \frac{2A^2}{\lambda} \quad r \gg A \quad r \gg \lambda \quad (5-1)$$

In these relations  $r$  is the distance between the transmitting and receiving antenna,  $\lambda$  is the wavelength of the radiated wave, and  $A$  is the physical aperture of the antenna. These conditions result from a phase approximation requirement, an amplitude approximation requirement in the expansion of the vector potential integral of a source at a point of observation located in the far field, from an approximation requirement in the expansion of the H field component of that source.

### 5.4.2.3 Radiation pattern measuring setup

Figure (5.5) shows the setup used in the measurements. Due to instrumentation problems met with the anechoic room installation, the measurements were performed in the exterior. In this setup the distance  $D$  is 120 cm, for far field measurement, and the height of the transmitter and receiver antennas was chosen sufficiently large to practically eliminate the reflection from the earth. A good matching at the port of the handset is necessary to lead to a sufficiently high level of receiving signal to be measured. This is vital specially at those points of the radiation pattern where there are deep nulls. In the system used the receiver has a minimum detectable signal of  $-53$  dBm at 1.9 GHz. In addition up to  $+10$  dBm, the output of the detector is linearized by software. This gives us sufficient dynamic range to perform the measurements in the linear part of the measuring system. It is sufficient to adjust the transmitted signal level. Then the maximum received signal, corresponding to the peak of the antenna pattern determines 0 dB in the measured pattern. In order to eliminate some small reflections due to cables some ferrite beads have been used. In the measuring steps, one should be careful to set the source point of the antenna on the axis of rotation and at the same height of the transmitting antenna.

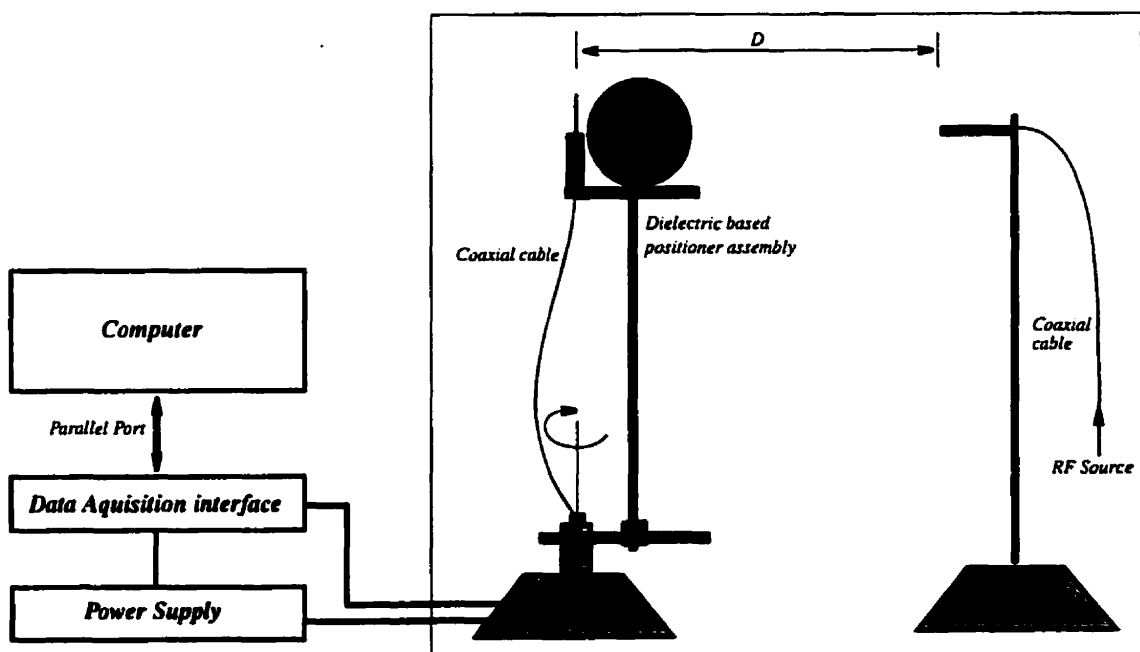


Figure (5.5) Radiation pattern measurement setup

## CHAPTER 6

### Numerical and Experimental results

#### 6.1 Introduction

This chapter presents the steps of the calculations, along with the related results, to quantify the effects of the head on the performance of a radio-handset on the one hand and the effects of the radio-handset on the human head on the other hand. In order to verify the code used in our calculations a comparison with the results of other researchers is given and to validate our results, experimental data are indicated. The steps covered in this chapter are, problem definition, preliminary calculations, validation of the code with the results in the literature, calculations and results at 1.9 GHz, and experimental verification of the results. In the following details of them are explained.

#### 6.2 Problem definition

The object of this study is to analyse the interaction between a radio-handset and human head at a frequency of 1.9 GHz, as illustrated on Figure (6.1).

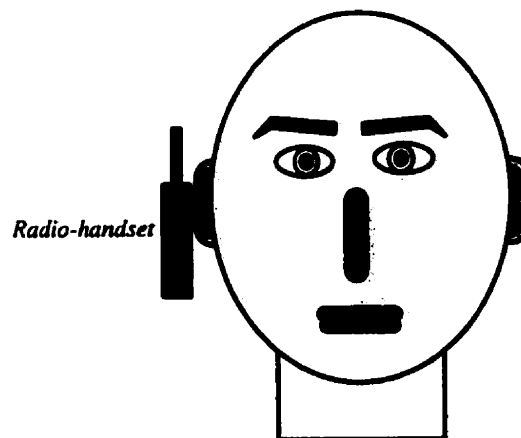


*Figure (6.1) Head-handset system.*

Simple homogeneous and heterogeneous models of the human head are considered. First, the antenna radiation pattern and input impedance are calculated to study radio-handset performance in the presence of the head. Secondly, the SAR in the head model is calculated to quantify the effects of the radio-handset on the head.

### 6.3 Preliminary considerations

Two sets of informations should be supplied to our programs to calculate the field distribution. The first ones are related to the head model and the second ones are general FDTD parameters. In the following these informations are studied. These data and their related considerations will be studied in the following subsections.

#### 6.3.1 Head model

Regarding the head model, the anatomic information about the human head should be considered as our starting point. Then a careful consideration and study of its geometry, the distribution of biological material in it, the values of the dielectric constant of related tissues, sensitivity of the organs based on the existing reports, working frequency, required information, and available computer resources are the important factors that will help us to develop a relevant head model

##### 6.3.1.1 Dielectric constants of the tissues

In the literature there is not a good compatibility among the various data sources for dielectric constants of related tissue types. Sometimes there are different values for the dielectric constant of the same tissue type. Table (6.1), taken from Gandhi et al., [15], includes the dielectric constant of various tissues used in our calculations

**Table 6.1-** Dielectric properties and specific gravities of various tissues of the head on 1900 MHz

<i>Tissue</i>	<i>Brain</i>	<i>Lens</i>	<i>Humour</i>	<i>Skin</i>	<i>Fat</i>	<i>Muscle</i>	<i>Bone</i>
$\epsilon_r$	43.22	42.02	67.15	37.21	9.38	49.41	16.40
$\sigma$ [S/m]	1.29	1.15	2.14	1.25	0.26	1.64	0.45
<i>Specific Gravity</i> $10^3 \text{ Kg/m}^3$	1.04	1.10	1.01	1.01	0.92	1.04	1.81

### ***6.3.1.2 Anatomic head***

Figure (6.2a) shows the vertical cross section of a human head taken from an atlas of anatomy, [50], which contains cross sectional diagrams of horizontal sections with a spacing of about one inch in human cadavers. This is the starting point of our head model

### ***6.3.1.3 Developing a relevant head model***

As there is not a unique anatomic head, there is also no unique head model. As already mentioned, differences between individual heads depend on the size, shape, gender, ethnic group and so on. Really, in the realm of head models there are some factors which influence the final form of the model and its difference from a real head. The number of tissue types may be considered as a parameter of resemblance to the real head. Our models are derived from the above mentioned anatomical model as indicated in Figure (6.2a-e), using 3 tissue types for brain, muscle, and eye humor. Two cases, with neck and without neck, have been considered for each homogeneous and nonhomogeneous model. In radiation pattern calculations, cell sizes of  $5\text{mm} \times 5\text{mm} \times 5\text{mm}$  give us good results but, in impedance calculations, precise results are obtainable using finer meshes. In our calculations, cell sizes of  $2.5\text{mm} \times 2.5\text{mm} \times 2.5\text{mm}$  were used to find impedance variations in the 0-6 GHz band.

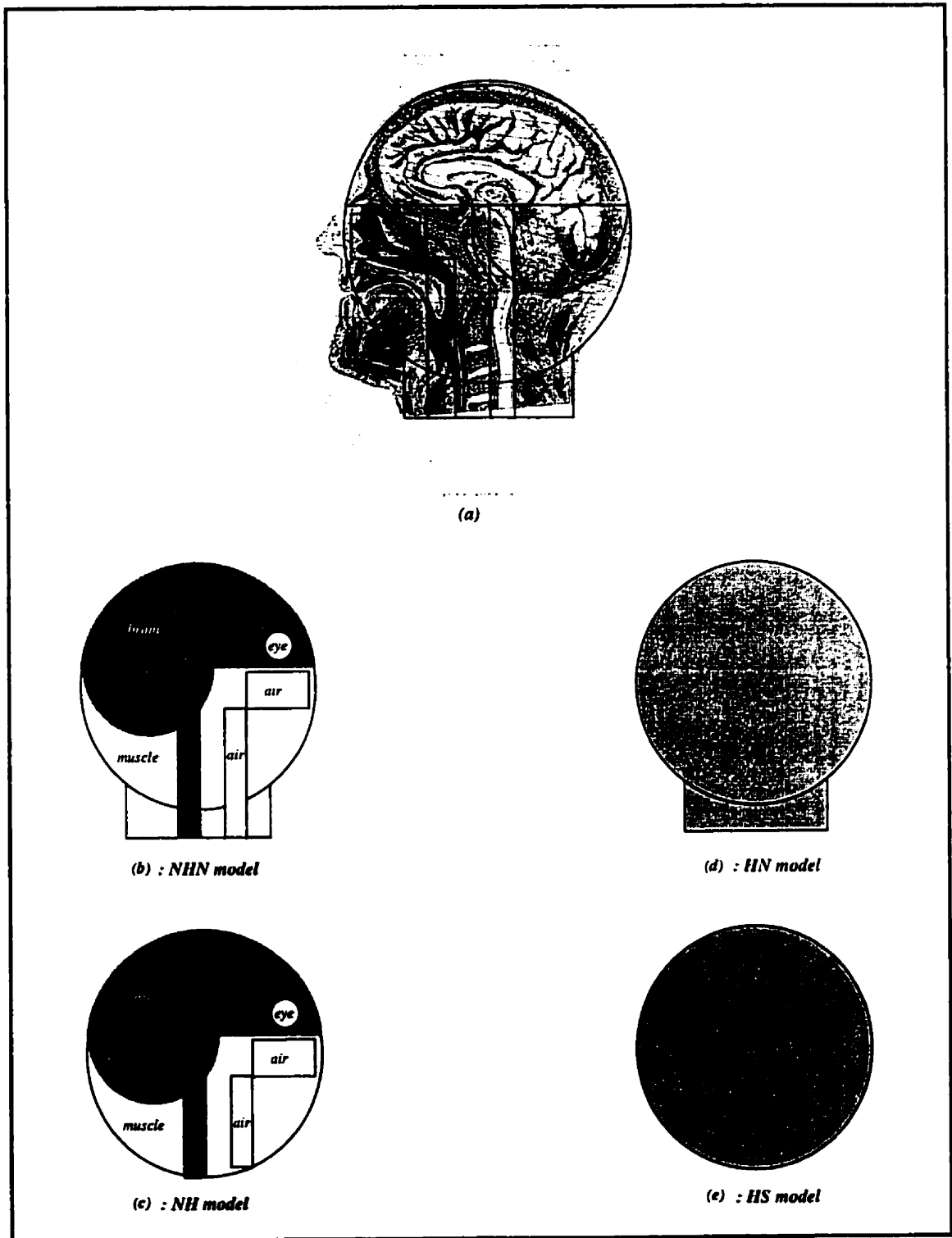
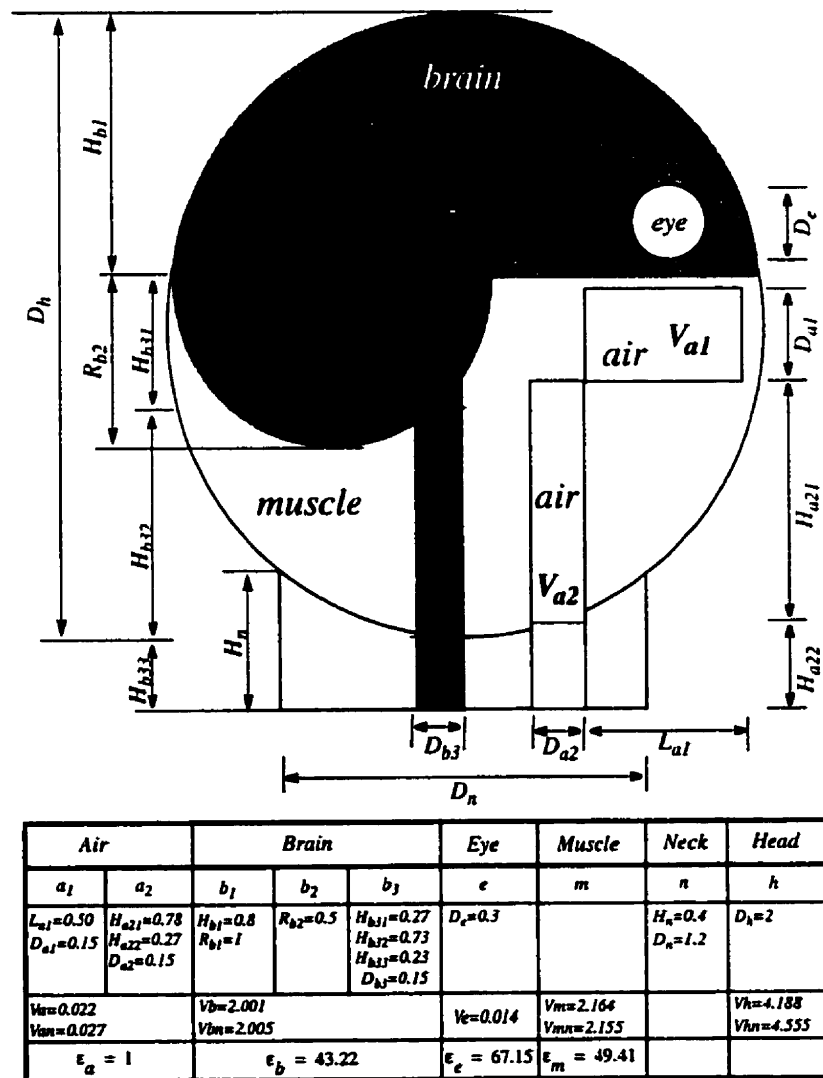


**Figure (6.2)** Developing of anatomical head into four homogeneous and heterogeneous head models

### 6.3.2 Calculation of the average dielectric properties of homogeneous models

Complete specification of homogeneous models requires us to find relevant values as equivalent dielectric constant, conductivity, and specific gravity of substituting material. These values should be derived from the respective parameters of the constituting component materials of the corresponding heterogeneous model. The most natural way to calculate these values seems to be volume averaging. Supposing a heterogeneous model as is shown in Figure (6.3), consisting of  $K$  parts each with a volume of  $V_i$  and specific property of  $P_i$ . The average property  $P_{ave}$  attributable to an equivalent homogeneous model is obtained using the



Figure(6.3) Nonhomogeneous model with neck and its constituent parts

following relation

$$P_{ave} = \frac{1}{V_T} \times \sum P_i \cdot V_i \quad (6-1)$$

In this relation  $V_T$  presents the total volume of the homogeneous model. To the extent that a FDTD equivalent homogeneous model is concerned, this relation is sufficient, but in order to construct a homogeneous phantom model using liquid mixtures, other factors, too, should be considered. Table (6.2) shows the average values of the required parameters.

**Table (6.2)** Calculated values for dielectric properties of homogeneous models

Parameter Model	$\epsilon_{ave}$	$\sigma_{ave}[S/m]$
HS	46.41	1.59
HN	46.60	1.60

#### 6.4 Component concentrations in a liquid filled phantom model

As explained in the chapter 5 the phantom model mixture may be in the solid, gel or in a liquid form. Due to practical limitations in fabrication of the phantom model, the author had to use finally a liquid mixture model. Calculations regarding the percentage of the mixture components is as follows.

In addition to their use in the FDTD calculations, the average properties of homogeneous models are also applicable to finding the concentrations of the constituting parts in the phantom model used in experimental validations of the results. As in our case a liquid mixture has been used as filling material in the phantom, our explanations in this section will concentrate on those aspects relevant to these mixtures. The component parts concentrations in the mixture are calculable using some mixture rules, [51], discussed in mixture theory. According to the simplest mixture rule the property  $P$  of a mixture is related to the properties  $P_1$  and  $P_2$  of its component parts through the following relation

$$P = P_1 C_1 + P_2 C_2 \quad (6-2)$$

The mixture used in the phantom model has three components of water, ethanol, and salt. Using the above relation and considering the dielectric constants of water ( $\epsilon_r = 78$ ) and ethanol ( $\epsilon_r = 24.30$ ) at 25 C,[17], the volume concentrations  $C_1$  and  $C_2$  are obtained as 41% and 59% respectively.

The amount of salt needed to adjust the conductivity of the mixture ( $\sigma = 1.59[S/m]$ ) is calcu-



lable using the following relation, [52]

$$\sigma = N(a_0 + a_1 \cdot N + a_2 \cdot N^2 + a_3 \cdot N^3 + a_4 \cdot N^4) \quad (6-3)$$

which gives us the normality  $N$  of the salt. The coefficients  $a_0$ ,  $a_1$ ,  $a_2$ ,  $a_3$  and  $a_4$  are parameters. Based on this equation a normality of  $N=0.159$  is required to give us the above mentioned conductivity. As the salt in the three component mixture will be distributed finally in a volume containing water and ethanol, the actual conductivity will be decreased by a factor amounting to  $C_1$ . Hence the final value of normality of salt should be  $N_f = N/C_1$ . Table (6.3) gives the volume concentrations for water and ethanol and normality for salt.

**Table (6.3)** Required volume concentration of water and ethanol and normality of salt

Water	Ethanol	Salt
$\epsilon_r = 78$	$\epsilon_r = 24.30$	$N=0.159$
41%	59%	$N_f=0.386$

#### 6.4.1 Error estimation for dielectric constant of the liquid mixture

In our experiments a liquid mixture has been provided using the above results. No measurement performed to find the dielectric constant of the mixture experimentally. In order to estimate the error in the dielectric constant various factors affecting each component should be considered. Regarding the salt, weighting error is less than 0.1 gram. Regarding the volume of the liquids the measurements were performed with a precision around 1%. Vaporization of liquids, temperature dependence of their parameters are negligible. They were kept in an environment with a temperature of 25 c degrees. The only factor that may have a considerable effect on the dielectric constant of the liquids is the working frequency, because our calculations are based on the parameters in the static case. Using the Debye equations [64], one may find the dielectric constants of the liquids, both the permittivities and the conductivities, at the working frequency, knowing their corresponding static values and their relaxation frequencies. The relaxation frequency of the ethanol is 1.111 GHz and in the case of water it is 19.23 GHz, [64]. In addition the ethanol used in the mixture had a 95% purity (5% water is associated with it). These points result in an error around 17% in

the permittivity of the mixture. Corresponding error in the conductivity amounts to 8%.

## 6.5 Impedance and radiation pattern results

### 6.5.1 Isolated radio-handset

The radio-handset model used in the study is shown in Figure (6.6). Dimensions are as indicated in the Table (6.4). Using cubic cell sizes of  $5 \times 5 \times 5 \text{ mm}$  for radiation pattern calculations and  $2.5 \times 2.5 \times 2.5 \text{ mm}$  for impedance calculations and around  $0.50 \cdot \lambda$  for the distance between the object and the boundary surfaces FDTD space sizes as indicated in Table (6.5) resulted. In this table “DWR” (Distance to Wavelength Ratio) and “ $d$ ” respectively indicate the white space around the object under analysis in wavelength and the distance between the head model and the reference plane on the radio-handset, shown in the figure.

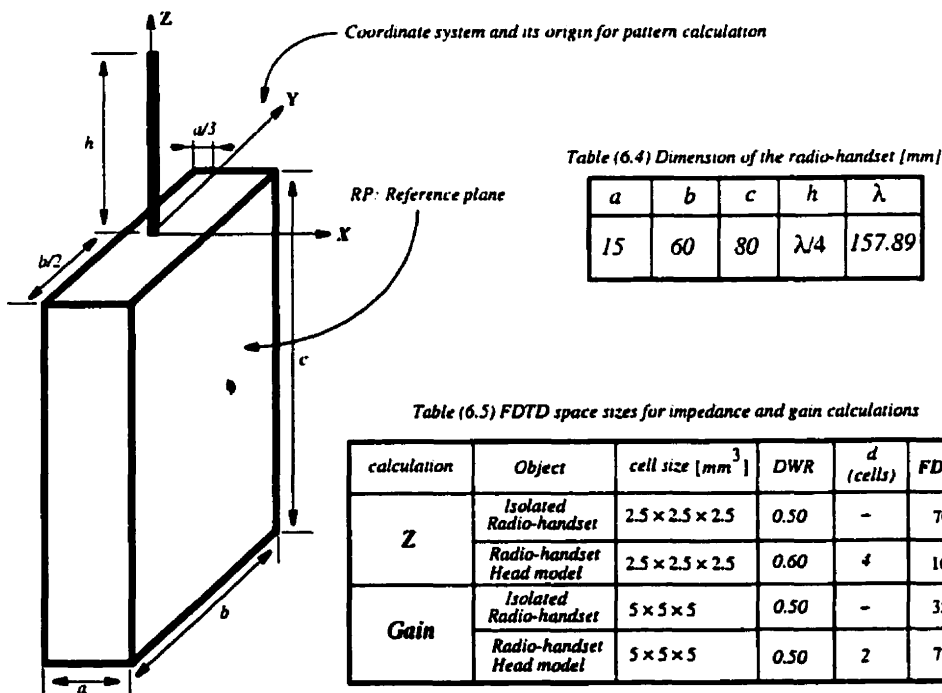


Figure (6.6) Radio-handset used in calculations and related FDTD space size information.

Figure (6.7) shows the input Gaussian voltage pulse as a function of time (a), the resulting input current of the antenna (b), real and imaginary parts of the input impedance of the antenna in the (0-6 GHz) frequency band (c) and (d). In Fig. (6.7-a) a  $250 \text{ ps}$  pulse has been imposed to give a sufficiently wideband frequency response. Fig.(6.7-b) shows the time do-

main input current response of the radio-handset to be used together with the input voltage for estimating the input impedance as function of frequency, by taking their FFT. Figures (6.7-a,b) exhibit the typical resonance behavior of a resonator. In (c) a near  $50\Omega$  resistance at  $1.9\text{ GHz}$  is seen accompanied with a near  $0\Omega$  reactance in (d) at the same frequency. In addition to this series resonance Figs (6.7-a,b) indicate another series resonance around  $5.4\text{ GHz}$  and a parallel resonance around  $3.2\text{ GHz}$ . Figure (6.8) shows the same information in another form. In Figure (6.8a) real and imaginary parts of the antenna input impedance in the (1.8-2 GHz) frequency band are indicated. As is seen at the frequency of  $1.9\text{ GHz}$  the relations  $R(f) = 50\Omega; X(f) \approx 0\Omega$  are satisfied. Figure (6.8c), magnitude of  $S_{11}$  in the band of (0-6 GHz), indicates the above mentioned series resonances at  $1.9\text{ GHz}$  and  $5.4\text{ GHz}$ , the first one representing a much higher resonance relative to the second one. This is due to a higher loss at higher frequency. This aspect is clear from the curve (b), the magnitude of the input impedance in the (0-6 GHz) frequency band which gives a somewhat higher value at  $5.4\text{ GHz}$  with respect to the value at  $1.9\text{ GHz}$ . Figure (6.8d) gives the magnitude of the  $S_{11}$  in the 0-3 GHz frequency band.

Figures (6.9) through (6.11) show the radiation pattern of the isolated radio-handset in different cuts of the XZ, XY, and YZ planes respectively. The reference level for these diagrams is the maximum value of the gain in the XZ and YZ cuts. In each figure, in addition to the gain, the E field components ( $20\log|E_\phi|$  and  $20\log|E_\theta|$ ) in dB have been indicated, both in rectangular and in polar coordinates.

In Figure (6.9), the pattern diagram in the XZ cut, the level of  $|E_\phi|$  is negligible with respect to the  $|E_\theta|$  (50 dB weaker). This explains readily the resemblance of figures (6.9 a with b) or (6.9 d with f) considering the following relation for gain

$$Gain(\theta) = 10\log\frac{4\pi|E|^2}{\eta_0} = 10\log\frac{4\pi}{\eta_0} + 10\log\left(|E_\phi|^2 + |E_\theta|^2\right) \quad (6-4)$$

$$Gain(\theta) = -14.775 + 20\log\left(|E_\phi|^2 + |E_\theta|^2\right) \quad (6-5)$$

Symmetry is another aspect in this figure to be mentioned. This symmetry reflects the physical symmetry of the radio-handset as the radiator.

Figure (6.10) indicates the patterns in the XY cut. Here too the  $|E_\phi|$  component is negligible with respect to  $|E_\theta|$  (11 dB below it), and patterns (a, and c) or (d, and f) are similar,

again considering the above equations. Figures (d, and f) are not exactly circular because of the presence of the box.

Figure (6.11) shows the patterns in the YZ cut. In this case,  $|E_{\phi}|$  is around 25 dB below  $|E_{\theta}|$  and this explains the similarity of figures (a, and c) or (d, and f). Here in (e), an asymmetry is seen between the upper and lower part of the pattern which reflects a similar asymmetry in the geometry of the radio-handset with respect to the XY plane in the coordinate system with its origin just at the base of the antenna as indicated in the figure (6.6).

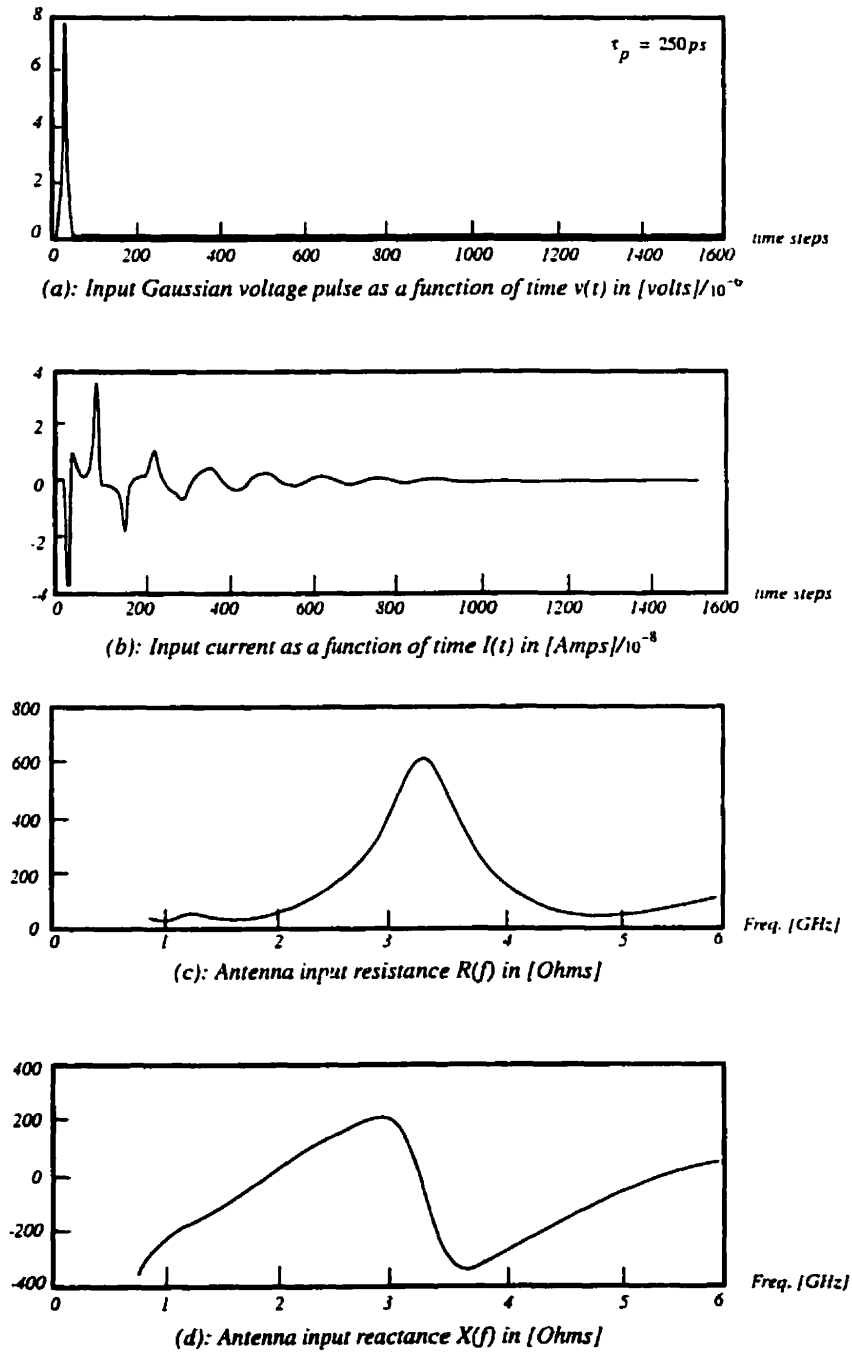
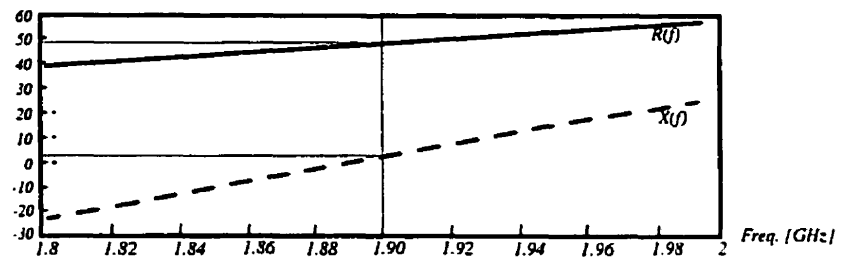
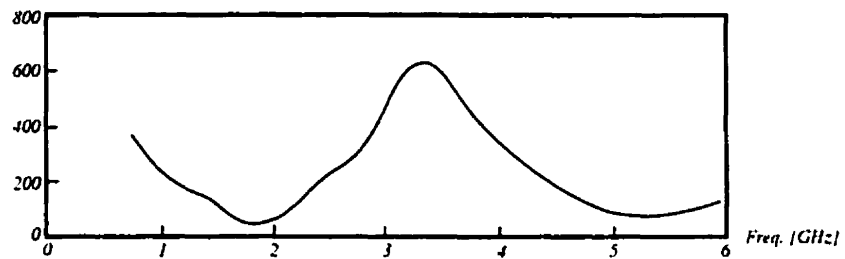


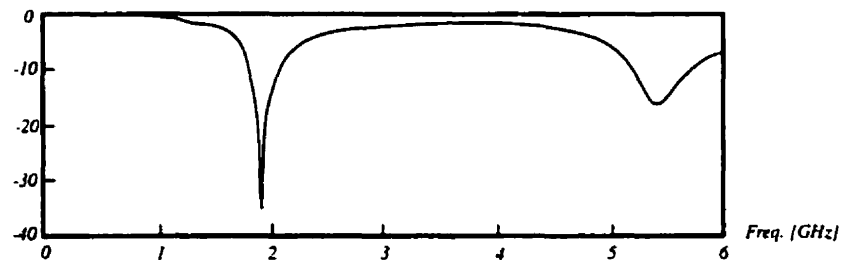
Fig 6.7: Input excitation, resulting current, and input impedance for the isolated radio-handset



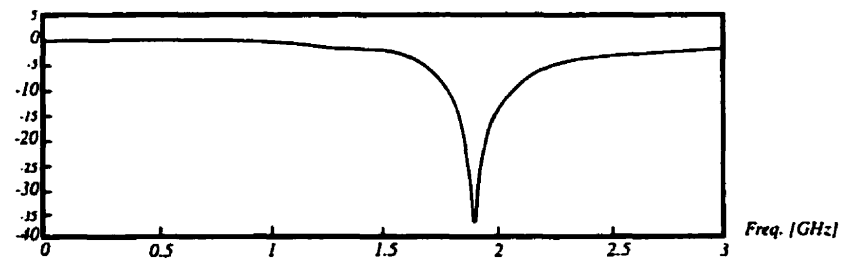
(a):  $R(f)$  and  $X(f)$  in the 1.8-2 GHz band in [Ohms]



(b):  $|Z(f)|$  in the 0-6 GHz band in [Ohms]



(c):  $|S11(f)|$  (dB) in the 0-6 GHz band



(d):  $|S11(f)|$  (dB) in the 0-3 GHz band

**Fig 6.8:**  $|Z(f)$ ,  $R(f)$ ,  $X(f)$ , and  $|S11(f)|$  in various frequency bands for the isolated radio-handset

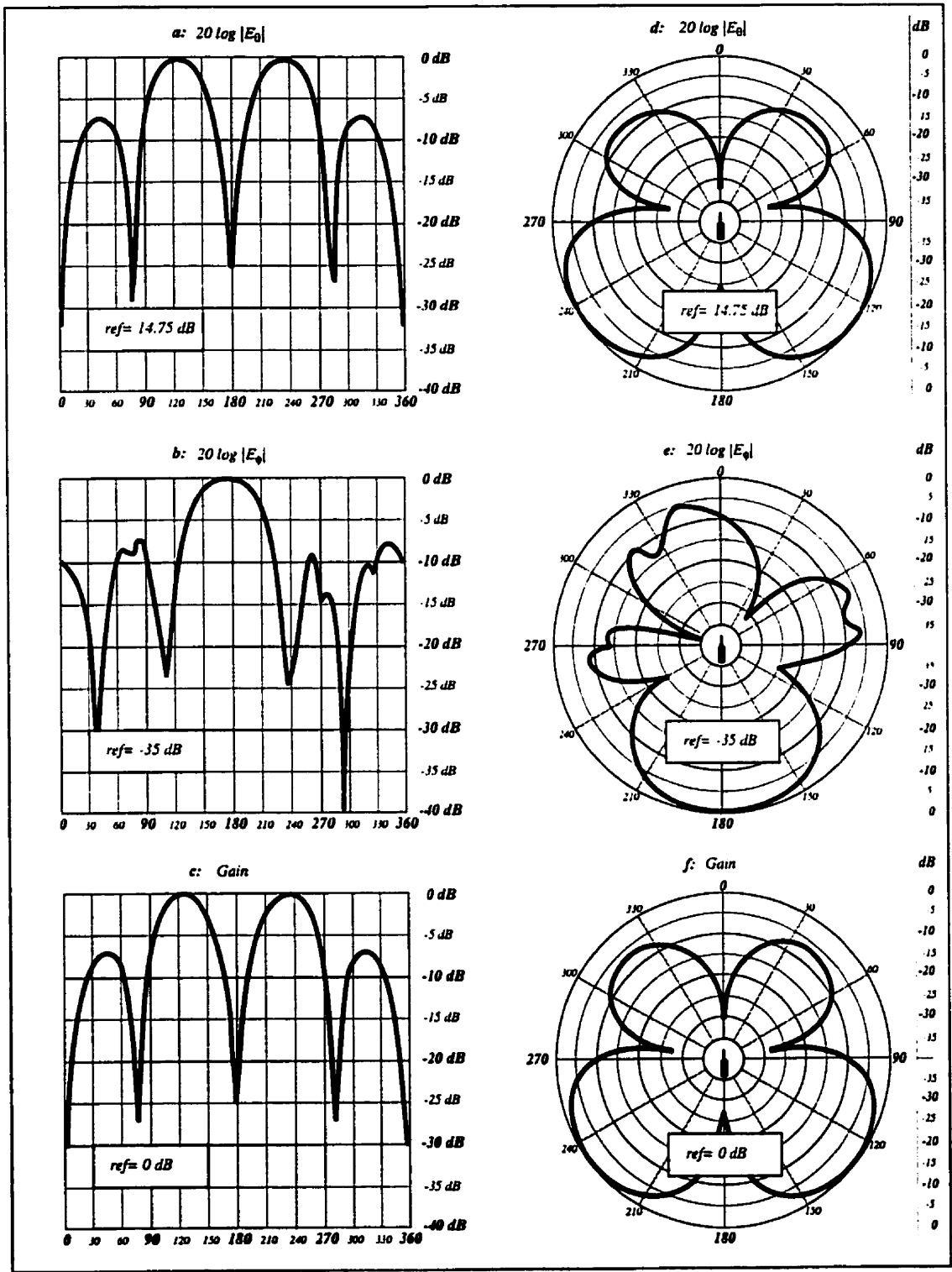


Fig 6.9: Radiation pattern of the isolated radio-handset in the XZ plane



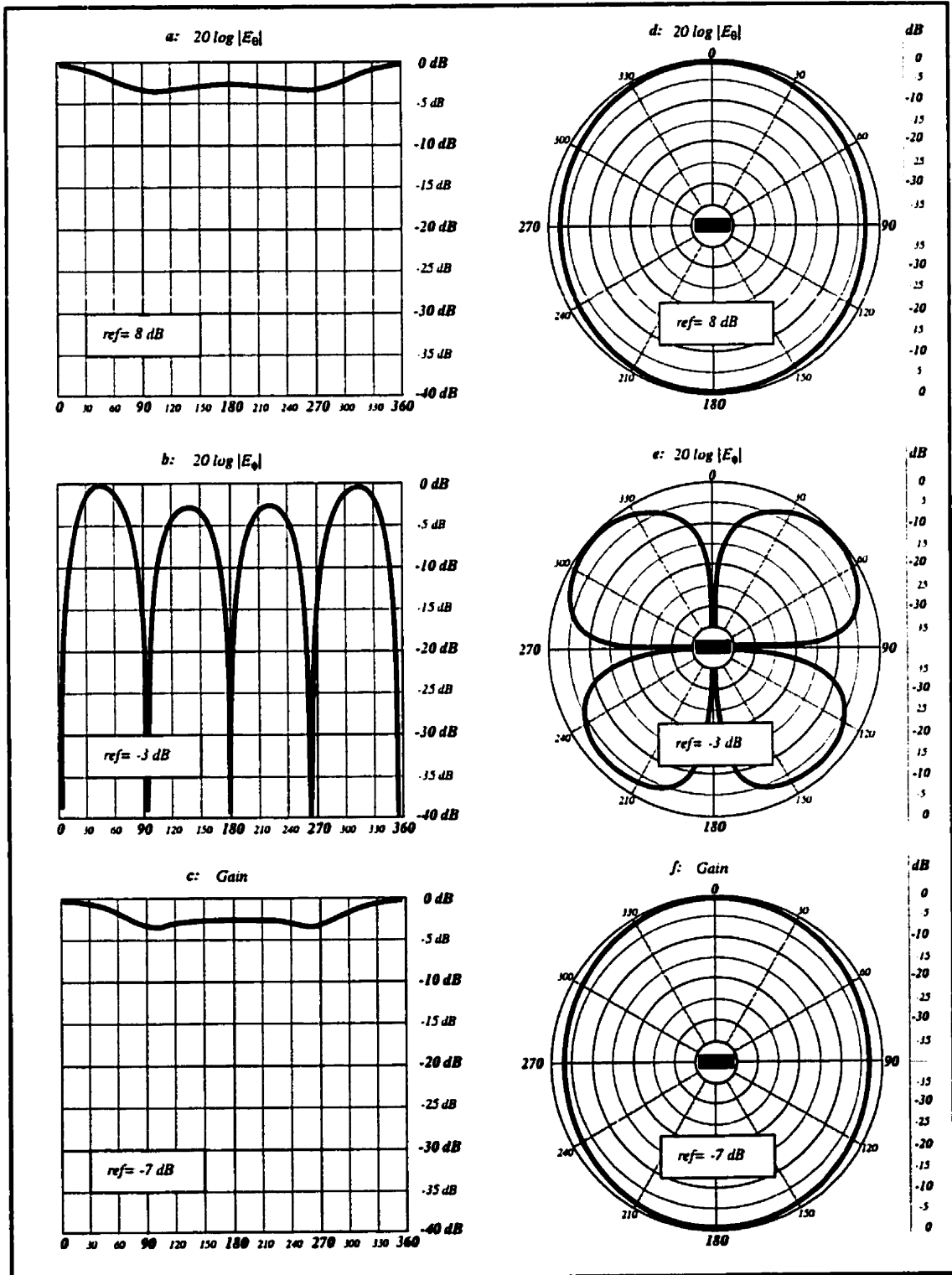
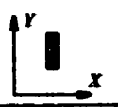


Fig 6.10: Radiation pattern of the isolated radio-handset in the XY plane





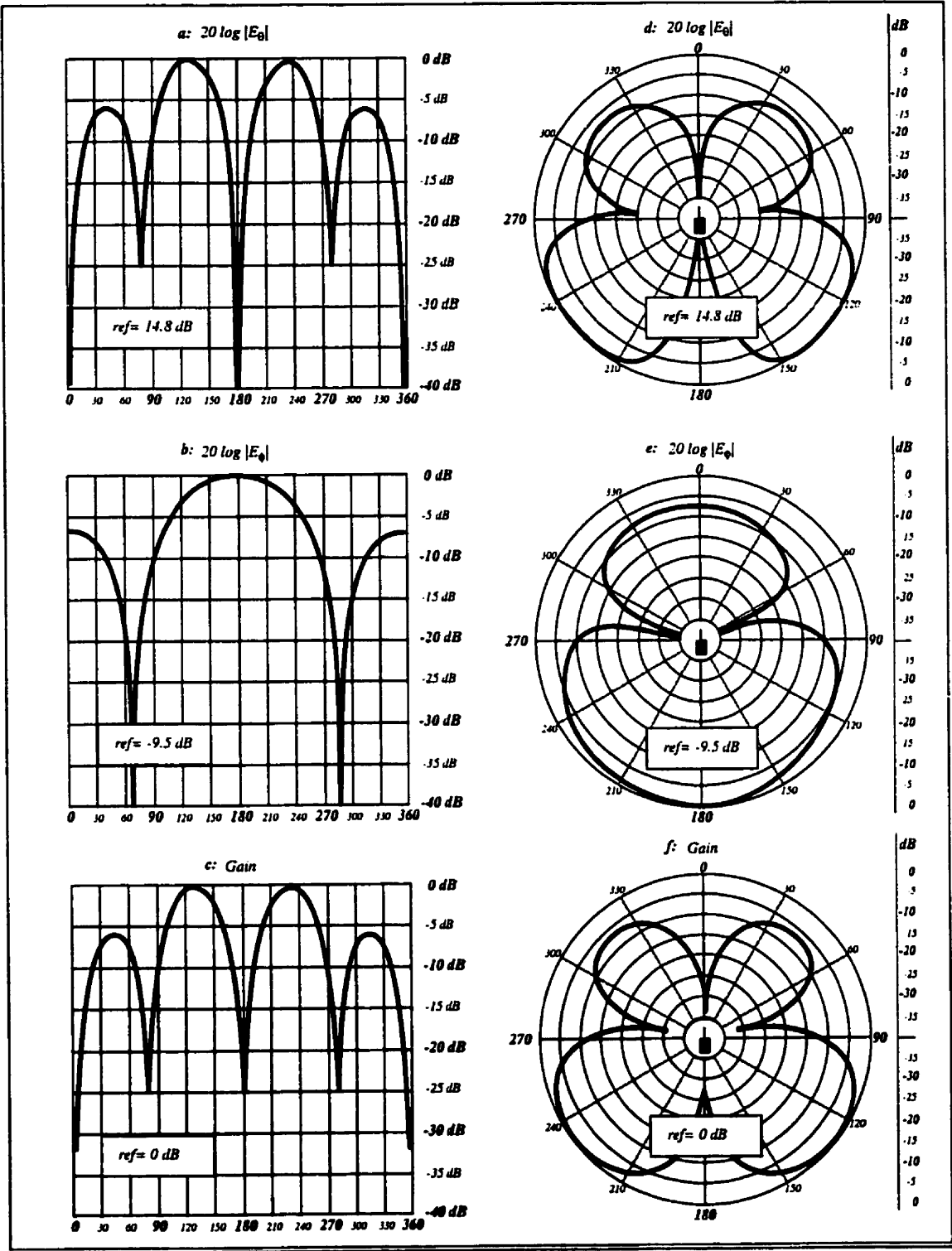
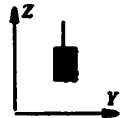


Fig 6.11: Radiation pattern of the isolated radio-handset in the YZ plane



### 6.5.2 Radio-handset in the presence of the human head model

In this case for impedance and radiation pattern calculations a homogeneous spherical model of the head (HS model) with radius  $RH=10\text{ cm}$  has been used. Figure (6.12) shows the system composed of the radio-handset and head model.

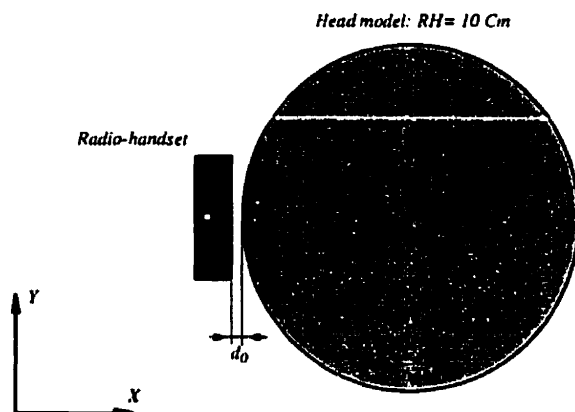
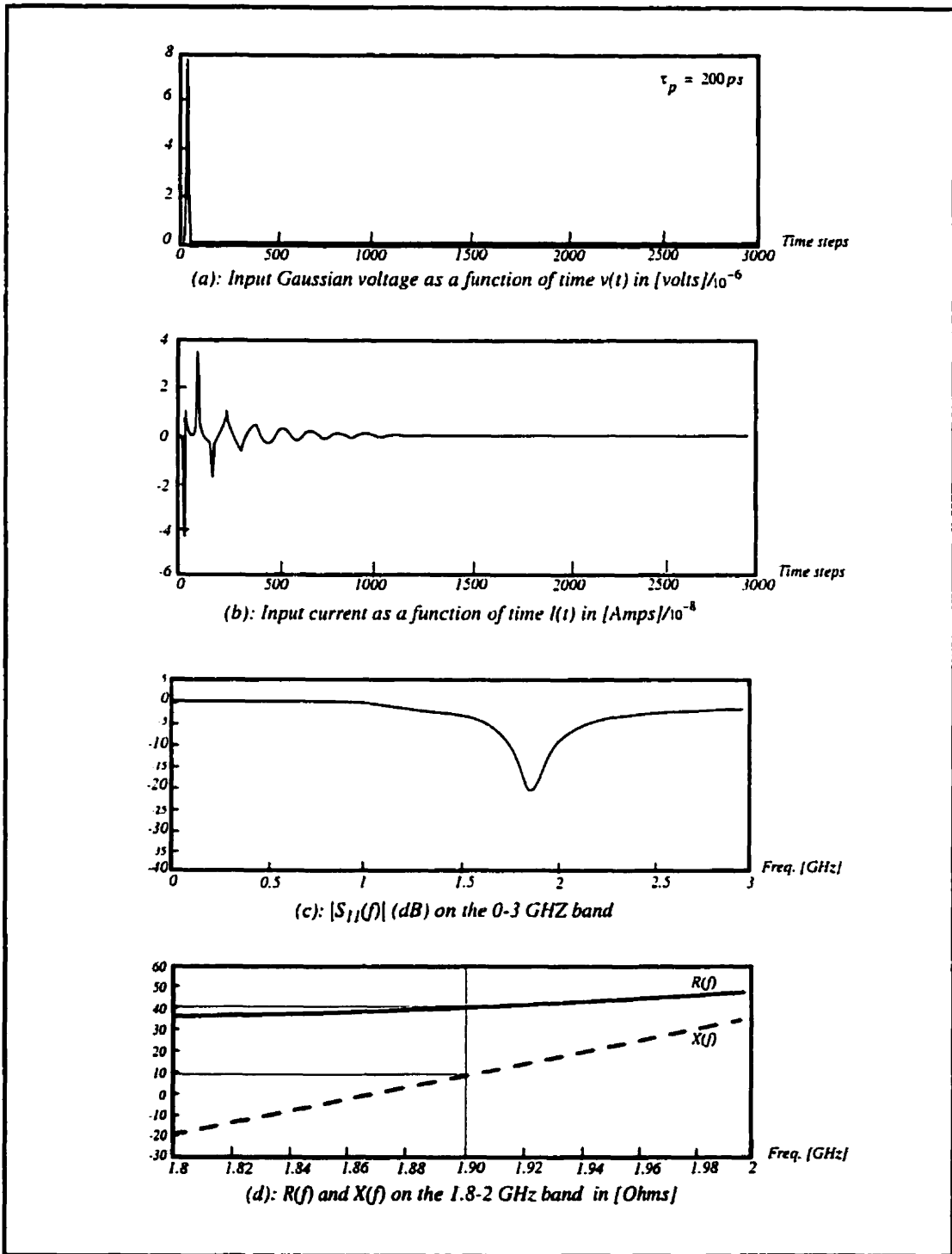


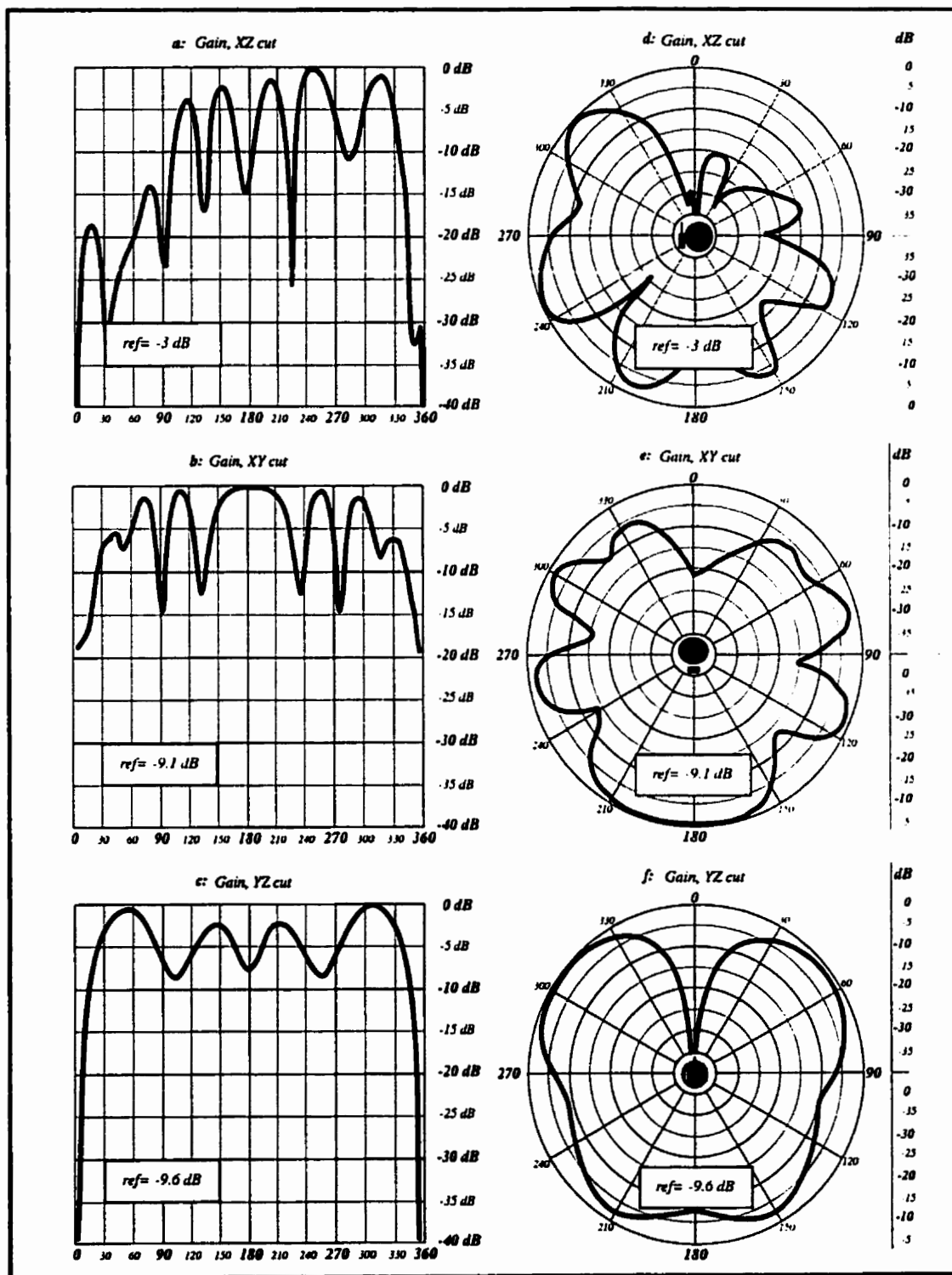
Figure (6.12) System composed of the radio-handset and head model

Figure (6.13) shows the input voltage, input current,  $|S_{11}(f)|$ , and real and imaginary parts of input impedance of the antenna on the 0-3 GHz and 1.8-2.0 GHz frequency bands. As is indicated on the figure (6.13 a and b), the total number of steps in this case is 3000. From Figure (6.13-d), the following values are estimated for the real and imaginary parts of the input impedance at the frequency of 1.9 GHz:  $R(f) \approx 40\Omega$ ;  $X(f) \approx 10\Omega$ .

Radiation patterns are indicated in the Figure (6.14) and represents the gains in three cuts of XZ, XY, and YZ cuts and were calculated for  $d_0=1\text{ cm}$



**Fig 6.13:** Input excitation, resulted current,  $|S_{11}(f)|$  in the 0-3 GHz band, and input impedance parts, in the 1.8-2 GHz band, for head-handset of figure 6.12



**Fig 6.14:** Radiation pattern in the XZ, XY and YZ cuts for the system of head-handset of figure 6.12

### **6.5.3 Effects of the head on the radiation pattern and input impedance**

#### **6.5.3.1 Effects on the radiation patterns**

Figure (6.15) shows the radiation patterns in the above mentioned cuts for the two cases of the isolated radio-handset and of the system composed of the radio-handset and the head model. The  $\lambda/4$  monopole antenna is situated at a distance of 2 cm ( $0.13 \lambda$ ) from the head model (a lossy dielectric with a radius of  $8.6 \lambda_{\epsilon}$  approximately). As is seen from the figure (a and b), due to shadow effect there is a 20 dB difference between the two sides of the head. The head blocks the radiation patterns in the head direction. In the XZ plane the radiation into half space where the head is situated is affected seriously, in the XY plane more attenuation is seen directly towards the head's direction, and in the YZ plane radiation into the lower half space is affected.

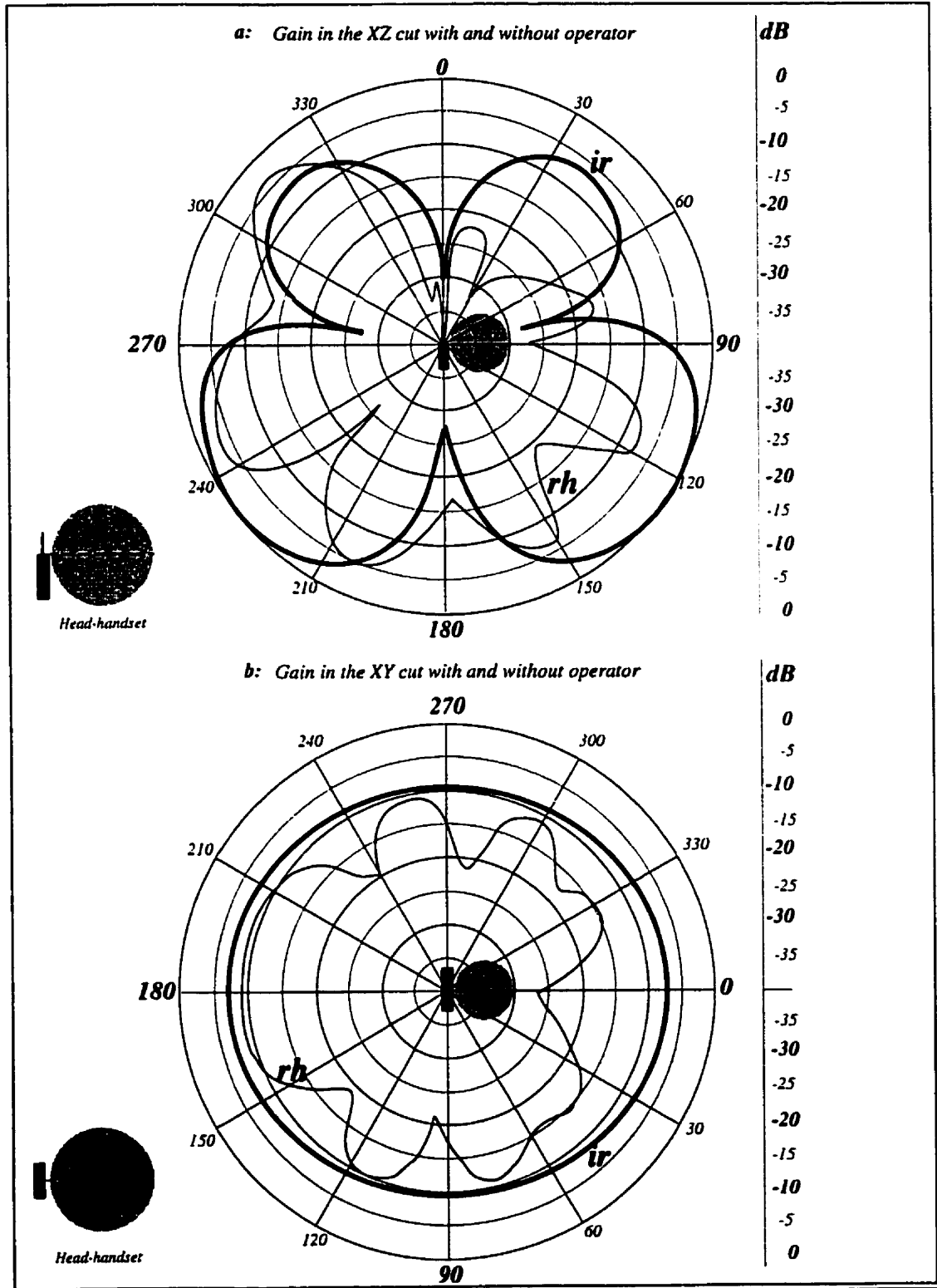
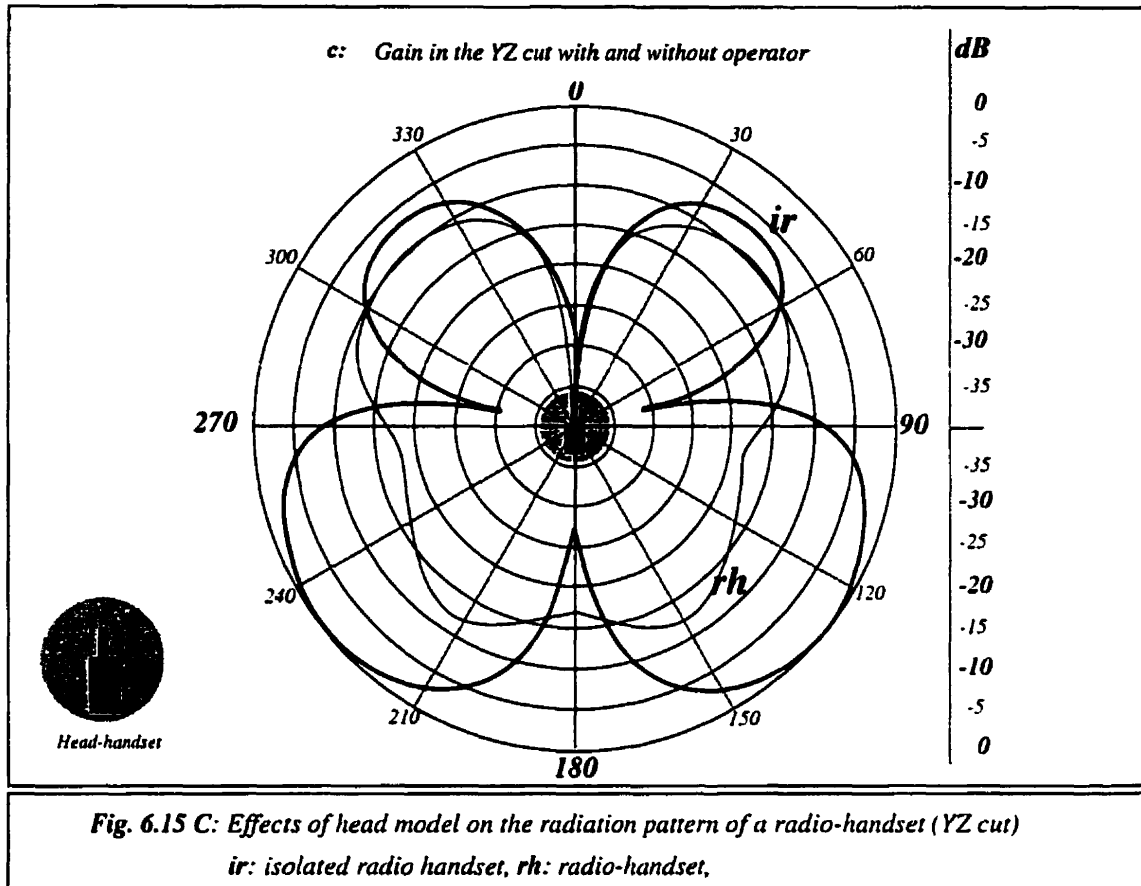


**Fig. 6.15 a, b: Effects of head model on the radiation pattern of a radio-handset;**  
 (a) XZ cut, (b) XY cut.  
*ir*: isolated radio handset, *rh*: radio-handset head,



### 6.5.3.2 Effects of the head on the input impedance

Figure (6.16 a) shows the real and imaginary parts of the input impedance of the antenna in two cases of isolated radio-handset and head-handset. As already mentioned, at this distance of 2 cm between the source point and the head the effect of the head on the input impedance of the antenna model used, is not so high. The effect in the figure (6.16 a) is a small frequency shift (to 1.87 GHz). At the working frequency of 1.9 GHz the impedance components are:  $R(f) \approx 40\Omega$ ;  $X(f) \approx 8\Omega$ . The same effects are observable in the figure (6.16 b), in which a frequency shift and a small impedance change is clearly seen. In this study a distance of 2 cm has been used. Regarding the geometry of the box with a distance of 1 cm from the source point to the box edge, which is a reasonable value, adding 1 cm as the distance between the head and the box, which is an acceptable estimation, the above mentioned distance between the source point and the head (2 cm) seems to be reasonable.

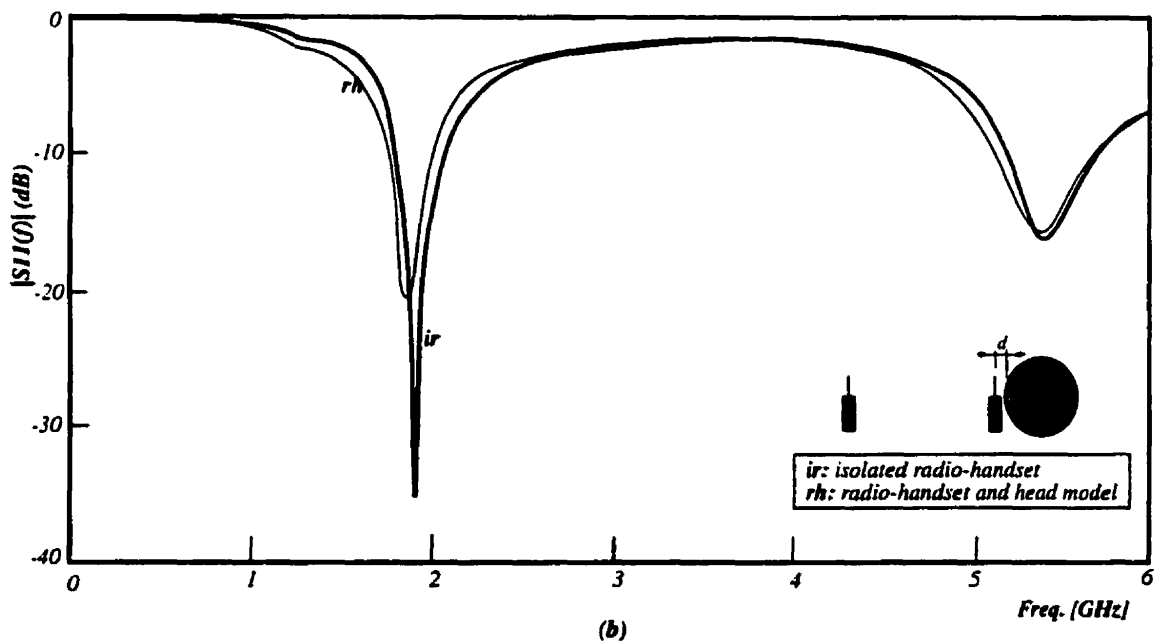
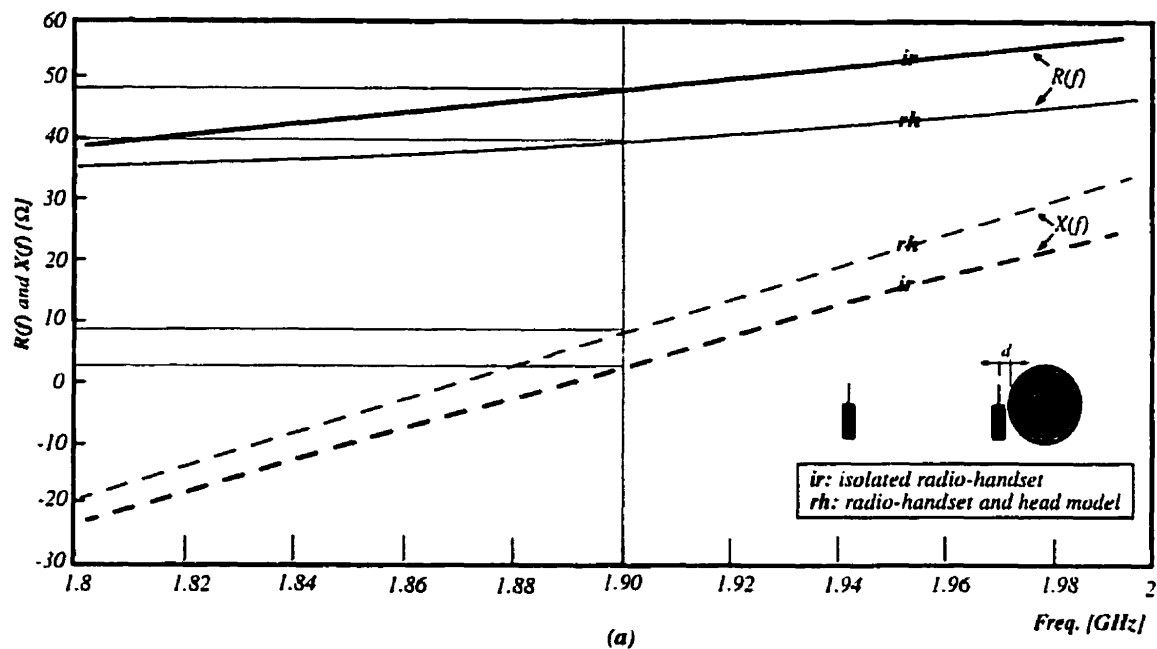


**Fig. 6.16:** Effects of the head model on the input impedance of the radio-handset. Comparison of results for two cases of isolated radio-handset (*ir*), and radio-handset near the head model (*rh*).  $d=2$  Cm

(a):  $R(f)$  and  $X(f)$  in the 1.8-2 GHz band

(b):  $|S_{11}(f)|$  (dB) in the 0-6 GHz band

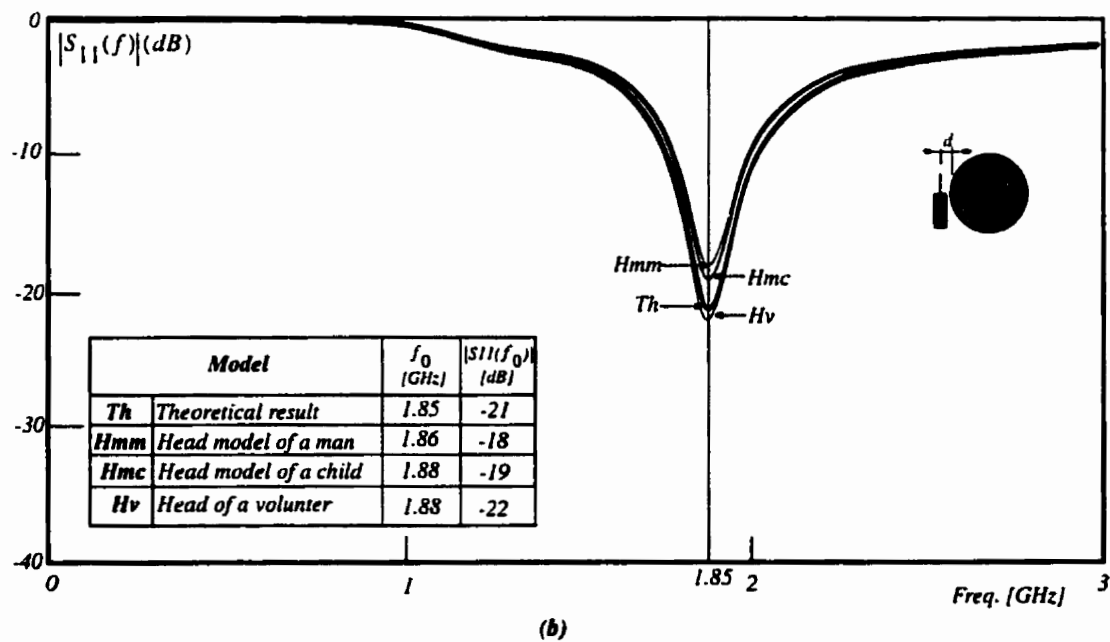
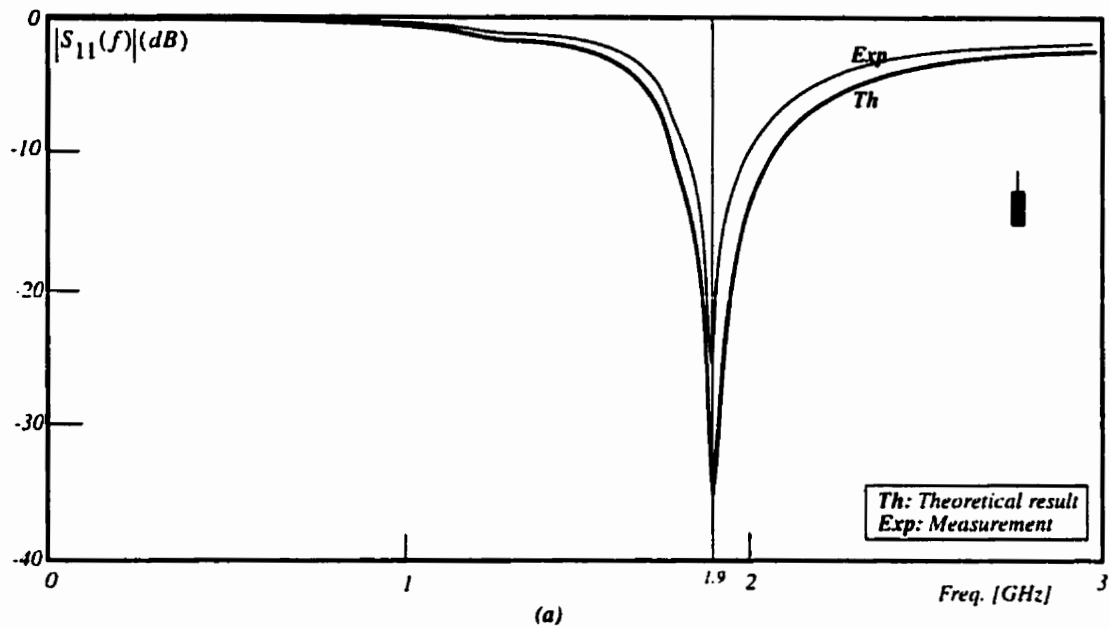


#### **6.5.4 Experimental verification of the results**

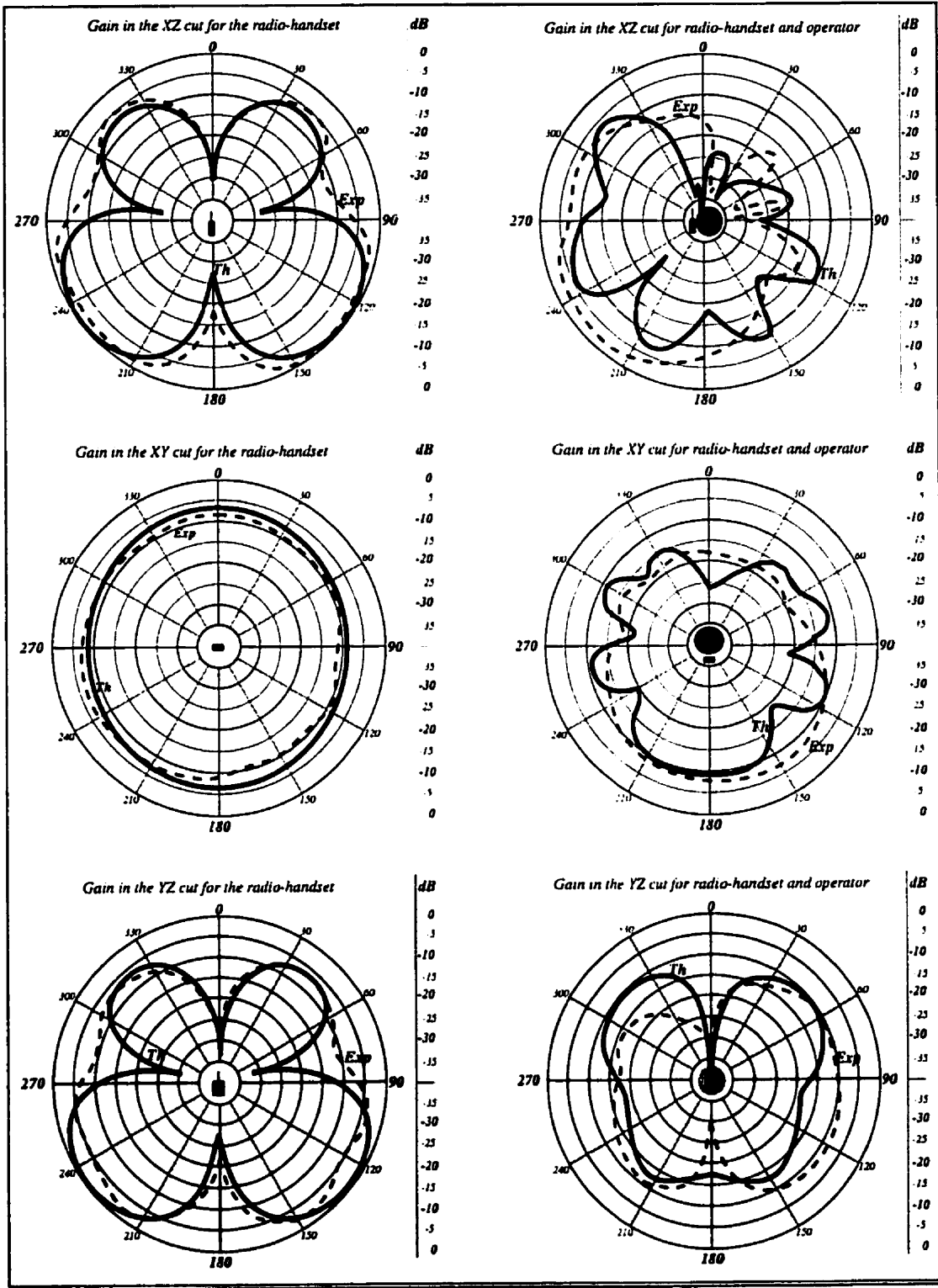
Figure (6.17) shows the results of measurement on  $|S_{11}|$  at the antenna input to verify the impedance calculations for the two cases. It is seen that the measurement confirms the impedance calculations regarding the centre frequency and impedance match. The effect of the head on the impedance curve is a small shift in centre frequency. In addition both size effect and homogeneity have a negligible effect on the frequency response of the radio-handset.

Figure (6.18) shows the results of the measurements on the radiation patterns in three different cuts in comparison with their related theoretical results. Regarding the conditions of the experiments, specifically in comparison with the theoretical cases, two points are important. Firstly, the head model has the form and size of the head of an adult versus a spherical head used in the calculations. Secondly, the head handset distance was around 5 mm versus 10 mm in the theoretical case. In addition experiments have been performed in the exterior, due to lack of a suitable anechoic chamber. The receiver transmitter antennas distance was 120 cm to set a far field measurement condition. A reference level is considered for all cases. This is the level of the maximum gain in the radiation pattern of the xz cut for the radio-handset. This level has been used already in our presentations of the theoretical patterns. In the case of experimental results, too, the same relation existed between the gain levels in different cuts, and naturally the maximum value in the experimental gain for that cut was considered to be coincident with its counterpart in the theoretical results. In the following the experimental results will be considered in comparison with their theoretical counterparts.

Generally there are good agreements between the theoretical and the experimental results. Nearly in all cases of the experimental patterns, the deep nulls present in the theoretical patterns have been removed to a large extent. This is understandable and may be due to reflections in the medium. In the case of the isolated radio-handset, experiments confirm closely the theoretical results. In the case of the head-handset, more pronounced differences between theoretical and experimental results are observed. These may be attributed, in addition to the above mentioned reflections, to the two differences in the configurations of the head-handset for the theoretical and experimental cases as is explained above.



**Figure (6.17):** Comparison of the simulation results and the results of measurements for  $|S_{11}(f)|$  (dB) at the antenna in the (0-3 GHz) frequency band.  $d=2$  cm  
 (a): For the isolated radio-handset  
 (b): For the system composed of the radio-handset and human head models.



**Fig. (6.18) Experimental verification of the radiation patterns**

## 6.6 Results of the SAR calculations

In SAR calculations four different head models have been used. These relatively simple models are named NHN (NonHomogeneous model with Neck), NH (Nonhomogeneous model without neck), HN (Homogeneous model with Neck), and HS (Homogenous Spherical model). Models NHN, NH, and HN have been developed for this study by the author and model HS has already been used by Toftgard et al. [36]. The SAR calculations are based on  $5\text{ mm} \times 5\text{ mm} \times 5\text{ mm}$  cell sizes. Although in the case of SAR calculations smaller cell sizes lead to better results, our choice of the above cell size was mainly due to limitations of memory at the time of the SAR calculations.

For this series of calculations the FDTD space size varies from  $82 \times 78 \times 78$  cells for models without neck (NH and HS models) and minimum head-source point distance of 15 mm, to  $89 \times 78 \times 83$  cells for models with neck (NHN and HN models) and maximum head-source point distance of 50 mm.

A single frequency voltage has been used as the excitation of the radio-handset. The forcing function was imposed in a vertical gap of one cell size at the base of monopole. The calculated  $E$  field distribution has been used to calculate the SAR distribution. This SAR distribution is a time harmonic function. Its maximum at any time step has been specified both in its magnitude and its location. From these data the time average of the spatial peak values of the SAR distribution has been calculated as a function of the distance “ $d$ ” between the head model and the source point of the radio-handset. Then the following aspects have been studied using the resulted data: Time average of the spatial peak of the SAR distribution in different tissue types, Effect of the neck on the peak of the SAR, Effect of nonhomogeneity of the model on the SAR, and the effect of head size on the resulting SAR. In the following the results obtained will be explained referring to the related figures.

### 6.6.1 Peak of the SAR in different tissues

Figures (6.19) and (6.20) represent the time average spatial peak for the SAR in heterogeneous models (NHN and NH). In both cases the values of the spatial peak of SAR in muscle is higher than the corresponding values in the brain. For both models the corresponding values in the eyes are negligible. In addition these figures indicate that the peak of the SAR in the NH model is higher than the corresponding values in the NHN model.

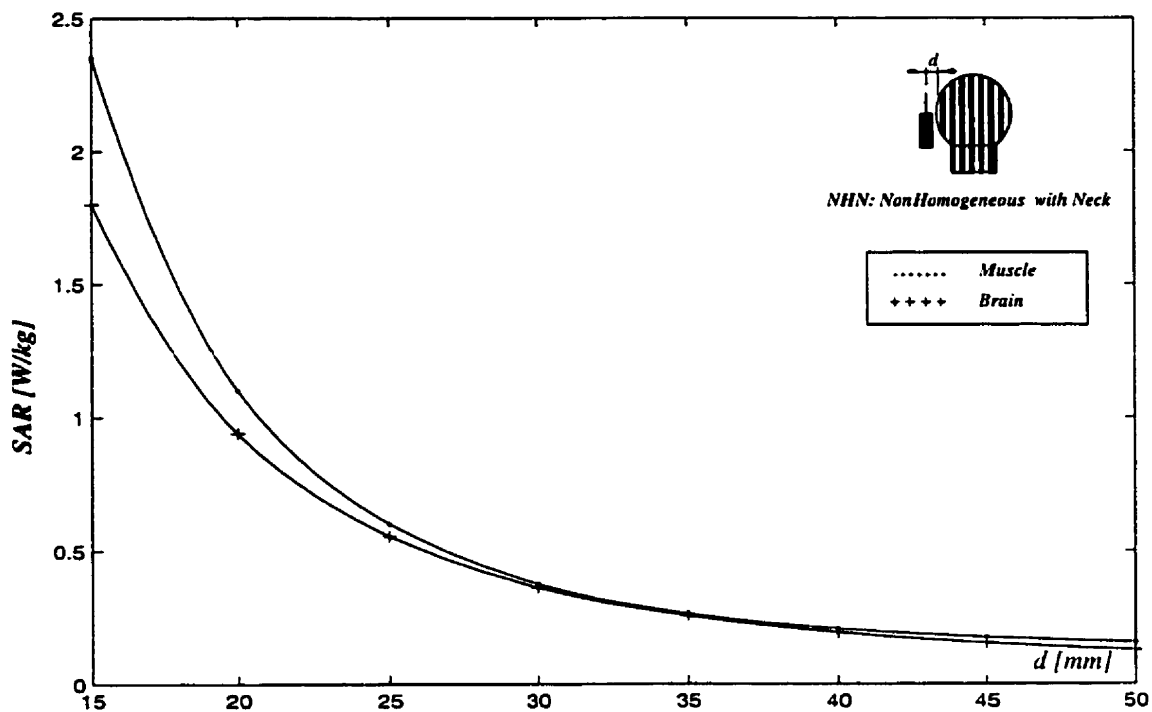


Fig. 6.19-Time averaged spatial peak of SAR [W/kg] in NHN model tissues as a function of distance "d"

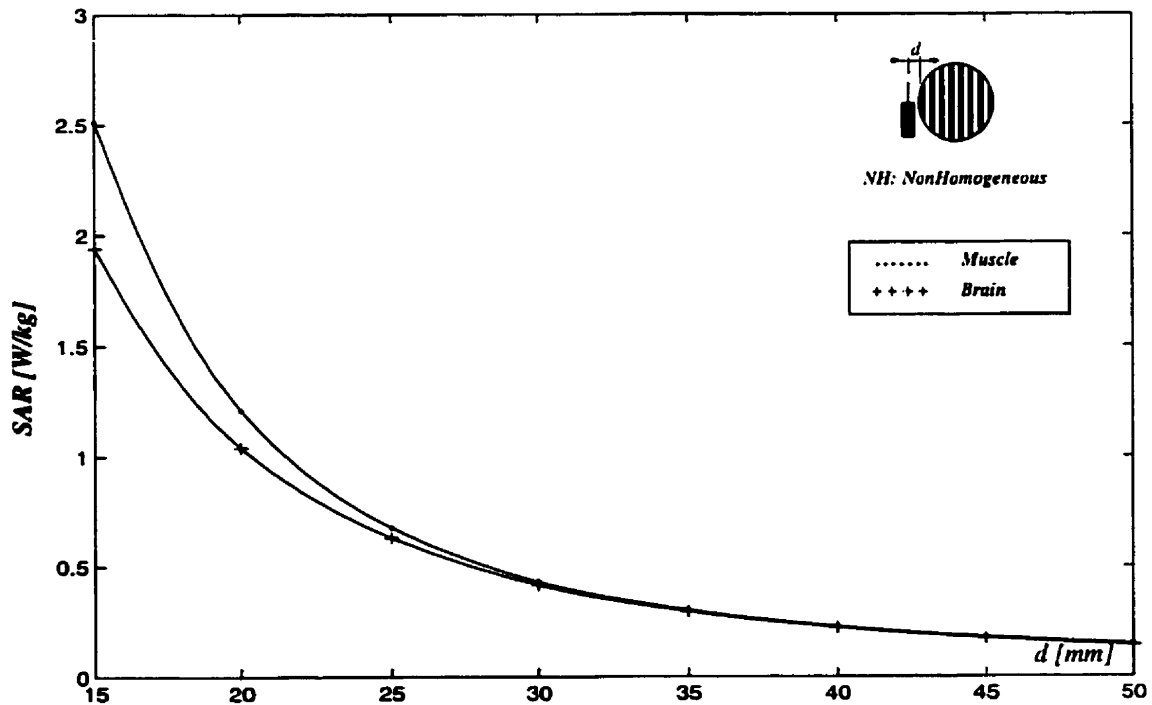
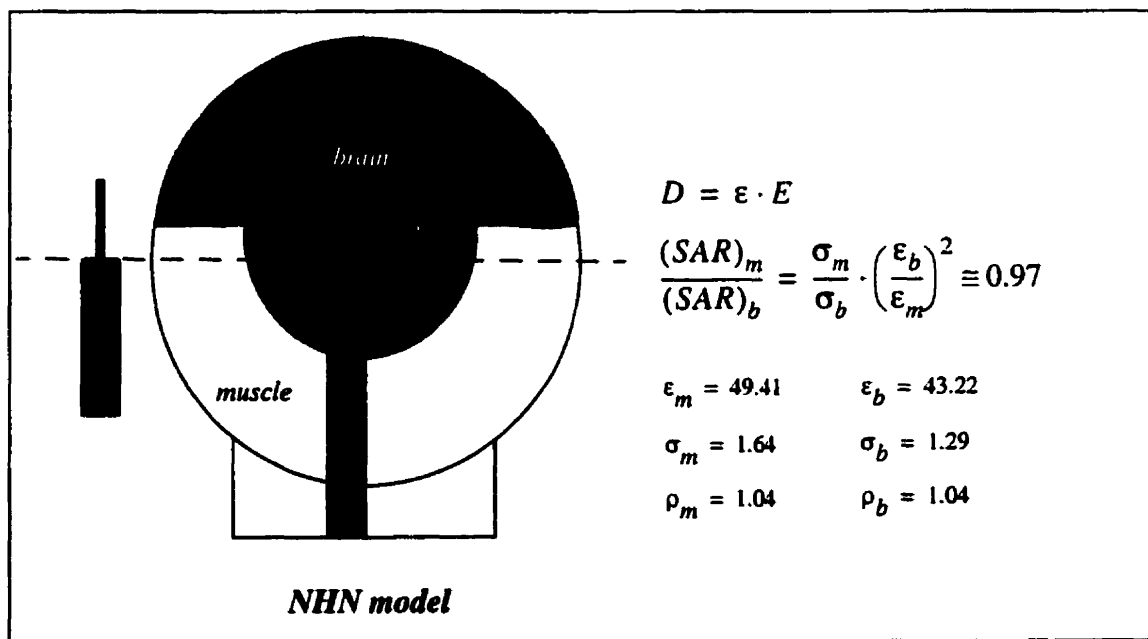


Fig. 6.20-Time averaged spatial peak of SAR [W/kg] in NH model tissues as a function of distance "d"

In addition, as is seen in Figures (6.19) and (6.20) for  $d > 30\text{mm}$  the peak values of the SAR in both tissues are the same. With decreasing the distance  $d$ , the difference between their values rises. This behavior may be explained considering the difference in the dielectric properties of the related tissues as follows: The source point of the antenna and the centre of the spherical part of the head are on the same level, Fig. (6.21). Field is inhomogeneous and more intense points are situated in the muscle. Up to the distance of  $d = 30\text{ mm}$  the SAR in the muscle is higher than its value in the brain. This may be attributed to the nonhomogeneity of the field. Using the relations  $D = \epsilon \cdot E$  and  $SAR = (\sigma \cdot E^2)/\rho$ , the ratio between the SAR values in these tissues under a uniform field distribution is around unity (0.97). With raising the distance the penetrated field in the head will be more homogeneous. For  $d > 30\text{mm}$  the SAR ratio of tissues is determined by their relative electrical properties and is practically equal to one. This is more pronounced in the case of NH model in which there is no neck and this eliminates a potential source of field heterogeneity. In fact the small difference between the SAR values in the tissues of the NHN model may be attributed to the effect of the neck.



**Figure (6.21)**-Tissues arrangement relative to the antenna point source.

### **6.6.2 Effect of the neck on the peak of SAR**

Figures (6.22) and (6.23) show the spatial peak values of the SAR in the NHN and HN models against the corresponding results in their corresponding model without neck (NH and HS model respectively). In both cases adding the neck resulted in a decrease in the SAR of around 5%. For  $d > 45\text{ mm}$  the neck has no effect on the peak of the SAR.

### **6.6.3 Homogeneity versus heterogeneity**

Figures (6.24) and (6.25) show comparison of spatial peak values for nonhomogeneous models (NHN and NH) with those of homogeneous models (NH and HS models respectively). In both cases a perfect match is seen between the corresponding results. That means that, heterogeneity has no effect on the peak of SAR value, and that homogeneous models are capable to give good results. Evidently in the process of development of homogeneous models one important step is to find a relevant value for the “equivalent dielectric constant” of the model. Our method to calculate this as explained earlier is based on a volume averaging, considering the volumes of each tissue and their dielectric constant. In these conditions, the equivalence of the SAR values for homogeneous and heterogeneous models seems to be natural.

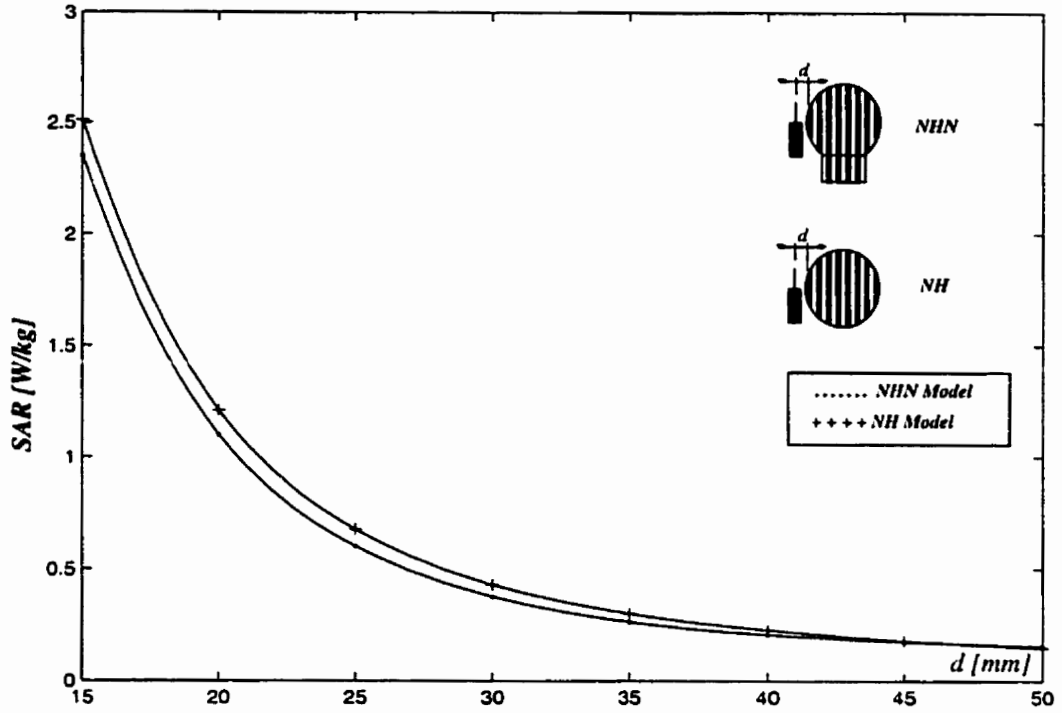


Fig. 6.22-Time averaged spatial peak of SAR [W/kg] in NHN and NH models

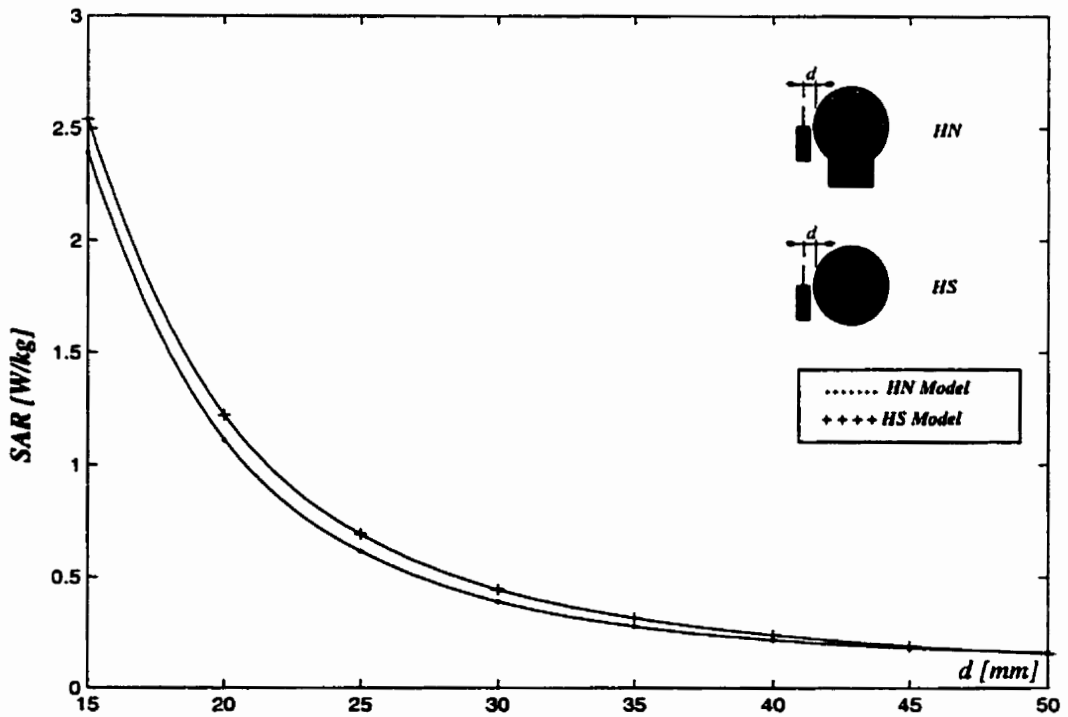


Fig. 6.23-Time averaged spatial peak of SAR [W/kg] in HN and NS models



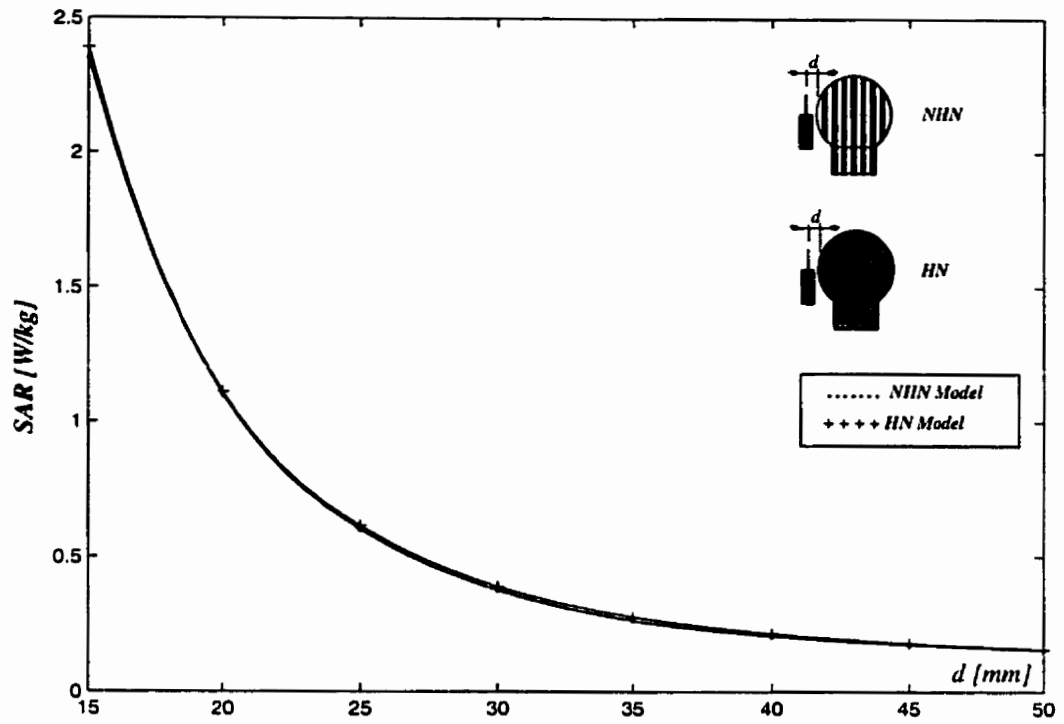


Fig. 6.24-Time averaged spatial peak of SAR [W/kg]: NHN model versus HN model

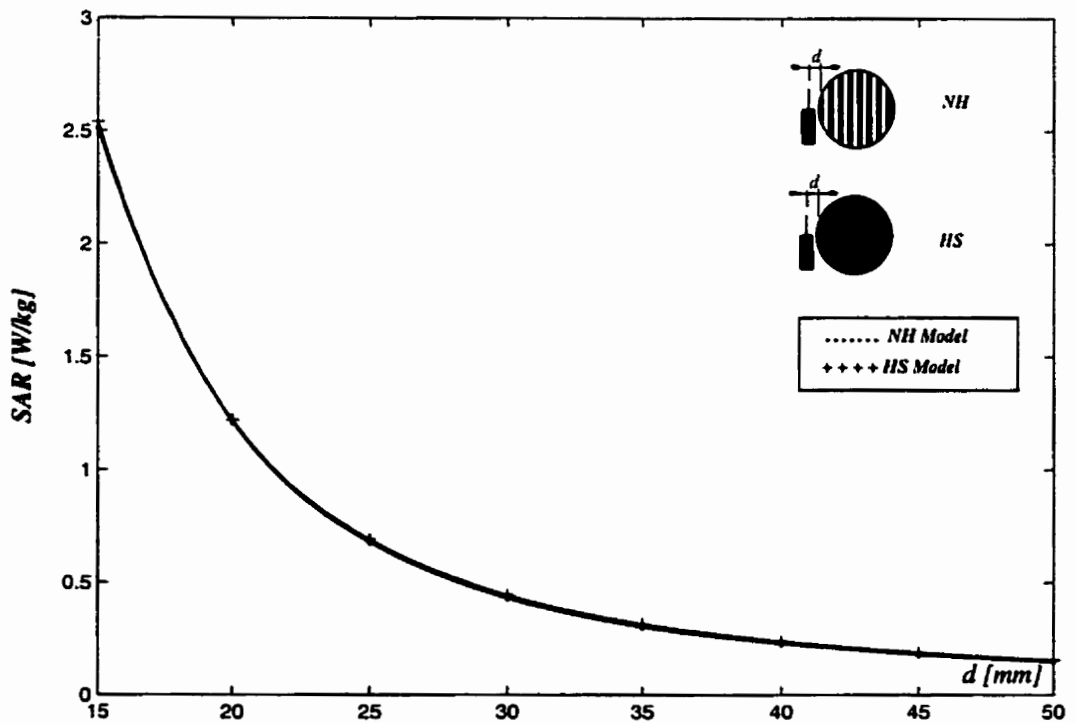


Fig. 6.25-Time averaged spatial peak of SAR [W/kg]: NH model versus HS model

#### 6.6.4 Effect of head size on the Peak of the SAR

Figure (6.26) shows a comparison of the results obtained for the NHN model of different sizes ( $RH=10\text{ cm}$  and  $RH=9\text{ cm}$ ). It is seen that decreasing the head size results into an increase in the spatial peak of the SAR value in the head. The above mentioned sizes have been used, because our calculations are based essentially on adult size models, and to the extent that spherical models are concerned, these sizes seem to be representative of real adult head sizes. It is interesting to note that, comparing Figure (6.26) and the two curves in Figure (6.25), the peak of the SAR for the smaller model is very close to the corresponding values for the model without neck. That means that adding the neck and reducing the radius of the spherical section in the head models by 10% has two compensating effects. As has already been explained adding the neck results in a decrease in the peak of the SAR.

#### 6.6.5 Power absorbed in the head and radiation efficiency

Figure (6.27) shows the percentage of the absorbed power in the NHN model of the head with respect to the antenna input power. The percentage of the radiated power of the head-handset or its radiation efficiency is also indicated in the same figure as another curve. In this figure too, the variable is the distance between the head model and the antenna source point. As is seen, under the normal distance of  $20\text{-}15\text{ mm}$  from the head to the source point ( $10\text{-}5\text{ mm}$  from the head model to the box) the radiation efficiency of the system would be 72% to 62%. In Table (6.6) the percentage of absorbed power in the head for three different values of " $d$ " ( $15\text{-}25\text{ mm}$ ) are indicated.

Table (6.6): Normalized absorbed power in the head

$d$ [mm]	$P_{\text{head}}/P_{\text{in}}$ [%]
15	37.21
20	27.18
25	21.13

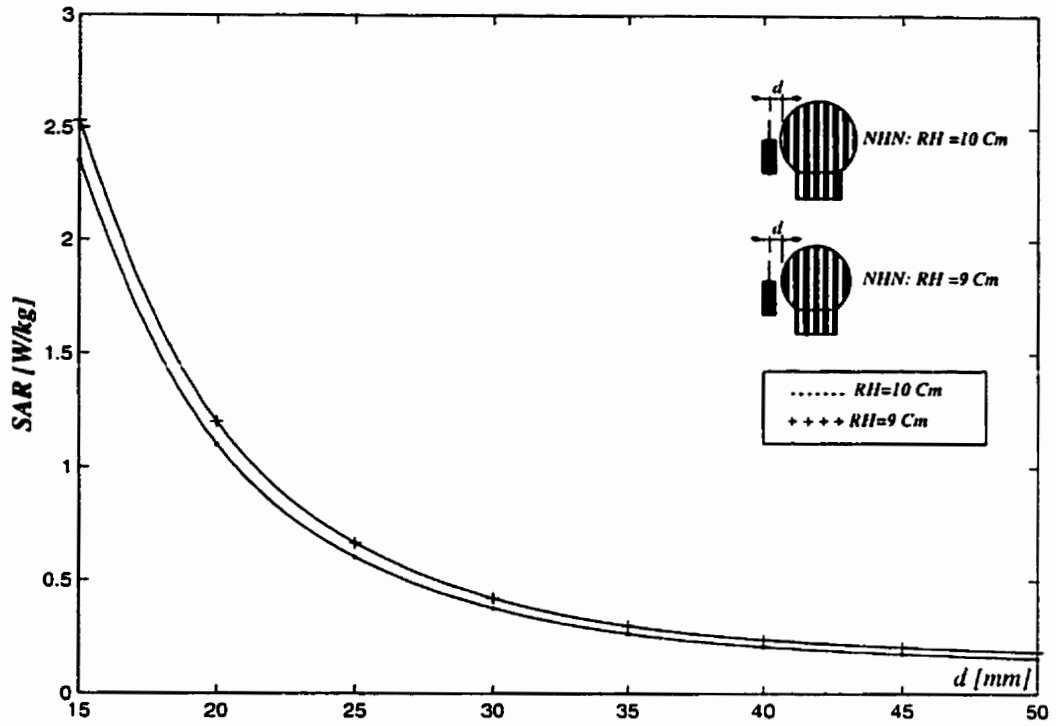


Fig. 6.26-Time averaged spatial peak of SAR [W/kg]: Effect of head size

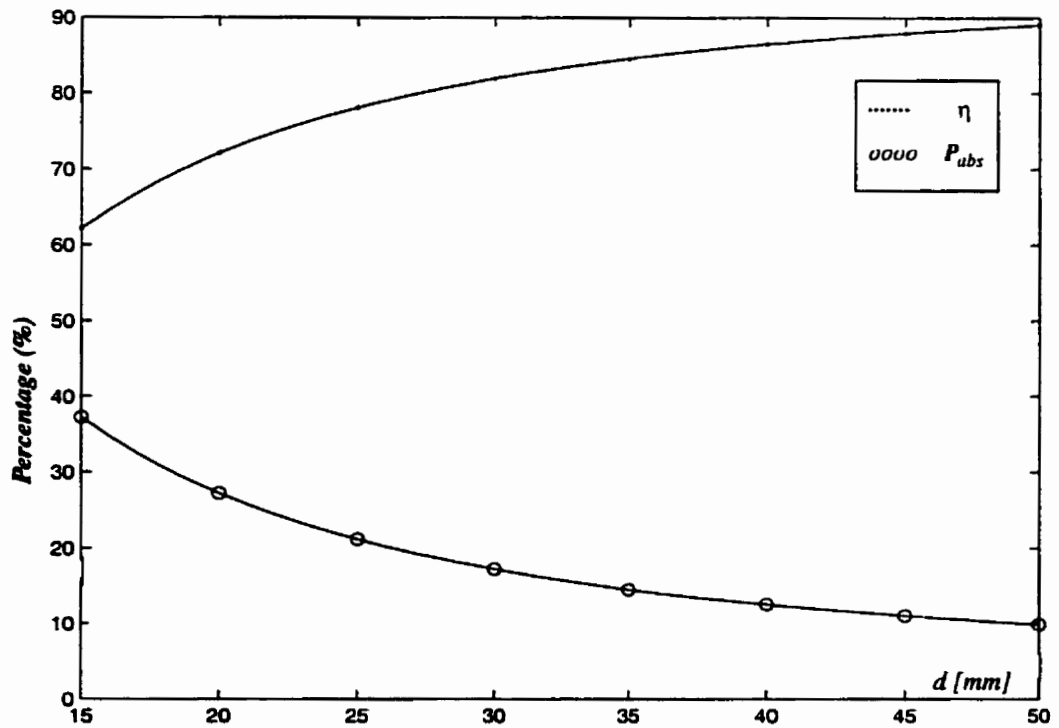


Fig. 6.27-Radiation efficiency ( $\eta$ ) and absorbed power percentage ( $P_{abs}$ ) % in the head

## Chapter 7

### Discussion and Conclusion

#### 7.1 Introduction

This study has considered the interaction between a radio-handset and the head of its user at the frequency of 1900 MHz, using the FDTD method and simple homogeneous and heterogeneous head models.

By interaction one refers to the effects of the head on the performance of the radio-handset, on the one hand, and the deposited power in the head, quantifiable by the SAR, on the other hand. The first class of effects is studied by calculating the input impedance and radiation patterns of the radio-handset both in the absence and in the presence of the head model. The effects of the radio-handset on the head is studied by calculating the time average of the spatial peak of the SAR in the head models. In the following a review of the general points about these studies and the results obtained, along with what should be done in the future, will be considered.

#### 7.2 Input impedance

In the input impedance calculations a spherical homogeneous model of the head with a radius of 10 cm has been used. The cell size was  $2.5\text{mm} \times 2.5\text{mm} \times 2.5\text{mm}$  and the distance between the head model and the source point of the antenna was 2 cm. Under these conditions the effect of the head on the input impedance was just a small shift in the centre frequency of the radio-handset. A good agreement has been observed between the results of input impedance calculations using the FDTD method, and experimental measurement on a wide band of frequencies (0-3 GHz), in both cases of the absence and the presence of the head model in the proximity of the radio-handset.

### **7.3 Radiation patterns**

Radiation patterns of the radio-handset, in the two cases of isolated handset and head-handset and in three cuts (XZ, XY, and YZ), have been calculated. In both cases good agreements is seen between the numerical results and those obtained by measurements. In both cases  $5\text{ mm} \times 5\text{ mm} \times 5\text{ mm}$  cells are used and head model was spherical homogeneous one at a distance of 2 cm from the source point of the radio-handset. Calculations and measurements show that the head blocks the radiation patterns in the head direction. In the XZ plane the radiation into half space where the head is situated is affected seriously, in the XY plane more attenuation is seen directly towards the head's direction, and in the YZ plane radiation into the lower half space is attenuated moderately.

### **7.4 Specific Absorption Rate (SAR)**

Four different models of the head have been used in the SAR calculations: NHN, or Non-Homogeneous model with Neck; NH, or NonHomogeneous model without neck; HN, or Homogeneous model with Neck; and HS Homogeneous Spherical model. The common element of all the above four models is a spherical section with a radius of 10 cm. The NHN model contains 3 tissue types of muscle, brain and humor. In addition nasal and mouth cavities have been considered in the model. Corresponding to each heterogeneous model a homogeneous model with the same size and geometry has been calculated with an equivalent dielectric constant equal to the volume average of the dielectric constant of its counterpart heterogeneous model.

Time average of the spatial peak for the SAR as a function of the distance between the head and radio-handset in the range (15-50 mm) in all the above models have been calculated. The effects of the size, neck, and heterogeneity is detectable by comparing the results, as follows.

Spatial peaks of the SAR in the homogeneous models and in their equivalent heterogeneous models are equal. That means, at least to the extent that just the problem of the heterogeneity is concerned, no effect in the spatial peak of the SAR is detectable. This may be due to our method of volume averaging to find the equivalent dielectric constant of the homogeneous models.

Regarding the effects of the size and neck, there are some points to be noted. Firstly, the

spatial peak of the SAR in the head model with neck used is less than that of the model without neck. Secondly, reducing the size of the head model leads to an increase in the spatial peak of the SAR. Thirdly, it is seen that adding the neck reduces the spatial peak value of the SAR by 5%, while reducing the size of the head by decreasing the radii of the spherical section and the cylindrical neck by 10% leads to a 5% increase in the peak value of the SAR. That means a compensating effect related to reducing the head size and adding the neck to the model at the same time. This aspect may be useful, in the comparison of the results obtained for MRI based head models with those for simple head models, specifically when these comparisons will serve to judge the value of simple models.

### 7.5 Radiation efficiency

In another series of calculations, the percentage of the absorbed and lost powers in the head and the radiated power from the head-handset system with respect to the input power as a function of head-handset distance in the range of (15-50 mm) were calculated. Calculations show that, at a distance of 15 mm, more than 37.5% of the input power is absorbed in the head, which corresponds to a radiation efficiency around 62.5%. These values are in a very good agreement with similar results reported by Gandhi, [15], using an MRI based model of the head. Around 50% of the absorbed power in the head is lost as heat. Table (7.1) indicates a comparison of SAR calculation results,  $P_{abs}\%$ , and  $\eta\%$  with those obtained by Gandhi [15].

Table (7.1)-Comparison of results of SAR,  $P_{abs}$ , and efficiency with those obtained by Gandhi [15]

Model	Peak 1-voxel SAR [W/kg]	$P_{abs}\%$	$\eta\%$
NHN	2.5	37.5	67.5
NH	2.35	-	-
HN	2.5	-	-
HS	2.35	-	-
Gandhi-1	1.54	45.4	54.6
Gandhi-2	-	35.6+13.8	50.6
Gandhi-1: 1800 Mhz, distance: 13.8 mm			
Gandhi-2: 1900 Mhz, $P_{abs}(\text{head and neck})\%=35.6$ , $P_{abs}(\text{hand})\%=13.8$			

## **7.6 Difficulties and factors influencing these studies**

Analyzing the head-handset system may encounter difficulties originating from its interacting parts, handset and head, from their relative positioning referred to as configuration of the system, or from the working frequency. These aspects will be considered below.

Regarding the head, one should note that the human head is not a unique object. It may have a vast variety of forms and sizes. In these conditions no head model should be considered as a representative model of the real head, and using the adjective “adult sized” can not remove all ambiguities present in the nature of these models. Regarding dielectric constants of tissues, there are some conflicts in the literature. To these one may add the problem of dependence of the dielectric constants of tissues on the physiological conditions, [39].

Considering the handset, there is not a unique geometry for its box, not even for its antenna. The only requirement is its working frequency, a parameter which should be considered important for other reasons, too. However in the literature, normally, a  $\lambda/4$  monopole mounted on a metallic box is considered. This helps the researcher to compare his results with those of other researchers, although exact positioning of the monopole on the top of the box is not given carefully, a problem which adds some ambiguity to the distance between the head and the source point on the antenna, and hence makes difficult the comparison of results.

Working frequency is another important factor. As has been observed by Meier et al., [40], in the range 1.5-2.5 GHz the thicknesses of some tissue layers are in the range of  $\lambda/4$ - $\lambda/2$ , whereby the attenuation in these layers is not significant enough to exclude possible enhancement effects due to reflection at the boundaries or due to matching effects. This may mean that the researchers working in this frequency range should pay more attention to the modeling of the head and be aware that the results obtained for other frequencies, in majority in the 900 MHz band, may not be considered as a reliable inspiring guide.

## **7.7 Values of the simple head models**

As has already been discussed, it seems that simple models can be used satisfactorily to calculate the input impedance, and the radiation patterns. In the case of the SAR values under similar conditions these models lead to comparable results. There is not a set of clear criteria to evaluate the values of simple head models for SAR calculations at the present time.

Setting up these criteria may be useful, but it needs a careful classification of the forms of the real heads and trying to establish a corresponding class of simple head models incorporating most important features of the real heads. This is a multistage project. This study has considered the potentials present in simple models, and shows their capabilities. Via these models global aspects of the interaction problem, even in SAR calculations which are essentially a study of local distribution of EM power deposition, may be tractable. Among these aspects one may note the effects of the neck, effects of the size, effects of the ear, effects of the polarization, and so on, on the peak of the SAR value in the head. One may insist on the natural differences between a simple model and an anatomic or MRI based model; but one may add the important features of the real head to a simple model, and keep it always mathematically expressible. In this case the resulting code would be usable in different cell sizes, and hence at different frequencies.

### **7.8 Issues for future research**

Our study shows that there is a domain of problems in which the interaction between a radio-handset and human head is tractable using just simple models. Knowing the exact boundaries of this domain needs more work by researchers. As has been discussed earlier, careful study of the problem involves a large number of parameters and considerations. The variations in all these properties lead to a spread in the analyzed absorption distribution. A strategy on how to obtain scientifically valuable information from this large parameter range has not been worked out yet. This basic approach is reliable, but it is costly and time consuming. At the present time a compromise tendency adopted by researchers in the field is a sort of study, which may be called type-approval, which considers a specific model of handset, some simplifications and looks for a relatively reliable, time-efficient and cost-effective solution to the problem, [39],[54].

It seems that work based on simple models, would not be limited in the context of the above logic. These studies can be conducted in a manner to consider at the same time the results of the type-approval approach, developing simple models via incorporating more features of the real head in simple models, doing some type of parametrization of the head, and looking for potential biohazard considering the fine structure of the head tissues related to the wavelength at the working frequency.



## Bibliography

- [1]-Silverman, Ch., Epidemiologic studies of microwave effects, Proc. IEEE, Vol. 68, No. 1, pp. 78-84, Jan 1980.
- [2]-Schwan, H.P., Foster, K.R., RF-field interaction with biological systems: electrical properties and biophysical mechanisms, Proc. IEEE, Vol. 68, No. 1, Jan. 1980. pp. 104-113
- [3]-Vander Vorst, A., Duhamel, F., 1990-1995 advances in investigating the interaction of microwave fields with the nervous system, IEEE Trans. MTT, Vol. 44, No. 10, pp.1898-1909, Oct. 1996.
- [4]-Possible health effects related to the use of radiotelephones; Proposal for a research programme by a european commission expert group, available on the internet at the add.: <http://europa.eu.int/en/record/other/radiosum.htm>. The proposal has been presented to the Commission of the European Communities, Brussels, COM(98).
- [5]-Moulder, J. E., Cellular Phone Antennas and Human Health, available on the internet at the add.: <http://www.mcw.edu/gcrc/cop/cell-phone-health-FAQ/toc.html>. The author is Professor of Radiation Oncology at the Medical College of Wisconsin.
- [6]-Blank, M., ed., Electromagnetic fields: Biological interactions and mechanisms, Advances in chemistry series, Vol. 250, American Chemical Society, pp. 3-4, 1995
- [7]-Gandhi, O.P., ed., Biological effects and medical applications of electromagnetic energy, Prentice Hall, 1990
- [8]-Lin, J.C., ed., Electromagnetic interaction with biological systems, Plenum, 1989
- [9]-Kuster, N., Balzano, Q., and Lin, J.C., eds., Mobile communications safety, Chapman and Hall, 1997
- [10]-Adey, W.R., Tissue interaction with nonionizing electromagnetic fields. Physiol. Rev. 61, pp 435-514, 1981.

- [11]-Adey, W.R., Bioeffects of mobile communications fields. chapter 4 in Kuster, N., Balzano, Q., and Lin, J.C., eds., Mobile communications safety, Chapman and Hall, 1997.
- [12]-Wertheimer, N., and Leeper, E., Electrical wiring configurations and childhood cancer Am. J. Epidemiol., 109, pp. 273-284, 1979.
- [13]-Balzano, Q., EM metrology issues in wireless communication, in: Stuchly, M.A., ed., Modern Radio Science, U.R.S.I., Oxford University Press 1999, pp.79-90.
- [14]-Jensen, M. A., and Rahmat-Samii, Y., EM interaction of handset antennas and a human in personal communications, Proc. IEEE, Vol. 83, No. 1, pp. 7-17 Jan. 1995.
- [15]-Gandhi, O.P., Lazzi, G., and Cynthia, M.F., Electromagnetic absorption in the human head and for mobile telephones at 835 and 1900 MHz, IEEE Trans. MTT., Vol. 44, No. 10, Oct. 1996, pp. 1884-1897.
- [16]-Duck, F.A., Physical properties of tissue; A comprehensive reference book. Academic Press, 1990
- [17]-Weast, R.C., Lide, D.R., et al., eds., CRC handbook of chemistry and physics, 70th ed. CRC press, 1989-1990
- [18]-Stuchly, M.A., Stuchly, S.S., Dielectric properties of biological substances- Tabulated, Journal of Microwave power, Vol. 15, No. 1, 1980, pp. 19-26
- [19]-Foster, K.R., Schwan, H.P., Dielectric properties of tissues and biological materials: a critical review, Critical reviews in biomedical engineering, Vol. 17, Issue 1, 1989, pp. 25-104
- [20]-Gabriel, S. Lau, R.W., Gabriel, C., The dielectric properties of biological tissues: II, Measurements in the frequency range 10Hz to 20 GHz, Phys. Med. Biol. Vol. 41, 1996, pp. 2251-2269
- [21]-Polk, C., Postow, E., eds., Handbook of biological effects of electromagnetic fields, CRC press, 1986
- [22]-Pething, R., Dielectric and electronic properties of biological materials, Wiley, 1979
- [23]-Mrozowski, M., Stuchly, M. A., Parametrization of media dispersive properties for FDTD, IEEE Trans. AP, Vol. 45, No. 9, Sept. 1997. pp. 1438-1439
- [24]-Balzano, Q. Garay, O. and Steel, F.R., Heating of biological tissue in the induction field of VHF portable radio transmitters, IEEE Trans. Veh. Technol., VT-27, 2, pp.51-56, 1978

- [25]-Balzano, Q. Garay, O. and Steel, F.R., Energy deposition in simulated human operators of 800 MHz portable transmitters, *IEEE Trans. Veh. Technol.*, VT-27, 4, pp.174-181, 1978
- [26]-Chatterjee, I., Gu, Y., and Gandhi, O.P., Quantification of electromagnetic absorption in humans from body-mounted communication transceivers, *IEEE Trans. Veh. Technol.*, VT-34, 2, pp.55-62, 1985
- [27]-Cleveland, R.F., and Athey, T.W., Specific absorption rate (SAR) in models of the human head exposed to hand-held UHF portable radios, *Bioelectromagnetics*, 10, pp.173-186, 1989
- [28]-Balzano, Q., Garay, O. and Manning, Jr., T.J., Electromagnetic energy exposure of simulated users of portable cellular telephones, *IEEE Trans. Veh. Technol.*, VT-44, 3, pp.390-403, 1995
- [29]-Amemiya, Y., and Uebayashi, S., The distribution of absorbed power inside a sphere simulating human head in the near field of a  $\lambda/2$  dipole antenna, *Trans. IECE Japan*, J66-B, 9, pp. 1115-1122, Nov. 1983.
- [30]-Kmimura, Y., Yamanaka, Y., and Kotani, M., EM exposure of a human head to the near field of portable radio transmitters, *Intl. Symp. Elec. Comp. Vol. 2*, 1989, pp. 735-740.
- [31]-Sullivan. D.M., Borup, D.T., and Gandhi, O.P., Use of the finite-difference time-domain method in calculating EM absorption in human tissues, *IEEE Trans. Biom. Eng.*, Vol. BME-34, No. 2, Feb. 1987.
- [32]-Kunz, K. S., Luebbers, R. J., *The finite difference time domain method for electromagnetics*, CRC press 1993.
- [33]-Iskander, M.F., *Computational techniques in bioelectromagnetics*, *Computer phys. comm.*, 68, pp: 224-254, 1991.
- [34]-Dimbylow, P.J., Gandhi, O.P., Finite-difference time-domain calculations of SAR in a realistic heterogeneous model of the head for plane-wave exposure from 600 MHz to 3GHz, *Phys. Med. Biol.*, 1991, Vol. 36, No 8, 1075-1089.
- [35]-Dimbylow, P.J., FDTD calculations of the SAR for a dipole closely coupled to the head at 900 MHz and 1.9 GHz, *Phys. Med. Biol.*, 1991, Vol. 38, 361-368.
- [36]-Toftgard, J., Hornsleth, H., and Anderson, B., Effects on portable antennas of the

- presence of a person, *IEEE Trans. Ant. and Propagat.*, AP., Vol. 41, No. 6, June 1993.
- [37]-Martens, L. Electromagnetic field calculations for wireless telephones. *The Radio Science Bulletin* No. 271, Dec. 1994, pp. 9-11.
- [38]-Martens, L., Moerloose, J. De., and Zutter, D. De., Calculation of the electromagnetic fields induced in the head of an operator of a cordless telephone. *Radio Science*, Vol. 30, No. 1, pp. 283-290, Jan-Feb 1995.
- [39]-Hombach, V., Meier, K., Burkhardt, E.K., and Kuster, N., The dependence of EM energy absorption upon human head modeling at 900 MHz, *IEEE Trans. MTT.*, Vol. 44, No. 10, Oct. 1996, pp. 1865-1873.
- [40]-Meier, K., Hombach, V., Kastle, R., Yew-Sio Tay, R., and Kuster, N., The dependence of electromagnetic energy absorption upon human-head modeling at 1800 MHz, *IEEE Trans. MTT.*, Vol. 45, No. 11, Nov. 1997, pp. 2058-2062.
- [41]-Watanabe, So-ichi., Taki, M., Nojima, T., Fujiwara, O., Characteristics of the SAR distributions in a head exposed to electromagnetic fields radiated by a hand-held portable radio, *IEEE Trans. MTT.*, Vol. 44, No. 10, Oct. 1996, pp. 1874-1883.
- [42]-Okoniewsky, M., and Stuchly, M.A., A study of the handset antenna and human body interaction, *IEEE Trans. MTT.*, Vol. 44, No. 10, Oct. 1996, pp. 1855-1864
- [43]-Umashankar, K., Taflove, A., and Becker, A., Calculation and experimental validation of induced currents on coupled wires in an arbitrary shaped cavity, *IEEE Trans. Ant. Prop.*, 35, 1284, 1987.
- [44]-Dimbylow, P.J., Finite difference calculations of current densities in a homogeneous model of a man exposed to extremely low-frequency electric fields, *Bioelectromagnetics*, 8, 355-377, 1987.
- [45]-Smith, G. S., and Scott, JR., W.R., The use of emulsions to represent dielectric materials in electromagnetic scale models. *IEEE Trans. Ant. and Propagat.*, AP, Vol. 38, No. 3, pp. 323-334, March, 1990
- [46]-Nikawa, Y., Chino, M., and Kikuci, K., Soft and dry phantom modeling material using silicon rubber with carbon fiber, *IEEE Trans. MTT.* Vol. 44, No. 10, Oct. 1996, pp. 1949-1953.
- [47]-Jasik, H., ed., *Antenna engineering handbook* Mc Graw-Hill 1961
- [48]-Kraus, J.D., *Antennas*, Mc Graw-Hill, 1988

- [49]-Stutzman, W. L., *Antenna theory and design*, Wiley, 1981.
- [50]-Eycleshymer, A. C., and Schoemaker, D. M., *A cross-section anatomy*, Appleton-Century-Crofts 1970
- [51]-Nielsen, L.E., *Predicting the properties of mixtures; mixture rules in science and engineering*, Marcel Dekker, Inc., 1978.
- [52]-Stogryn, A., Equations for calculating the dielectric constant of saline water. *IEEE Trans. MTT*, Vol. 19, pp. 733-736, Aug. 1971.
- [53]-Luebbers, R., Chen, L., Uno, T., and Adachi, S., FDTD calculation of radiation patterns, impedance, and gain for a monopole antenna on a conducting box, *IEEE Trans. Ant. and Propagat.*, AP, Vol. 40, pp. 1577-1583, DEC. 1992.
- [54]-Yu, Q., Gandhi, O.P., Aronson, M., and Wu, D., An automated SAR measurement system for compliance testing of personal wireless devices, *IEEE Trans. Electromag. Compat.*, Vol. 41, No. 3, pp. 234-245, Aug. 1999.
- [55]-Balanis, C. A., *Advanced Engineering electromagnetics*; Wiley 1989
- [56]-Yee, K.S., Numerical solution of initial boundary value problems involving Maxwell's equations in isotropic media, *IEEE Trans. Ant. Prop.*, vol. 14, no. 3, p-302 1966.
- [57]-Mur, G., Absorbing boundary conditions for the finite-difference approximation of the time-domain electromagnetic-field equations, *IEEE Trans. Electromag. Compat.*, Vol. 23, pp. 377-382, 1981.
- [58]-Enquist, B., and Majda, A., Absorbing boundary conditions for the numerical simulations of waves, *Math. Comput.*, 629, 1977.
- [59]-American National Standards Institute, *IEEE C95.1-1991: IEEE Standard for safety Levels with Respect to Human Exposure to Radio Frequency Electromagnetic Fields, 3 kHz to 300 GHz*, 1991, Piscataway, NJ 08855-1331.
- [60]-Watanabe, S. and Taki, M., An Improved FDTD model for the feeding of a thin-wire antenna, *IEEE Microwave and Guided Wave Letters*, Vol. 8, No. 4, pp. 152-154, April 1998
- [61]-Hockanson, D.M., Drewniak, J. L., Hubing, T.H., and Vandoren, T.P., FDTD modeling of thin wires for simulating common-mode radiation from structures with attached cables, *IEEE International Symposium on Electromagnetic Compatibility Aug 14-18 1995* 1995 p 168-173

- [62]-Douglas, M., Okoniewski, M., and Stuchly, M. A., Accurate modeling of thin wires in the FDTD method, IEEE Antennas and Propagation Society, AP-S International Symposium (Digest) v 2 Jun 21-26 1998 1998 Sponsored by: IEEE IEEE p 1246-1249
- [63]-Douglas, M., Okoniewski, M., and Stuchly, M. A., Accurate modeling of thin-wire antennas in the FDTD method, Microwave and Optical Technology Letters v 21 n 4 1999 John Wiley & Sons Inc p 261-265
- [64]-Smyth, C. P., Dielectric behaviour and structure: dielectric constant and loss, dipole moment and molecular structure, McGraw-Hill, 1955.
- [65]-Vadjed Samiei, M.H., Delisle, G.Y., Analytical and experimental study of the EM /biological tissues interaction at 1900 MHz., submitted to the IEEE 2000 Intl. Symp. Electromagnetic compatibility, Aug. 21-25, 2000, Washington, DC, USA.